



Supporting Information

Supramolecular Chalcogen-Bonded Semiconducting Nanoribbons at Work in Lighting Devices

D. Romito, E. Fresta, L. M. Cavinato, H. Kählig, H. Amenitsch, L. Caputo, Y. Chen, P. Samorì, J.-C. Charlier, R. D. Costa, D. Bonifazi**

SUPPORTING INFORMATION

Table of Contents

1. General remarks

- 1.1 Instrumentation
- 1.2 Materials and methods
 - 1.2.1 Thin-film transistor fabrication
 - 1.2.2 Thin film preparation
 - 1.2.3 Device fabrication and characterization

2. Synthetic procedures

- 2.1 Synthesis of 2-bromo-3-iodopyridine **2**^[1]
- 2.2 Synthesis of 2-bromo-3-((trimethylsilyl)ethynyl)pyridine **3**_{TMS}^[2]
- 2.3 Synthesis of 2-bromo-3-(phenylethynyl)pyridine **3**_{Ph}
- 2.4 Synthesis of 2-(trimethylsilyl)telluropheno[2,3-β]pyridine **4**_{TMS}
- 2.5 Synthesis of 2-phenyltelluropheno[2,3-β]pyridine **4**_{Ph}
- 2.6 Synthesis of 2-bromo-3-ethynylpyridine **5**_{Pyr}^[3]
- 2.7 Synthesis of 2-bromo-3-ethynylbenzene **5**_{Benzo}
- 2.8 Synthesis of 2-bromo-3-((perfluorophenyl)ethynyl)pyridine **6**_{Pyr}
- 2.9 Synthesis of 1-((2-bromophenyl)ethynyl)-2,3,4,5,6-pentafluorobenzene **6**_{Benzo}
- 2.10 Synthesis of 7-butyl-6,8,9-trifluorobenzo[4',5']telluropheno[2',3':4,5]telluropheno[2,3-β]pyridine **7**_{Pyr}
- 2.11 Synthesis of 2-butyl-1,3,4-trifluorobenzo[b]benzo[4,5]telluropheno[2,3-d]tellurophene **7**_{Benzo}

3. NMR-HRMS Spectroscopic characterization (¹H, ¹³C, ¹⁹F, ¹²⁵Te, HRMS)

- 3.1 Characterization of **3**_{Ph}
- 3.2 Characterization of **4**_{TMS}
- 3.3 Characterization of **4**_{Ph}
- 3.4 Characterization of **6**_{Pyr}
- 3.5 Characterization of **6**_{Benzo}
- 3.6 Characterization of **7**_{Pyr}
- 3.7 Characterization of **7**_{Benzo}

4. Optoelectronic characterization

- 4.1 Photophysical properties
- 4.2 Electrochemical properties

5. Crystallographic data**6. Computational studies****7. Morphological features****8. Thin-film transistor outcome****9. Implementation of dichalcogenides **7**_{Pyr} and **7**_{Benzo} in LEC device****1. General remarks****1.1. Instrumentation**

Thin layer chromatography (TLC) was conducted on pre-coated aluminum sheets with 0.20 mm *Merck Millipore* Silica gel 60 with fluorescent indicator F254. *Column chromatography* was carried out using *Merck Gerduran* silica gel 60 (particle size 40–63 μm). *Melting points* (mp) were measured on a *Gallenkamp* apparatus in open capillary tubes and have not been corrected. *Nuclear magnetic resonance*: (NMR) spectra were recorded on a

SUPPORTING INFORMATION

Bruker Fourier 300 MHz spectrometer equipped with a dual (^{13}C , ^1H) probe, a Bruker AVANCE III HD 400 MHz NMR spectrometer equipped with a Broadband multinuclear (BBFO) SmartProbeTM, a Bruker AVANCE III HD 500 MHz Spectrometer equipped with Broadband multinuclear (BBO) Prodigy CryoProbe or a Bruker AV III HDX 700 MHz NMR spectrometer (Bruker BioSpin, Rheinstetten, Germany) with a quadruple (^1H , ^{13}C , ^{15}N , ^{19}F) inverse helium cooled cryo probe. ^1H spectra were obtained at 300, 400, 500, 600 or 700 MHz, $^{13}\text{C}\{^1\text{H}\}$ spectra were obtained at 75, 100, 125, 150 or 175 MHz NMR and ^{19}F spectra were obtained at 376, 470 and 659 MHz. ^{125}Te NMR experiments were done on a Bruker AV III 600 MHz NMR spectrometer using a nitrogen cooled broad band observe cryo probe at a resonance frequency of 189.38 MHz. All spectra were obtained at r.t. Chemical shifts were reported in ppm relative to tetramethylsilane using the residual solvent signal for ^1H or the solvent signal for ^{13}C as an internal reference (CDCl_3 : $\delta_{\text{H}} = 7.26$ ppm, $\delta_{\text{C}} = 77.16$ ppm; C_6D_6 : $\delta_{\text{H}} = 7.16$ ppm, $\delta_{\text{C}} = 128.06$ ppm). Chemical shifts for ^{19}F and ^{125}Te are reported on a unified scale relative to ^1H using the Ξ value for CDCl_3 .^[4] Coupling constants (J) were given in Hz. Resonance multiplicity was described as s (singlet), d (doublet), t (triplet), dd (doublet of doublets), ddd (doublet of doublets of doublets), dm (doublet of multiplets), q (quartet), m (multiplet) and bs (broad signal). Carbon spectra were acquired with ^1H decoupling. Solid state ^{125}Te NMR spectra were obtained on a Bruker Avance NEO 500 wide bore system (Bruker BioSpin, Rheinstetten, Germany) using a 4 mm triple resonance magic angle spinning (MAS) probe. The resonance frequency was set to 157.82 MHz, the MAS rotor spinning to 15 kHz. Up to 9000 transients with a relaxation delay of 20 s were acquired. During acquisition ^1H was high power decoupled using SPINAL with 64 phase permutations. To identify the isotropic chemical shifts the experiments were repeated at a second rotor spinning speed of 13.7 kHz. The line shape analysis was done within the TopSpin software (Bruker BioSpin, Rheinstetten, Germany) using the chemical shift anisotropy model. **Infrared spectra** (IR) were recorded on a Shimadzu IR Affinity 1S FTIR spectrometer in ATR mode with a diamond mono-crystal. **Mass spectrometry**: (i) High-resolution ESI mass spectra (HRMS) were performed on a Waters LCT HR TOF mass spectrometer in the positive or negative ion mode. **Photophysical analysis**: Absorption spectra were recorded on air equilibrated solutions at room temperature with an Agilent Cary 5000 UV-Vis spectrophotometer, using quartz cells with path length of 1.0 cm. Steady-state photoluminescence, phosphorescence spectra, and lifetime measurements were recorded on a Cary Eclipse spectrofluorometer. All photophysical properties at 298 K were measured in CH_2Cl_2 using a quartz cell with a 10x2 mm optical path. The photophysical properties at 77 K were measured in $\text{CHCl}_3/\text{EtOH}$ 1:1 glassy matrix using a quartz NMR tube (4 mm) placed in a quartz liquid nitrogen dewar. The absorbance at the excitation wavelength was adjusted to < 0.1 . **Electrochemical measurements**: Cyclic voltammetry (CV) measures in solution were carried out at room temperature in N_2 purged dry CH_2Cl_2 and TCE with an AUTOLAB PGSTAT 204. Glassy carbon electrode with a 3 mm diameter was used as a working electrode, an Ag wire as a pseudo-reference electrode (AgQRE) and a Pt spiral as a counter electrode. Working electrode and AgQRE electrodes were polished on a felt pad with 0.05 or 0.3 μm alumina suspension and then sonicated in deionized H_2O for few minutes before each experiment; the Pt wire was flame-cleaned. Tetrabutylammonium hexafluorophosphate (TBAPF_6) was exploited as a supporting electrolyte at a concentration 0.1 M. Ferrocene (Fc) was added as internal reference: $E_{1/2}(\text{Fc}^+/\text{Fc}) = 0.43$ V vs

SUPPORTING INFORMATION

AgQRE in CH_2Cl_2 ; $E_{1/2}(\text{Fc}^+/\text{Fc}) = 0.41 \text{ V}$ vs AgQRE in TCE. CV measurements of PET/ITO spin coated thin films were carried out at room temperature in Ar purged Propylene Carbonate (PC) with an AUTOLAB PGSTAT 204. A strip of PET with sputtered ITO ($60 \Omega/\text{sq}$) was used as working electrode, a non-aqueous Ag/Ag⁺ electrode as reference and a Pt wire as a counter electrode. **Scanning Electron Microscopy (SEM):** SEM images were recorded with a Zeiss Supra 55 Variable Pressure instrument with an acceleration voltage of 5 kV. **X-ray measurements:** Crystallographic studies of **4_{Ph}** (2063971) were undertaken on single crystal mounted in paratone and studied on an Agilent SuperNova Dual three-circle diffractometer using Mo-K α ($\lambda = 0.7093187 \text{ \AA}$) radiation and a CCD detector. Measurements were made at 150(2) K with temperatures maintained using an Oxford Cryostream. Data were collected, integrated and corrected for absorption using a numerical absorption correction based on gaussian integration over a multifaceted crystal model within CrysAlisPro.^[5] The structures were solved by direct methods and refined against R^2 within SHELXL-2013.^[6] A summary of crystallographic data are available as ESI and the structures deposited with the Cambridge Structural Database (CCDC) deposition numbers: These data can be obtained free of charge from The Cambridge Crystallographic Data Centre via www.ccdc.cam.ac.uk/data_request/cif. The X-ray intensity data of **7_{PyR}** (2057472) and **7_{Benzo}** (2057473) were measured on Bruker D8 Venture diffractometer equipped with multilayer monochromator, Mo and Cu K/ α INCOATEC micro focus sealed tubes and Oxford cooling system. The structures were solved by Direct Methods and Intrinsic Phasing. Non-hydrogen atoms were refined with anisotropic displacement parameters. Hydrogen atoms were inserted at calculated positions and refined with riding model. The following software was used: Bruker SAINT software package^[7] using a narrow-frame algorithm for frame integration, SADABS^[8] for absorption correction, OLEX2^[9] for structure solution, refinement, molecular diagrams and graphical user-interface, Shelxle^[10] for refinement and graphical user-interface SHELXS-2015^[11] for structure solution, SHELXL-2015^[11] for refinement, Platon^[12] for symmetry check. Crystal data, data collection parameters, and structure refinement details are given in Tables 4 to 6. **Grazing incidence X-ray diffraction (GIXRD) measurements:** GIXRD patterns have been recorded at the Austrian SAXS beamline at ELETTRA^[13] with a Pilatus3 1M detector at a sample to detector distance of 407 mm using an X-ray energy of 16 keV. The spot size at the sample position has been set to 0.2 x 1.5 mm (horizontal x vertical). The data have been corrected for fluctuations of the primary intensity. GIXRD patterns have been taken at a grazing angle of 0.07° for **7_{PyR}** and 0.1° for **7_{Benzo}** (below the critical angle of Si). The data evaluation as well as the simulation of the GIXRD pattern from the crystal structure has been performed with the software package *GIXSGUI*.^[14] **Calculations** have been performed using density functional theory (DFT) with normconserving pseudopotentials from PseudoDojo^[15] and plane waves (PW) basis set as implemented in the Quantum Espresso code.^[16] The generalized-gradient approximation of Perdew, Burke and Ernzerhof (PBE) has been exploited for the exchange-correlation density functional.^[17] To properly describe the long-range electron correlation effects, D3 correction has been added^[18] as implemented in the Quantum Espresso code. In both **7_{PyR}** and **7_{Benzo}** structures, the butane chains have been substituted by a Hydrogen atom for simplicity. The vacuum thickness along non-periodical axes has been fixed after convergence study to 13°Å. Calculations have been performed using an energy cut off of 85Ry. Regarding the k-point sampling, a mesh of 1×2×1 has been used in

SUPPORTING INFORMATION

both monolayer systems where the denser grid is always along the periodicity axis while a 2×2 grid have been used for the multilayered structures along the periodic directions. The structural optimization has been performed by relaxing both ionic positions and cell parameters, keeping fixed the latter on the non-periodical axes, until the total forces reach values below 0.001 a.u.

1.2. Materials and methods

Chemicals were purchased from *Sigma Aldrich*, *Acros Organics*, *TCI*, *Apollo Scientific*, *ABCR*, *Alfa Aesar*, *Carbosynth* and *Fluorochem* and were used as received. Solvents were purchased from *Fluorochem*, *Fisher Chemical* and *Sigma Aldrich*, while deuterated solvents from *Eurisotop* and *Sigma Aldrich*. THF, Et₂O and CH₂Cl₂ were dried on a Braun MB SPS-800 solvent purification system. MeOH, CHCl₃ and acetone were purchased as reagent-grade and used without further purification. Et₃N was distilled from CaH₂ and then stored over KOH. Anhydrous dioxane and pyridine were purchased from *Sigma Aldrich*. Solution of iso-propyl magnesium chloride in THF were freshly prepared according to a procedure of Lin et al.^[19] and titrated with the Paquette method,^[20] or directly purchased from *Sigma Aldrich*. Low temperature baths were prepared using different solvent mixtures depending on the desired temperature: 0 °C with ice/H₂O. Anhydrous conditions were achieved by flaming two necked flasks with a heat gun under vacuum and purging with N₂. The inert atmosphere was maintained using Nitrogen-filled balloons equipped with a syringe and needle that was used to penetrate the silicon stoppers closing the flask's necks. Additions of liquid reagents were performed using dried plastic or glass syringes. All reactions were performed in dry conditions and under inert atmosphere unless otherwise stated.

1.2.1 Thin-film transistor fabrication

Thin-film transistors in a bottom-gate top-contact configuration were fabricated on the substrates of n++ Si coated with 230 nm thick thermally grown layer of SiO₂ acting as the gate dielectric (IPMS Fraunhofer Institute). The substrates were cleaned by ultrasonication in acetone and isopropanol for 20 min, blow dried with a nitrogen flow, and then treated by ozone for 5 min (Novascan, Digital UV Ozone system).

BCB dielectric layer was prepared by diluting Cyclotene 3022–46 (Dow Chemistry) to 20% vol with mesitylene. The solution was spin-coated onto the Si/SiO₂ substrates at 4000RPM and post-anneal at 290 °C for 1 hour resulting in a cross-linked film with thickness of 100 nm. A drop of 0.2 mg/mL solution in toluene of either **7_{Pyr}** or **7_{Benzo}** was applied onto the Si/SiO₂/BCB substrate. The as-prepared **7_{Pyr}** and **7_{Benzo}** samples were kept in a petri dish under dark overnight to allow the slow evaporation of the toluene solvent. The morphology of these films was explored by Optical Microscopy (OLYMPUS EX51) and by Atomic Force Microscopy topographical imaging. The latter type of investigation was carried out with using a Bruker Dimension Icon microscope in ambient conditions, operating in tapping mode and using TESPA-V2 tips with spring constant k = 42 N/m.

Gold electrodes with size of 40 μm × 200 μm and thickness of 120 nm were dry transferred and laminated on top of the individual **7_{Pyr}** crystals under the observation of optical microscopy. Electrical characterization was realized by semiconductor parameter analyzer (Keithley 2636) inside a dry and nitrogen-filled glove-box.

SUPPORTING INFORMATION

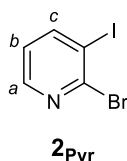
1.2.2 Thin film preparation

A 5 mg/mL toluene solution of **7_{Pyr}/7_{Benzo}** pristine or combined with a ion-doped matrix consisting of **7_{Pyr}/7_{Benzo}**:TMPE:LiOTf 1:0.15:0.03 mass ratio was prepared by using toluene solutions of TMPE with M_w 450,000 (20 mg/mL), and LiOTf (10 mg/ml). The solution was heated at 60° C, sonicated and filtered. Then, it was either spin coated onto cleaned naked glass substrate at a speed of 700 rpm for 60 s, or drop casted directly.

1.2.3 Device fabrication and characterization

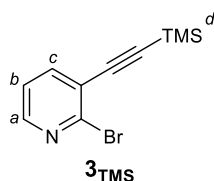
ITO substrates were purchased from Naranjo Substrates with an ITO thickness of 130 nm. They were extensively cleaned using detergent, water, ethanol, and propan-2-ol as solvents in an ultrasonic bath (frequency 37-70 Hz) for 15 min each. Afterwards, the slides were dried with N₂ gas and put in an UV-ozone cleaner for 8 min. The clean plates were then coated with 60 nm PEDOT:PSS layers via spin coating. To this end, an aqueous solution of PEDOT:PSS was filtered and mixed with propan-2-ol in a ratio of 3:1.3. From this solution, 60 μL were dropped onto the substrate at a rotation speed of 2000 rpm and spun for 60 s. The resulting layers were dried on a hotplate at 120 °C and stored under N₂. The active layers in single-layered LEC devices (60-70 nm) were deposited from a 5 mg/mL toluene solution of **7_{Pyr}/7_{Benzo}** combined with a ion-doped matrix consisting of **7_{Pyr}/7_{Benzo}**:TMPE:LiOTf 1:0.15:0.03 mass ratio. This was prepared using toluene solutions of TMPE with M_w 450,000 (20 mg/mL), and LiOTf (10 mg/ml) and spin coated at 700 rpm for 30 s, at 1200 rpm for 30 s and at 2500 rpm for an additional 10 s. Before spin-coating, the solution was heated at 60° C, sonicated and filtered. In the case of double-layered devices, the first active layer comprising **7_{Pyr}/7_{Benzo}** was prepared as aforementioned and spin coated for 60 s at a speed of 3000 rpm. Then, a layer of **Cu-iTMC** was spin coated on top. **Cu-iTMC** was dissolved in THF in a concentration of 12 mg/mL and spin coated at 800 rpm for 30 s, 1500 rpm for 30 s and 3000 rpm for an additional 10 s, reaching a thickness of 80 nm. In all cases, after the deposition of the active layer(s) the devices were dried under vacuum for 2 h and transferred to an inert atmosphere glovebox (<0.1 ppm O₂ and H₂O, Angstrom Engineering). Finally, Aluminum cathodes (90 nm) were thermally evaporated onto the active layer using a shadow mask under high vacuum (<1 x 10⁻⁶ mbar) in an Angstrom Covap evaporator integrated into the inert atmosphere glovebox. The device statistics involve up to five different devices- *i.e.*, a total number of 20 pixels. Time dependence of luminance, voltage, and current was measured by applying constant and/or pulsed voltage and current by monitoring the desired parameters simultaneously by using Avantes spectrophotometer (Avaspec-ULS2048L-USB2) in conjunction with a calibrated integrated sphere Avasphere 30-Irrad and Botest OLT OLED Lifetime-Test System.

SUPPORTING INFORMATION

2. Synthetic procedure**2.1 Synthesis of 2-bromo-3-iodopyridine 2_{Pyr} ^[1]**

To a solution of *i*-Pr₂NH (2.04 g, 2.8 mL, 20 mmol) in dry THF (40 mL) under anhydrous condition, *n*-BuLi (1.6 M in hexane, 12.5 mL, 20 mmol) was added dropwise at -40 °C. The mixture was stirred at the same temperature for 30 minutes, then a solution of 2-bromopyridine **1** (3.16 g, 1.9 mL, 20 mmol) in dry THF (8 mL) was added dropwise at -95 °C. The reaction was stirred at -95 °C for 4 h, followed by the addition dropwise of a solution of I₂ (5.1 g, 20 mmol) in dry THF (16 mL) at -95 °C. The reaction was allowed to warm up to room temperature and stirred for 50 minutes, then quenched by a saturated aqueous Na₂S₂O₃ solution (30 mL) and extracted with Et₂O (3 × 50 mL). The combined organic extracts were washed with brine (20 mL), dried over Na₂SO₄, filtered and solvents removed under reduced pressure. The crude was purified by silica gel chromatography (CHCl₃/MeOH 99.5:0.05) to give pure 2_{Pyr} as a yellow solid (4.26 g, 75% yield). Spectral properties are in agreement with those reported in the literature.^[21]

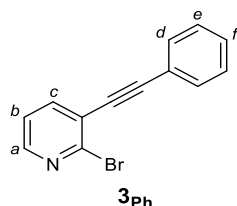
mp: 98-100 °C (lit.: 95-97 °C); ¹H NMR (300 MHz, CDCl₃) δ: 8.35 (dd, *J*_{H,H} = 4.6, 1.8 Hz, 1H, *H*_a), 8.11 (dd, *J*_{H,H} = 7.8, 1.8 Hz, 1H, *H*_c), 7.00 (dd, *J*_{H,H} = 7.8, 4.6 Hz, 1H, *H*_b); ¹³C{¹H} NMR (75 MHz, CDCl₃) δ: 148.9, 148.6, 148.3, 123.6, 99.6.

2.2 Synthesis of 2-bromo-3-((trimethylsilyl)ethynyl)pyridine 3_{TMS} ^[2]

A solution of 2-bromo-3-iodopyridine 2_{Pyr} (284 mg, 1 mmol) in NEt₃ (2 mL) and 1,4-dioxane (2 mL) was degassed for 30 minutes, then [Pd(PPh₃)₂Cl₂] (35 mg, 0.05 mmol) and CuI (19 mg, 0.1 mmol) were added, followed by the addition of trimethylsilylacetylene (18 mg, 0.17 mL, 1.2 mmol). The reaction was stirred at room temperature for 1.5 h, then diluted with Et₂O (10 mL) and filtered over celite. The filtrate was washed with a saturated aqueous NH₄Cl solution (30 mL) and extracted with Et₂O (3 × 30 mL). The combined organic extracts were washed with brine (20 mL), dried over Na₂SO₄, filtered and solvents removed under reduced pressure. The crude was purified by silica gel chromatography (CHCl₃) to give pure 3_{TMS} as a yellow oil (254 mg, 98% yield). Spectral properties are in agreement with those reported in the literature.^[22]

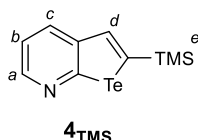
¹H NMR (300 MHz, CDCl₃) δ: 8.28 (dd, *J*_{H,H} = 4.8, 2.0 Hz, 1H, *H*_a), 7.73 (dd, *J*_{H,H} = 7.7, 2.0 Hz, 1H, *H*_c), 7.21 (dd, *J*_{H,H} = 7.7, 4.8 Hz, 1H, *H*_b), 0.28 (s, 9H, *H*_d); ¹³C{¹H} NMR (75 MHz, CDCl₃) δ: 148.7, 144.8, 141.3, 123.6, 122.1, 103.3, 100.9, -0.2; ESI-LRMS: *m/z* required: 252.99; found: 254.00.

SUPPORTING INFORMATION

2.3 Synthesis of 2-bromo-3-(phenylethynyl)pyridine **3_{Ph}**

A solution of 2-bromo-3-iodopyridine **2_{Pyr}** (284 mg, 1 mmol) in NEt₃ (2 mL) and 1,4-dioxane (2 mL) was degassed for 30 minutes, then [Pd(PPh₃)₂Cl₂] (35 mg, 0.05 mmol) and CuI (19 mg, 0.1 mmol) were added, followed by the addition of ethynylbenzene (123 mg, 0.13 mL, 1.2 mmol). The reaction was stirred at room temperature for 1.5 h, then diluted with Et₂O (10 mL) and filtered over celite. The filtrate was washed with a saturated aqueous NH₄Cl solution (30 mL) and extracted with Et₂O (3 × 30 mL). The combined organic extracts were washed with brine (20 mL), dried over Na₂SO₄, filtered and solvents removed under reduced pressure. The crude was purified by silica gel chromatography (CHCl₃/MeOH 99.75:0.25) to give pure **3_{Ph}** as a yellow powder (105 mg, 41% yield).

mp: 78-80 °C; FTIR (ATR): ν (cm⁻¹): 3048, 2253, 1523, 1472, 1426, 1396, 1374, 1291, 1250, 1189, 1110, 1094, 954, 862, 781, 723, 654; ¹H NMR (300 MHz, CDCl₃) δ : 8.31 (dd, $J_{H,H} = 4.8, 2.0$ Hz, 1H, H_a), 7.82 (dd, $J_{H,H} = 7.7, 2.0$ Hz, 1H, H_c), 7.63 – 7.56 (m, 2H, H_e), 7.43 – 7.35 (m, 3H, $H_{d,f}$), 7.28 (dd, $J_{H,H} = 7.7, 4.8$ Hz, 1H, H_b); ¹³C{¹H} NMR (100 MHz, CDCl₃) δ : 148.5, 144.5, 140.7, 131.7, 129.2, 128.5, 123.7, 122.3, 122.2, 96.6, 85.9; HRMS (ESI): m/z calcd for C₁₃H₈NBr+H⁺: 257.9913 [$M+H$]⁺; found: 257.9915.

2.4 Synthesis of 2-(trimethylsilyl)telluropheno[2,3- β]pyridine **4_{TMS}**

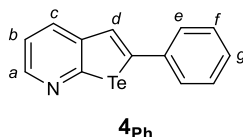
To a diluted solution of *i*-PrMgCl (2 M in THF, 0.59 mL, 1.18 mmol) in dry and degassed THF (2 mL) under anhydrous condition, *n*-BuLi (1.6 M in hexane, 1.47 mL, 2.35 mmol) was added dropwise at 0 °C. The mixture was stirred at the same temperature for 10 minutes, then a solution of 2-bromo-3-((trimethylsilyl)ethynyl)pyridine **3_{TMS}** (250 mg, 0.98 mmol) in dry and degassed THF (2 mL) was added dropwise at 0 °C. The mixture was stirred at the same temperature for 1 h, and freshly grounded elemental tellurium powder (375 mg, 2.94 mmol) was added in once while a brisk flux of nitrogen was passed through the flask. The reaction was slowly allowed to warm up to room temperature and stirred for 3 h, then degassed EtOH (2 mL) was added. The mixture was stirred at room temperature for 3 h, then poured in cold water (20 mL) and extracted with Et₂O (5 × 30 mL). The combined organic extracts were washed with brine (20 mL), dried over Na₂SO₄, filtered and solvents removed under reduced pressure. The crude was purified by silica gel chromatography (CHCl₃/MeOH 99.75:0.25) to give pure **4_{TMS}** as a brown oil (128 mg, 43% yield).

FTIR (ATR): ν (cm⁻¹): 3049, 2932, 1798, 1580, 1474, 1400, 1356, 1290, 1180, 1063, 1012, 970, 874, 801, 752, 688, 631, 420; ¹H NMR (300 MHz, CDCl₃) δ : 8.47 (dd, $J_{H,H} = 4.6, 1.7$ Hz, 1H, H_a), 8.00 (s, 1H, H_d), 7.96 (dd,

SUPPORTING INFORMATION

$J_{\text{H,H}} = 7.9, 1.7$ Hz, 1H, H_c), 7.30 (dd, $J_{\text{H,H}} = 7.9, 4.6$ Hz, 1H, H_b), 0.35 (s, 9H, H_e); $^{13}\text{C}\{^1\text{H}\}$ NMR (75 MHz, CDCl_3) δ : 163.8, 146.9, 145.9, 145.8, 138.9, 133.7, 120.0, 0.4; HRMS (ESI): m/z calcd for $\text{C}_{10}\text{H}_{13}\text{NSi}^{130}\text{Te}+\text{H}^+$: 305.9958 $[\text{M}+\text{H}]^+$; found: 305.9968.

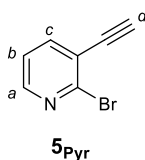
2.5 Synthesis of 2-phenyltelluropheno[2,3- β]pyridine **4_{Ph}**



To a diluted solution of *i*-PrMgCl (2 M in THF, 0.21 mL, 0.42 mmol) in dry and degassed THF (1 mL) under anhydrous condition, *n*-BuLi (1.6 M in hexane, 0.53 mL, 0.84 mmol) was added dropwise at 0 °C. The mixture was stirred at the same temperature for 10 minutes, then a solution of 2-bromo-3-(phenylethynyl)pyridine **3_{Ph}** (90 mg, 0.35 mmol) in dry and degassed THF (1 mL) was added dropwise at 0 °C. The mixture was stirred at the same temperature for 1 h, then freshly grounded elemental tellurium powder (134 mg, 1.05 mmol) was added in once while a brisk flux of nitrogen was passed through the flask. The reaction was slowly allowed to warm up to room temperature and stirred for 3 h, then degassed EtOH (1 mL) was added. The mixture was stirred at room temperature for 3 h, then poured in cold water (20 mL) and extracted with Et₂O (5 × 30 mL). The combined organic extracts were washed with brine (20 mL), dried over Na₂SO₄, filtered and solvents removed under reduced pressure. The crude was purified by silica gel chromatography ($\text{CHCl}_3/\text{MeOH}$ 99.5:0.5) to give pure **4_{Ph}** as an orange solid (44 mg, 41% yield).

mp: 98-99 °C; FTIR (ATR): ν (cm⁻¹): 3053, 2957, 1842, 1558, 1520, 1485, 1375, 1315, 1219, 1194, 1061, 1045, 849, 781, 752, 723, 687, 650, 590, 442; ^1H NMR (300 MHz, CDCl_3) δ : 8.42 (br, 1H, H_a), 7.92 (dd, $J_{\text{H,H}} = 7.9, 1.4$ Hz, 1H, H_c), 7.76 (s, 1H, H_d), 7.53 (m, 2H, H_f), 7.38 (m, 3H, $H_{e,g}$), 7.29 (dd, $J_{\text{H,H}} = 7.9, 4.7$ Hz, 1H, H_b); $^{13}\text{C}\{^1\text{H}\}$ NMR (75 MHz, CDCl_3) δ : 160.7, 146.0, 145.6, 145.1, 139.5, 133.4, 129.1, 128.6, 127.9, 127.7, 120.6; HRMS (ED): m/z caclcd for $\text{C}_{13}\text{H}_9\text{N}^{130}\text{Te}$: 308.9795 $[\text{M}^+]$; found: 308.9797. Crystal suitable for X-Ray diffraction was obtained by slow evaporation of solvent from a CHCl_3 solution (CCDC #2063971 – see page S30).

2.6 Synthesis of 2-bromo-3-ethynylpyridine **5_{Pyr}**^[3]

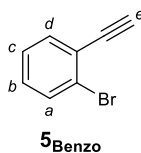


To a solution of 2-bromo-3-((trimethylsilyl)ethynyl)pyridine **3_{TMS}** (500 mg, 2 mmol) in CH_2Cl_2 (0.7 mL) under anhydrous condition, were added MeOH (1.4 mL) and K₂CO₃ (280 mg, 2 mmol). The mixture was stirred at room temperature for 1 h, then water (20 mL) was added and extracted with Et₂O (3 × 30 mL). The combined organic extracts were washed with brine (20 mL), dried over Na₂SO₄, filtered and solvents removed under reduced pressure. Pure **5_{Pyr}** was obtained as a brown solid without further purification (293 mg, 80% yield). Spectral properties are in agreement with those reported in the literature.^[22]

SUPPORTING INFORMATION

^1H NMR (300 MHz, CDCl_3) δ : 8.34 (dd, $J_{\text{H,H}} = 4.8, 2.0$ Hz, 1H, H_a), 7.79 (dd, $J_{\text{H,H}} = 7.7, 2.0$ Hz, 1H, H_c), 7.25 (dd, $J_{\text{H,H}} = 7.7, 4.8$ Hz, 1H, H_b), 3.52 (s, 1H, H_d); $^{13}\text{C}\{^1\text{H}\}$ NMR (75 MHz, CDCl_3) δ : 149.3, 144.6, 141.9, 122.7, 122.2, 84.8, 80.0.

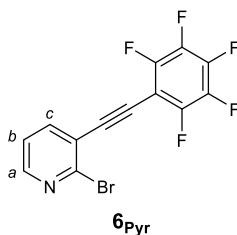
2.7 Synthesis of 1-bromo-2-ethynylbenzene **5_{Benzo}**



In a Schlenk flask [$\text{Pd}(\text{PPh}_3)_2\text{Cl}_2$] (621 mg, 0.89 mmol) and CuI (337 mg, 1.77 mmol) were added and three vacuum-nitrogen cycles were performed. A mixture of 2-bromoiodobenzene **2_{Benzo}** (5 g, 2.3 mL, 17.7 mmol) and NEt_3 (125 mL) was added and the resulting suspension immediately frozen in liquid N_2 . The mixture was degassed by two *fpt* cycles, then trimethylsilylacetylene (1.91 g, 2.7 mL, 19.4 mmol) was added. The resulting reaction mixture was subjected to further two *fpt* cycles and stirred at room temperature for 3.5 h, then diluted with CHCl_3 (30 mL) and filtered over celite. The filtrate was washed with a saturated aqueous NH_4Cl solution (30 mL), then the organic phase was dried over MgSO_4 , filtered and the solvents removed under reduced pressure. To a solution of resulting 2-bromo-3-((trimethylsilyl)ethynyl)benzene (2.9 g, 11.4 mmol) in CH_2Cl_2 (3.9 mL) under anhydrous condition, were added MeOH (7.8 mL) and K_2CO_3 (1.57 g, 11.4 mmol). The mixture was stirred at room temperature for 1 h, then water (30 mL) was added and extracted with Et_2O (3×30 mL). The combined organic extracts were washed with brine (30 mL), dried over Na_2SO_4 , filtered and solvents removed under reduced pressure. Pure **5_{Benzo}** was obtained as a brown solid without further purification (1.99 g, 62% yield over two steps). Spectral properties are in agreement with those reported in the literature.^[23]

^1H NMR (300 MHz, CDCl_3) δ : 7.59 (ddd, $J_{\text{H,H}} = 7.9, 1.4, 0.4$ Hz, 1H, H_a), 7.53 (dd, $J_{\text{H,H}} = 7.6, 1.9$ Hz, 1H, H_d), 7.27 (td, $J_{\text{H,H}} = 7.6, 1.4$ Hz, 1H, H_c), 7.20 (td, $J_{\text{H,H}} = 7.9, 1.9$ Hz, 1H, H_b), 3.38 (s, 1H, H_e); $^{13}\text{C}\{^1\text{H}\}$ NMR (75 MHz, CDCl_3) δ : 134.2, 132.6, 129.9, 127.2, 125.4, 124.2, 81.8, 81.6.

2.8 Synthesis of 2-bromo-3-((perfluorophenyl)ethynyl)pyridine **6_{Pyr}**



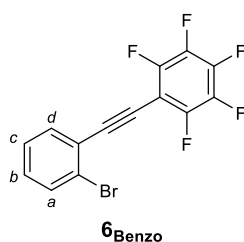
In a Schlenk flask [$\text{Pd}(\text{PPh}_3)_2\text{Cl}_2$] (32 mg, 0.046 mmol) and CuI (18 mg, 0.092 mmol) were added and three vacuum-nitrogen cycles were performed. A mixture of iodopentafluorobenzene (270 mg, 0.12 mL, 0.92 mmol), *i*- Pr_2NH (0.86 mL) and toluene (2 mL) was added and the resulting suspension immediately frozen in liquid N_2 . The mixture was degassed by two *fpt* cycles, then a solution of 2-bromo-3-ethynylpyridine **5_{Pyr}** (200 mg, 1.1 mmol) in toluene (0.9 mL) was added. The resulting reaction mixture was subjected to further two *fpt* cycles and stirred at 80 °C for 3 h, then diluted with CHCl_3 (30 mL) and filtered over celite. The filtrate was washed with a saturated aqueous NH_4Cl solution (30 mL), then the organic phase was dried over Na_2SO_4 , filtered and solvents removed

SUPPORTING INFORMATION

under reduced pressure. The crude was purified by silica gel chromatography (CHCl₃/MeOH 99.9:0.1) to give pure **6_{Pyr}** as an orange solid (125 mg, 40% yield).

mp: 112-114 °C. FTIR (ATR): ν (cm⁻¹): 3065, 2926, 1726, 1645, 1585, 1516, 1497, 1433, 1387, 1269, 1200, 1062, 1038, 986, 962, 802, 775, 660, 567, 540, 469; ¹H NMR (400 MHz, CDCl₃) δ : 8.39 (dd, $J_{H,H} = 4.8, 1.9$ Hz, 1H, H_a), 7.87 (dd, $J_{H,H} = 7.7, 1.9$ Hz, 1H, H_c), 7.32 (dd, $J_{H,H} = 7.7, 4.8$ Hz, 1H, H_b); ¹⁹F NMR (376 MHz, CDCl₃) δ_F : -134.81 (dd, $J_{F,F} = 22.2, 8.1$ Hz, 2F), -150.66 (t, $J_{F,F} = 22.2$ Hz, 1F), -161.00 (m, 2F); ¹³C{¹H} NMR (100 MHz, CDCl₃) δ_C : 149.8, 147.4 (dm, $J_{C,F} = 255$ Hz), 144.4, 142.1 (dm, $J_{C,F} = 259$ Hz), 141.3, 137.3 (dm, $J_{C,F} = 251$ Hz), 122.2, 99.4 (m), 97.2 (m), 80.1 (q, dm, $J_{C,F} = 3.8$ Hz); HRMS (ESI): m/z calcd for C₁₃H₃NF₅Br+H⁺: 347.9447 [$M+H$]⁺; found: 347.9447.

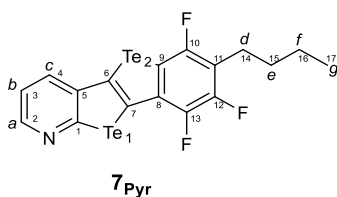
2.9 Synthesis of 1-((2-bromophenyl)ethynyl)-2,3,4,5,6-pentafluorobenzene **6_{Benzo}**



In a Schlenk flask [Pd(PPh₃)₂Cl₂] (53 mg, 0.075 mmol) and CuI (28 mg, 0.151 mmol) were added and three vacuum-nitrogen cycles were performed. A mixture of iodopentafluorobenzene (443 mg, 0.2 mL, 1.51 mmol) and NEt₃ (8 mL) was added and the resulting suspension immediately frozen in liquid N₂. The mixture was degassed by two *fpt* cycles, then a solution of 1-bromo-2-ethynylbenzene **5_{Benzo}** (300 mg, 1.66 mmol) in NEt₃ (3 mL) was added. The resulting reaction mixture was subjected to further two *fpt* cycles and stirred at 40 °C overnight, then diluted with CHCl₃ (30 mL) and filtered over celite. The filtrate was washed with a saturated aqueous NH₄Cl solution (30 mL), then the organic phase was dried over MgSO₄, filtered and the solvents removed under reduced pressure. The crude was purified by silica gel chromatography (petr. ether) to give pure **6_{Benzo}** as a white solid (343 mg, 65% yield).

mp: 88-90 °C. FTIR (ATR): ν (cm⁻¹): 3026, 2953, 1971, 1557, 1518, 1501, 1366, 1260, 1113, 1045, 1026, 986, 964, 756, 658, 563, 476, 449, 436, 419; ¹H NMR (300 MHz, CDCl₃) δ : 7.65 (dd, $J_{H,H} = 7.8, 1.4$ Hz, 1H, H_a), 7.60 (dd, $J_{H,H} = 7.6, 1.7$ Hz, 1H, H_d), 7.34 (td, $J_{H,H} = 7.6, 1.4$ Hz, 1H, H_c), 7.26 (td, $J_{H,H} = 7.6, 1.4$ Hz, 1H, H_b); ¹⁹F NMR (376 MHz, CDCl₃) δ : -135.29 (dd, $J_{F,F} = 23.0, 8.8$ Hz, 2F), -151.99 (t, $J_{F,F} = 23.0$ Hz, 1F), -161.68 (td, $J_{F,F} = 23.0, 8.8$ Hz, 2F); ¹³C{¹H} NMR (125 MHz, CDCl₃) δ : 147.4 (dm, $J_{C,F} = 254$ Hz), 141.8 (dm, $J_{C,F} = 258$ Hz), 137.9 (dm, $J_{C,F} = 251$ Hz), 133.8, 132.8, 130.9, 121.9, 125.7, 124.0, 100.1 (m), 100.0 (m); HRMS (ASAP): m/z calcd for [C₁₄H₄F₅⁷⁹Br+H]⁺: 346.9495 [$M+H$]⁺; found: 346.9490.

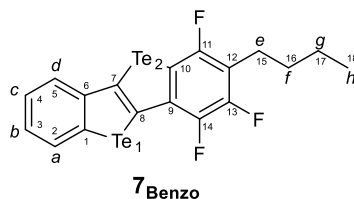
SUPPORTING INFORMATION

2.10 Synthesis of 7-butyl-6,8,9-trifluorobenzo[4',5']telluropheno[2',3':4,5]telluropheno[2,3-β]pyridine **7_{Pyr}**

To a diluted solution of *i*-PrMgCl (2 M in THF, 0.22 mL, 0.43 mmol) in dry and degassed THF (0.73 mL) under anhydrous condition, *n*-BuLi (1.6 M in hexane, 0.54 mL, 0.86 mmol) was added dropwise at 0 °C. The mixture was stirred at the same temperature for 10 minutes, then a solution of 2-bromo-3-((perfluorophenyl)ethynyl)pyridine **6_{Pyr}** (125 mg, 0.36 mmol) in dry and degassed THF (0.73 mL) was added dropwise at 0 °C. The mixture was stirred at the same temperature for 1 h, then freshly grounded elemental tellurium powder (129 mg, 1.01 mmol) was added in once while a brisk flux of nitrogen was passed through the flask. The reaction was slowly allowed to warm up to room temperature and stirred for 3 h, then degassed EtOH (0.73 mL) was added. The mixture was stirred at room temperature overnight, then poured in cold water (20 mL) and extracted with Et₂O (5 × 30 mL). The combined organic extracts were washed with brine (20 mL), dried over Na₂SO₄, filtered and solvents removed under reduced pressure. The crude was purified by silica gel chromatography (CHCl₃/MeOH 99.8:0.2) to give pure **7_{Pyr}** as a yellow solid (195 mg, 36% yield).

mp: 128-130 °C; FTIR (ATR): ν (cm⁻¹): 3526, 3146, 2990, 2955, 1634, 1537, 1477, 1435, 1435, 1389, 1364, 1287, 1202, 1173, 1142, 1051, 962, 914, 802, 785, 721, 583, 482, 436; ¹H NMR (600 MHz, C₆D₆) δ : 8.32 (dd, $J_{H,H} = 4.6, 1.6$ Hz, 1H, H_a), 6.95 (dd, $J_{H,H} = 7.8, 1.6$ Hz, 1H, H_c), 6.62 (dd, $J_{H,H} = 7.8, 4.6$ Hz, 1H, H_b), 2.56 (m, 2H, H_d), 1.49 (m, 2H, H_e), 1.22 (m, 2H, H_f), 0.82 (t, $J_{H,H} = 7.4$ Hz, 3H, H_g); ¹⁹F NMR (659 MHz, C₆D₆) δ : -106.25 (dd, $J_{F,F} = 16.8, 3.6$ Hz, 1F), -142.13 (dd, $J_{F,F} = 20.0, 16.6$ Hz, 1F), -142.29 (dd, $J_{F,F} = 20.0, 3.6$ Hz, 1F); ¹³C{¹H} NMR (150 MHz, CDCl₃) δ : 161.6 (d, $J_{C,F} = 10.5$ Hz, C₁), 157.2 (ddd, $J_{C,F} = 235.2, 7.9, 3.0$ Hz, C₁₂), 148.2 (dm, $J_{C,F} = 230.8$ Hz, C₁₀), 146.8 (C₃), 145.0 (ddd, $J_{C,F} = 252.4, 16.8, 3.1$ Hz, C₁₃), 142.1 (C₅), 136.1 (ddd, $J_{C,F} = 238.3, 7.9, 3.1$ Hz, C₈), 133.1 (C₄), 126.8 (C₆), 125.0 (t, $J_{C,F} = 4.1$ Hz, C₇), 120.6, 116.5 (dd, $J_{C,F} = 24.0, 18.7$ Hz, C₁₁), 110.8 (d, $J_{C,F} = 35.9$ Hz, C₉), 31.8 (C₁₄), 23.1 (C₁₅), 22.6 (C₁₆), 13.9 (C₁₇); ¹²⁵Te NMR (190 MHz, C₆D₆) δ : 901.6 (d, ⁴*TS* $J_{Te,F} = 290.4$ Hz, Te₁), 837.1 (d, ³ $J_{Te,F} = 26.5$ Hz, Te₂). HRMS (LD): m/z calcd for C₁₇H₁₂F₃NTe₂⁺: 546.9042 [*M*]⁺; found: 546.9044. Elemental Microanalysis: expected C = 38.89, H = 2.38, N = 2.60, S < 0.02; found: C = 38.24, H = 2.38, N = 2.58, S < 0.02. Crystal suitable for X-Ray diffraction was obtained by slow evaporation of solvent from a CHCl₃ solution (CCDC #2057472 – see page S31).

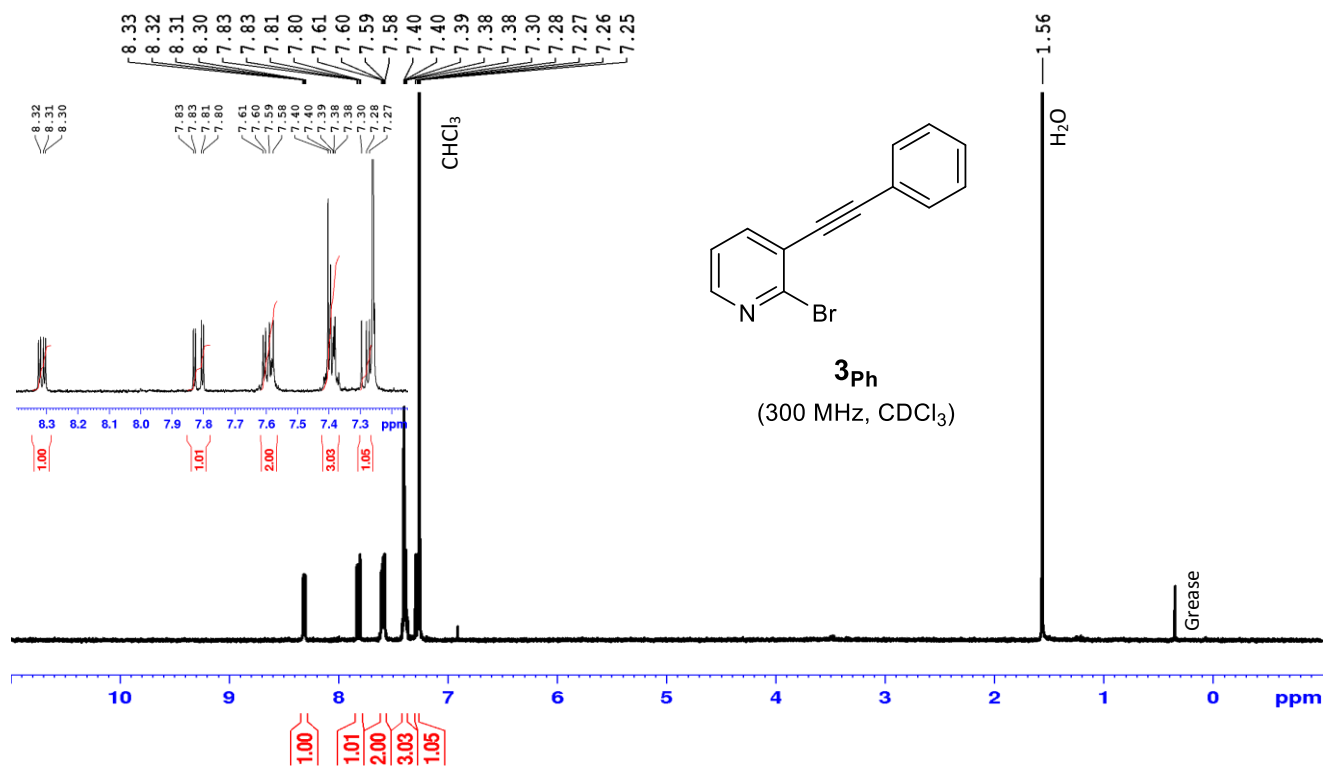
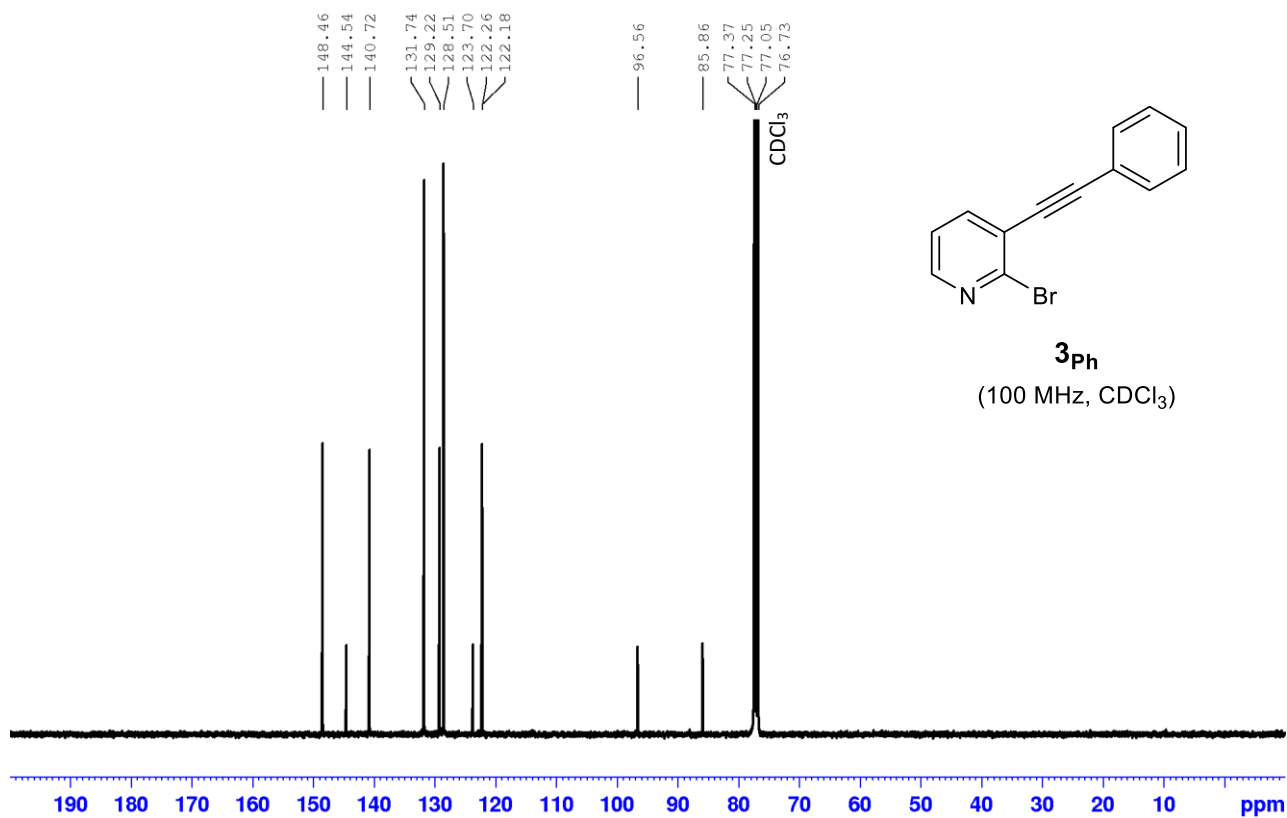
SUPPORTING INFORMATION

2.11 Synthesis of 2-butyl-1,3,4-trifluorobenzo[b]benzo[4,5]telluropheno[2,3-d]tellurophene **7**_{Benzo}

To a diluted solution of *i*-PrMgCl (2 M in THF, 1.3 mL, 2.59 mmol) in dry and degassed THF (4.4 mL) under anhydrous condition, *n*-BuLi (2.5 M in hexane, 2.1 mL, 5.18 mmol) was added dropwise at 0 °C. The mixture was stirred at the same temperature for 10 minutes, then a solution of 1-((2-bromophenyl)ethynyl)-2,3,4,5,6-pentafluorobenzene **6**_{Benzo} (900 mg, 2.59 mmol) in dry and degassed THF (4.4 mL) was added dropwise at 0 °C. The mixture was stirred at the same temperature for 1 h, then freshly grounded elemental tellurium powder (991 mg, 7.77 mmol) was added in once while a brisk flux of nitrogen was passed through the flask. The reaction was slowly allowed to warm up at room temperature and stirred for 3 h, then degassed EtOH (4.4 mL) was added. The mixture was stirred at room temperature overnight, then poured in cold water (40 mL) and extracted with Et₂O (3 × 50 mL). The combined organic extracts were washed with brine (50 mL), dried over MgSO₄, filtered and solvents removed under reduced pressure. The crude was purified by trituration from petr. ether to give pure **7**_{Benzo} as a yellow solid (547 mg, 39% yield).

mp: 100-102 °C. FTIR (ATR): ν (cm⁻¹): 2957, 2930, 2868, 1632, 1483, 1452, 1435, 1344, 1246, 1231, 1146, 1115, 1034, 970, 928, 806, 795, 750, 743, 706, 646, 621, 581, 552, 463, 438; ¹H NMR (700 MHz, C₆D₆) δ : 7.46 (d, $J_{H,H} = 6.7$ Hz, 1H, H_a), 7.20 (d, $J_{H,H} = 7.2$ Hz, 1H, H_d), 7.05 (t, $J_{H,H} = 6.7$ Hz, 1H, H_b), 6.86 (t, $J_{H,H} = 7.2$ Hz, 1H, H_c), 2.56 (m, 2H, H_e), 1.49 (m, 2H, H_f), 1.23 (m, 2H, H_g), 0.83 (t, $J_{H,H} = 7.0$ Hz, 3H, H_h); ¹⁹F NMR (659 MHz, C₆D₆) δ : -106.75 (d, $J_{F,F} = 16.5$ Hz, 1F), -142.71 (dd, $J_{F,F} = 18.9, 4.6$ Hz, 1F), -144.00 (dd, $J_{F,F} = 18.9, 16.5$ Hz, 1F); ¹³C{¹H} NMR (175 MHz, C₆D₆) δ : 157.1 (ddd, $J_{C,F} = 237.9, 8.0, 2.8$ Hz, C₁₃), 148.1 (ddd, $J_{C,F} = 243.7, 13.2, 8.0$ Hz, C₁₁), 146.3 (C₆), 144.8 (ddd, $J_{C,F} = 249.1, 15.0, 3.0$ Hz, C₁₄), 135.7 (dd, $J_{C,F} = 12.3, 10.1$ Hz, C₉), 133.6 (C₁), 132.8 (C₂), 132.1 (C₇), 128.2 (C₅), 126.4 (C₄), 125.4 (C₃), 122.1 (t, $J_{C,F} = 4.0$ Hz, C₈), 116.1 (dd, $J_{C,F} = 24.0, 19.1$ Hz, C₁₂), 110.4 (d, $J_{C,F} = 36.3$ Hz, C₁₀), 31.9 (C₁₅), 23.1 (C₁₆), 22.7 (C₁₇), 13.9 (C₁₈); ¹²⁵Te NMR (190 MHz, C₆D₆) δ : 881.6 (d, $^{47S}J_{Te,F} = 290.4$ Hz), 818.5 (d, $^3J_{Te,F} = 26.2$ Hz). HRMS (LD): m/z calcd for C₁₈H₁₃F₃Te₂⁺: 545.9088 [M]⁺; found: 545.9084. Elemental Microanalysis: expected C = 39.79, H = 2.45, N < 0.05, S < 0.02; found: C = 39.86, H = 2.50, N < 0.05, S < 0.02. Crystal suitable for X-Ray diffraction was obtained by slow evaporation of solvent from a petr. ether solution (CCDC #2057473 – see page S32).

SUPPORTING INFORMATION

3. NMR-HRMS Spectroscopic characterization (^1H , ^{13}C , ^{19}F , ^{125}Te , HRMS)3.1 Characterization of 3_{Ph} Figure S1: 300 MHz ^1H NMR in CDCl_3 of molecule 3_{Ph} .Figure S2: 100 MHz $^{13}\text{C}\{^1\text{H}\}$ NMR in CDCl_3 of molecule 3_{Ph} .

SUPPORTING INFORMATION

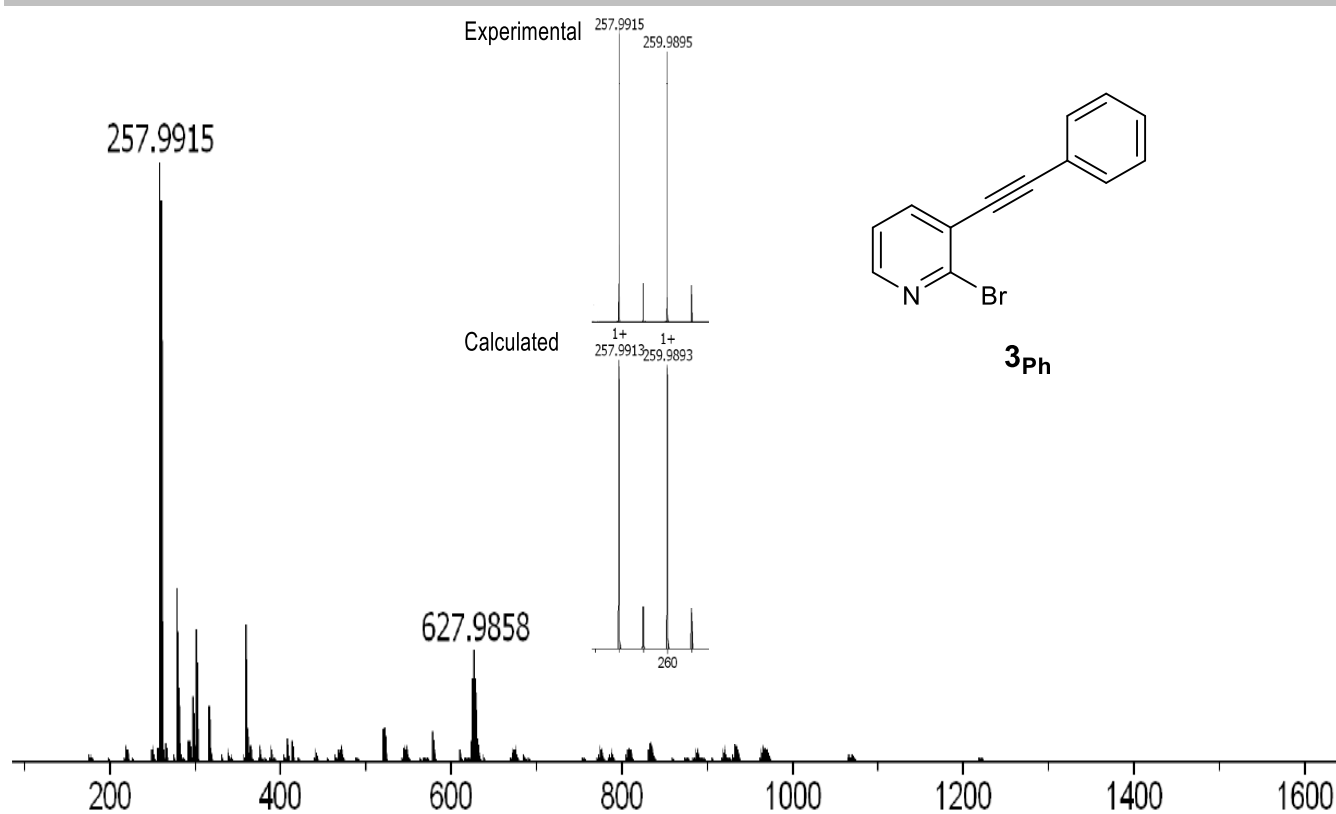


Figure S3: HRMS-ESI mass spectrum of molecule **3_{Ph}** in the positive ion mode.

3.2 Characterization of **4_{TMS}**

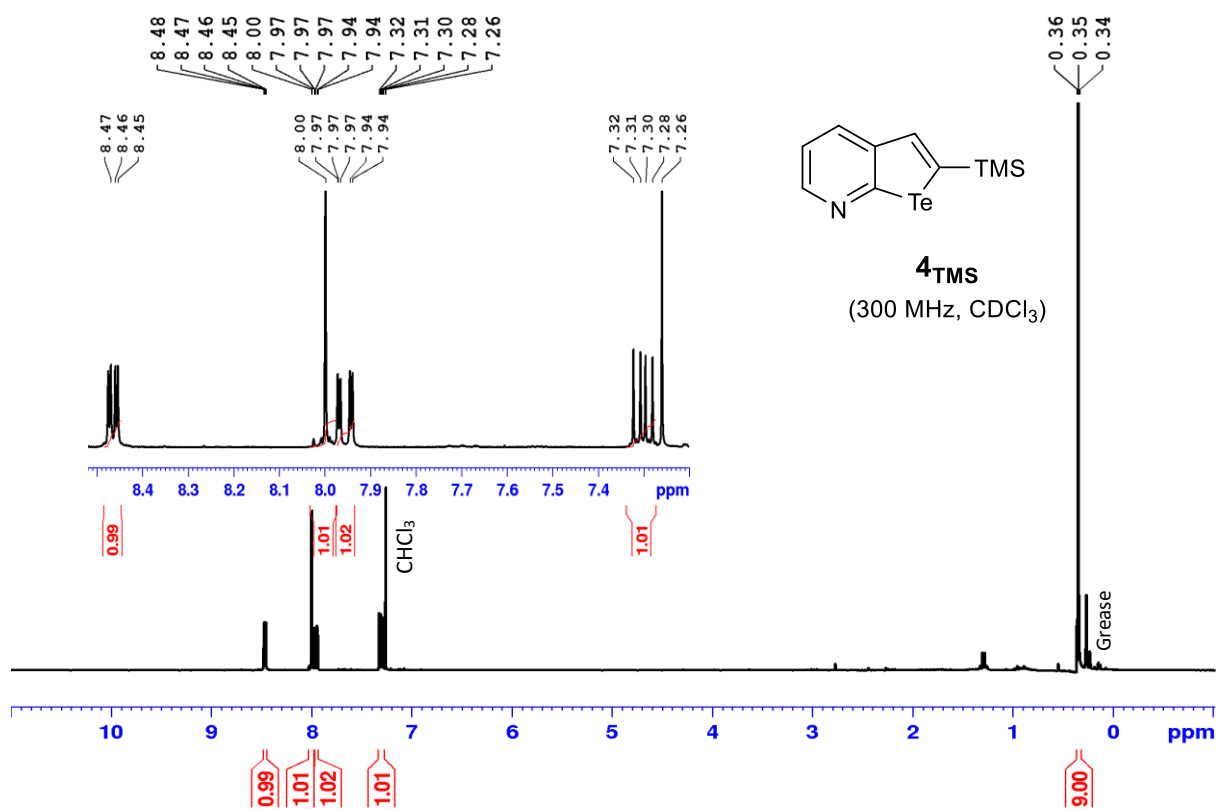
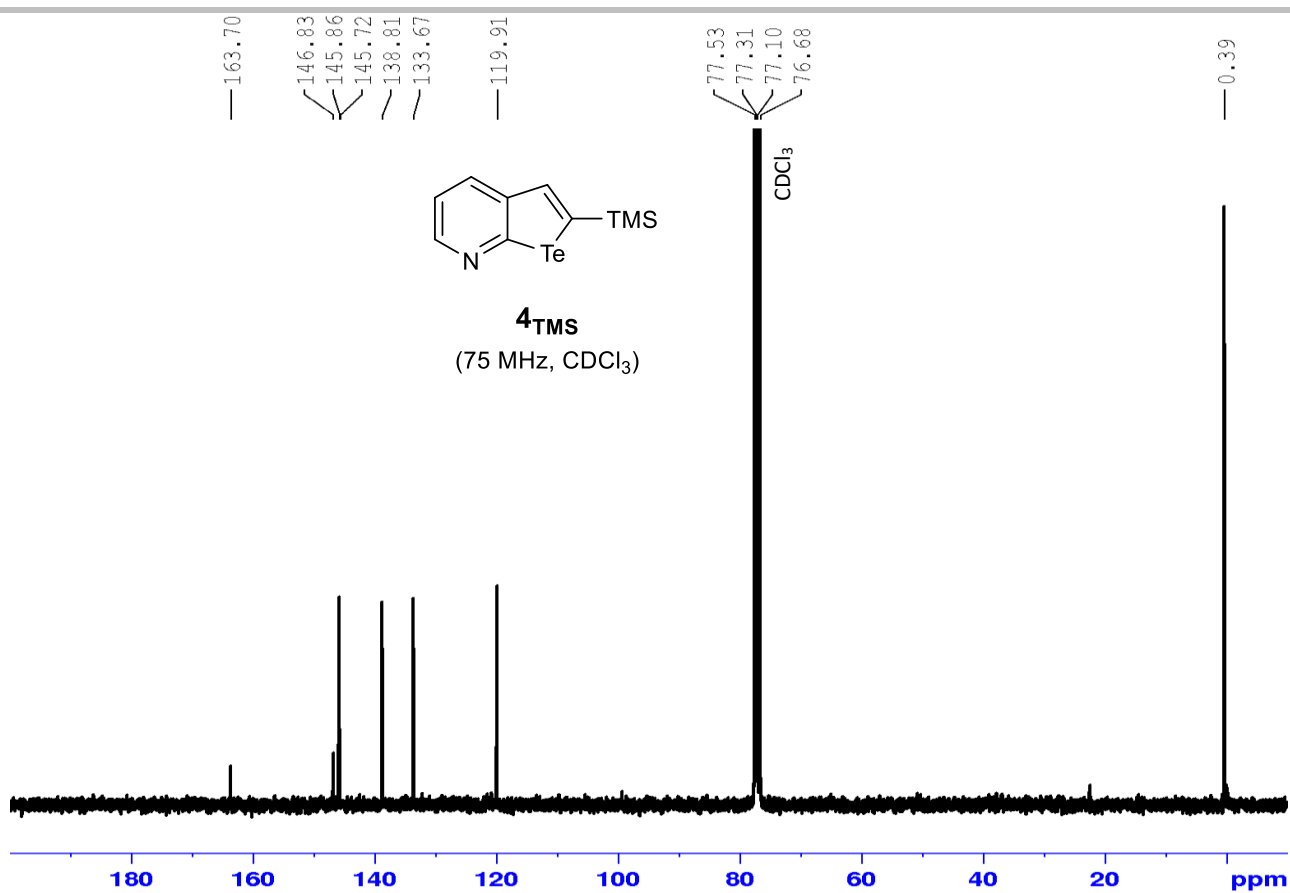
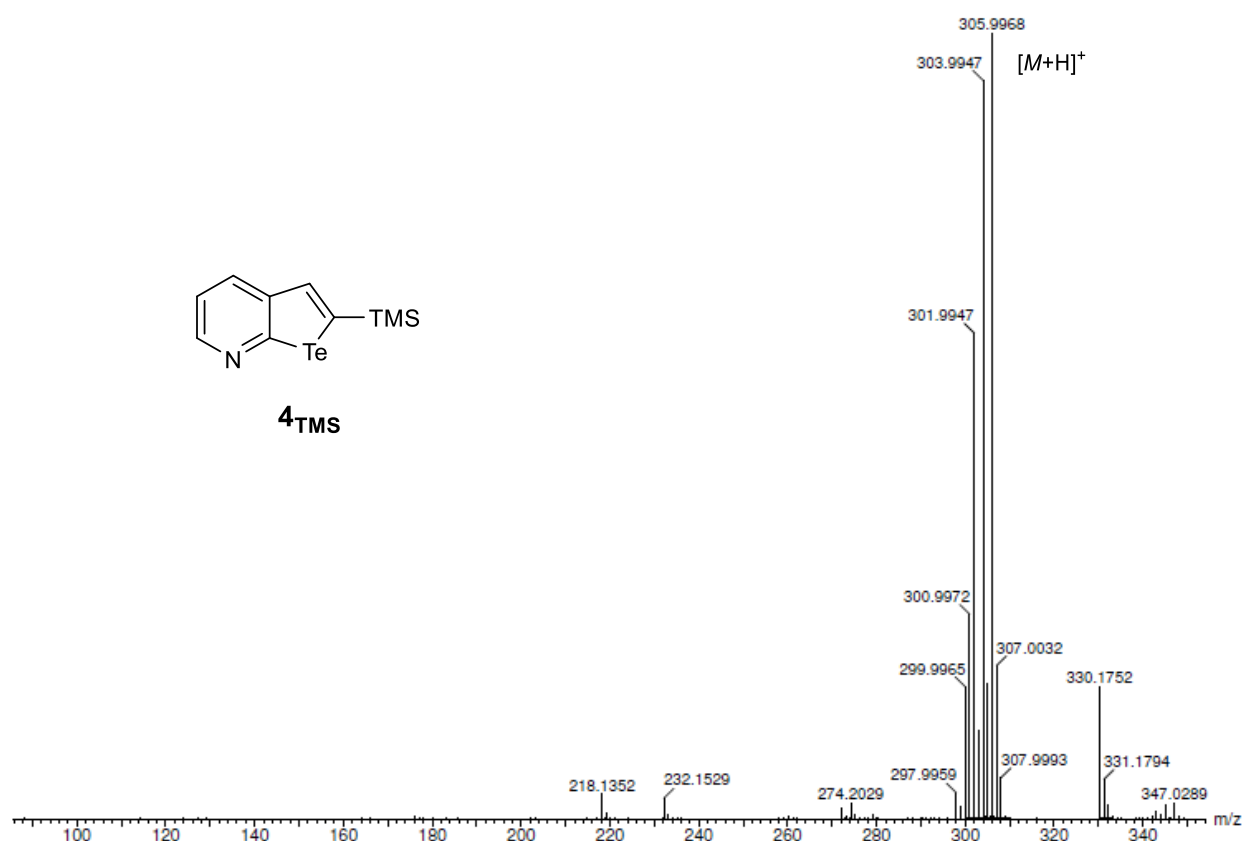
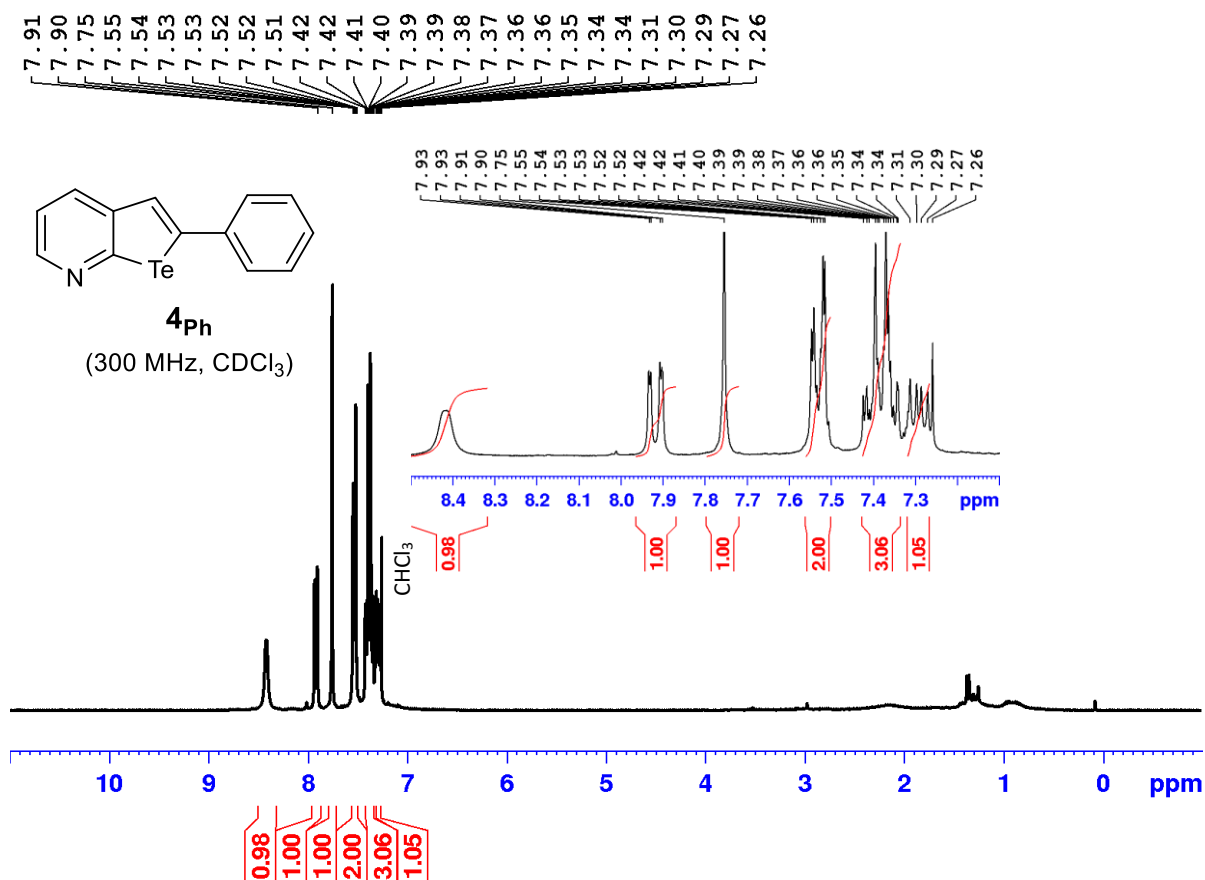
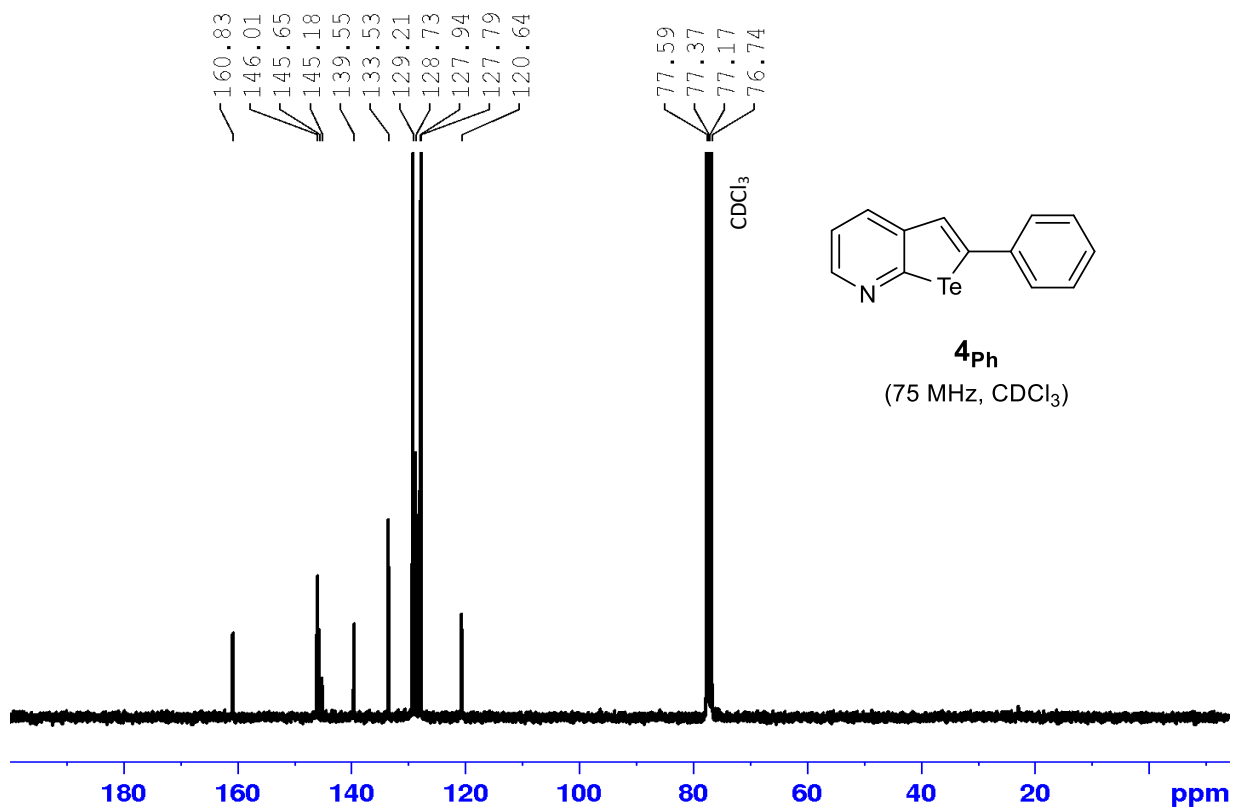


Figure S4: 300 MHz ¹H NMR in CDCl₃ of molecule **4_{TMS}**.

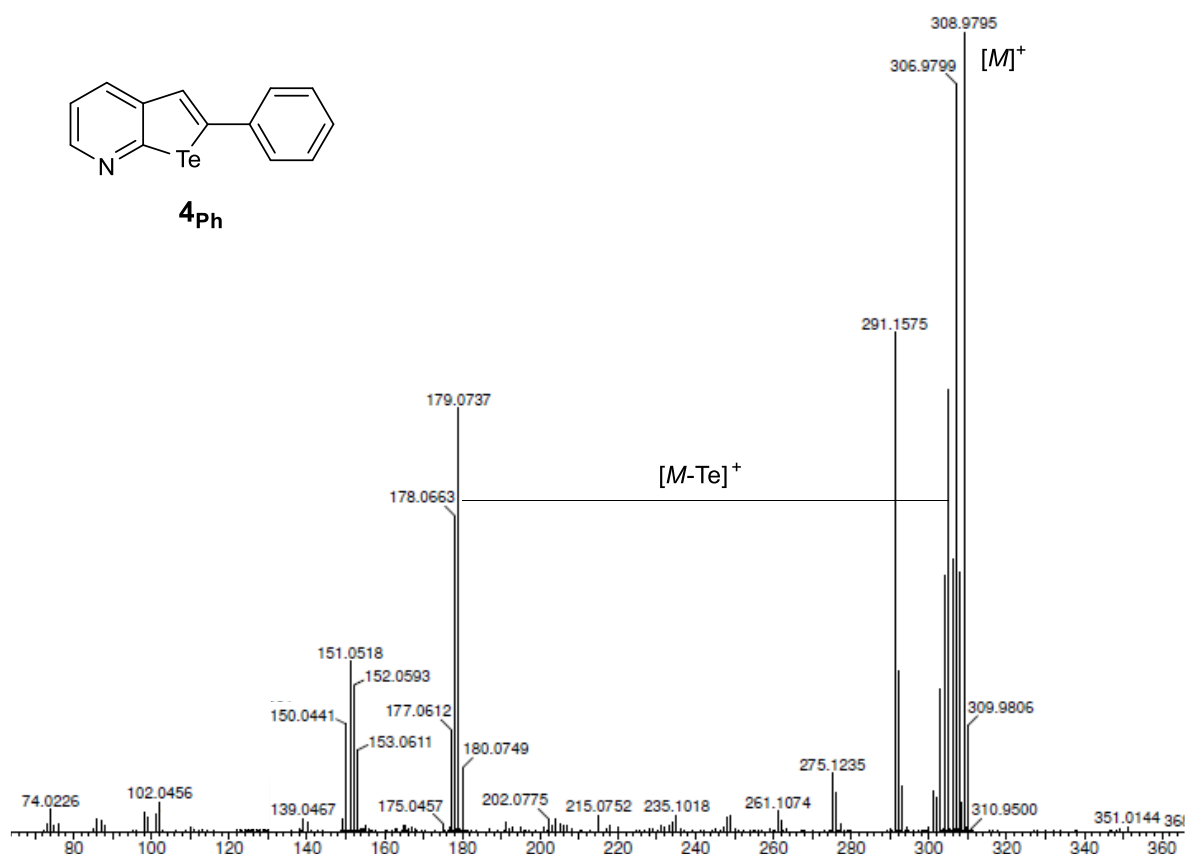
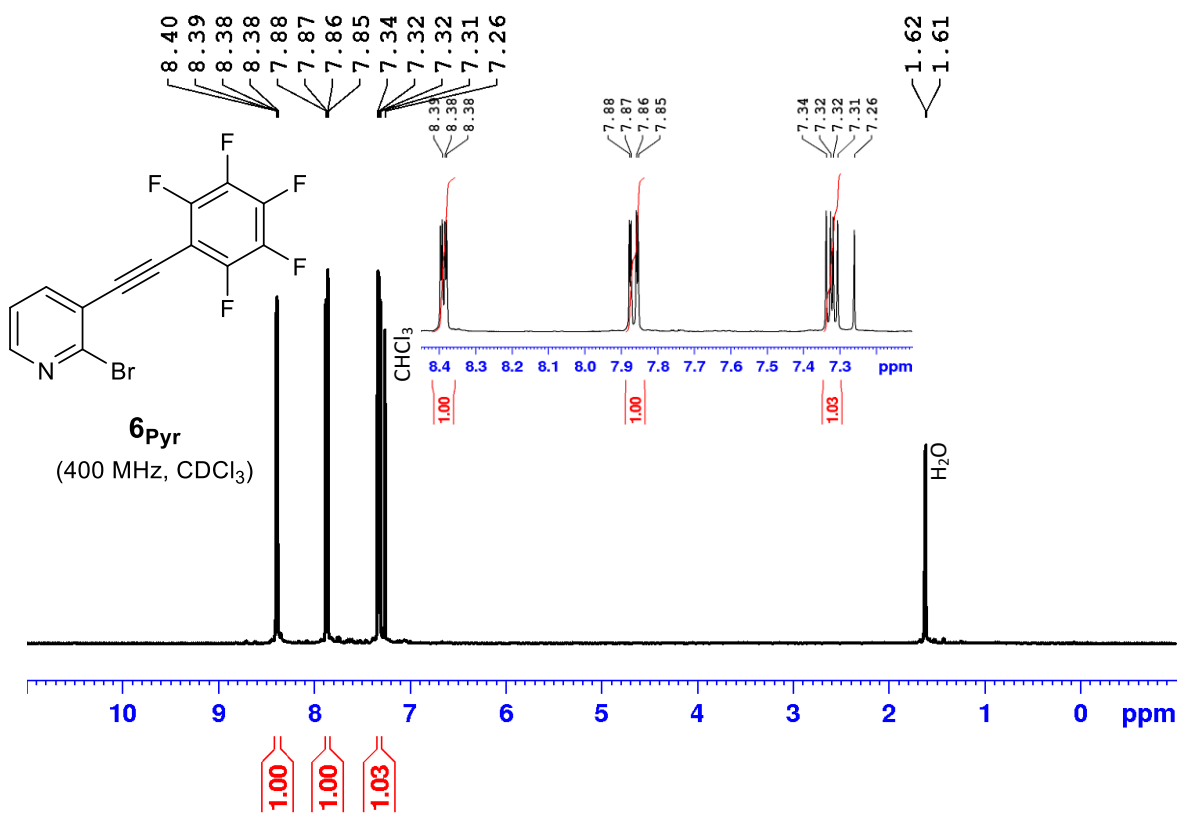
SUPPORTING INFORMATION

Figure S5: 75 MHz ¹³C{¹H} NMR in CDCl₃ of molecule **4_{TMS}**.Figure S6: HRMS-ESI mass spectrum of molecule **4_{TMS}** in the positive ion mode.

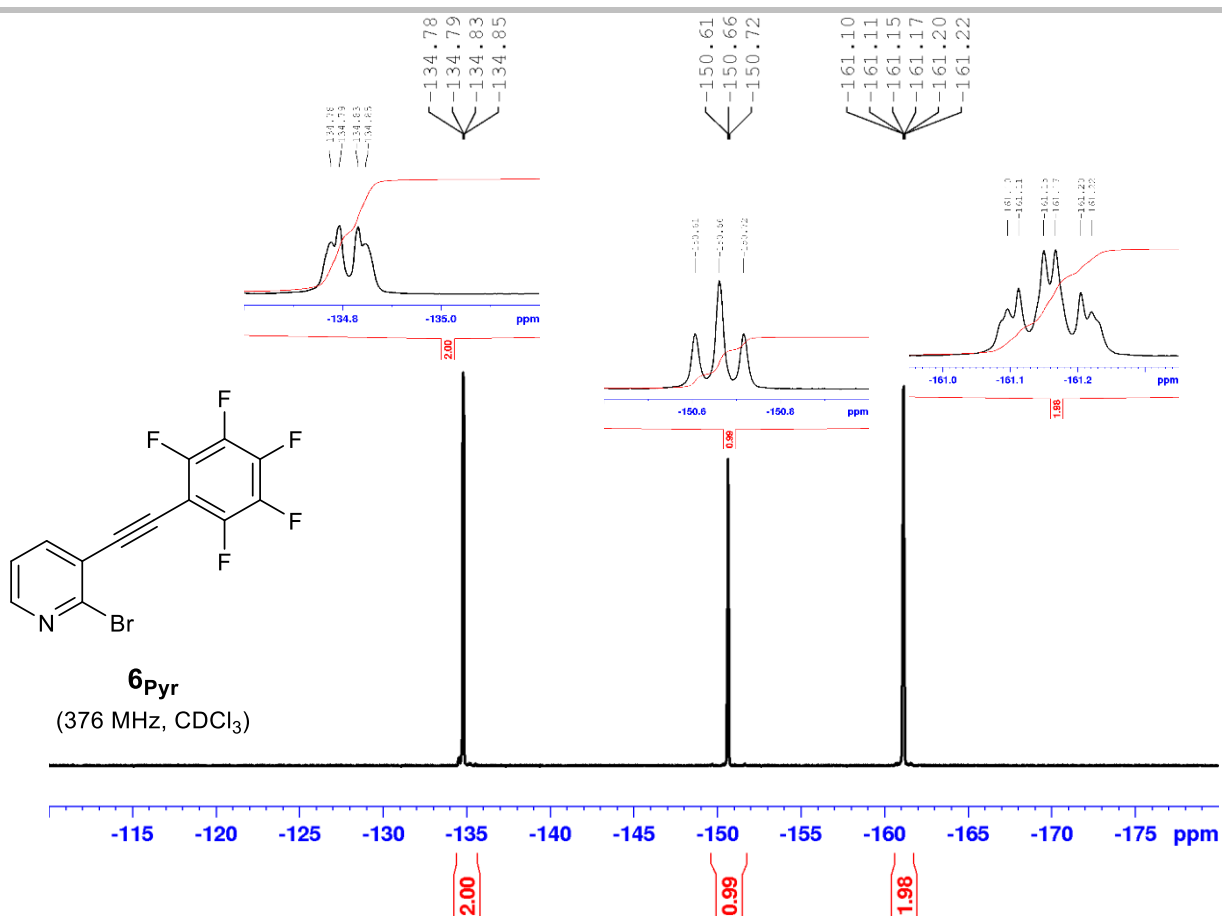
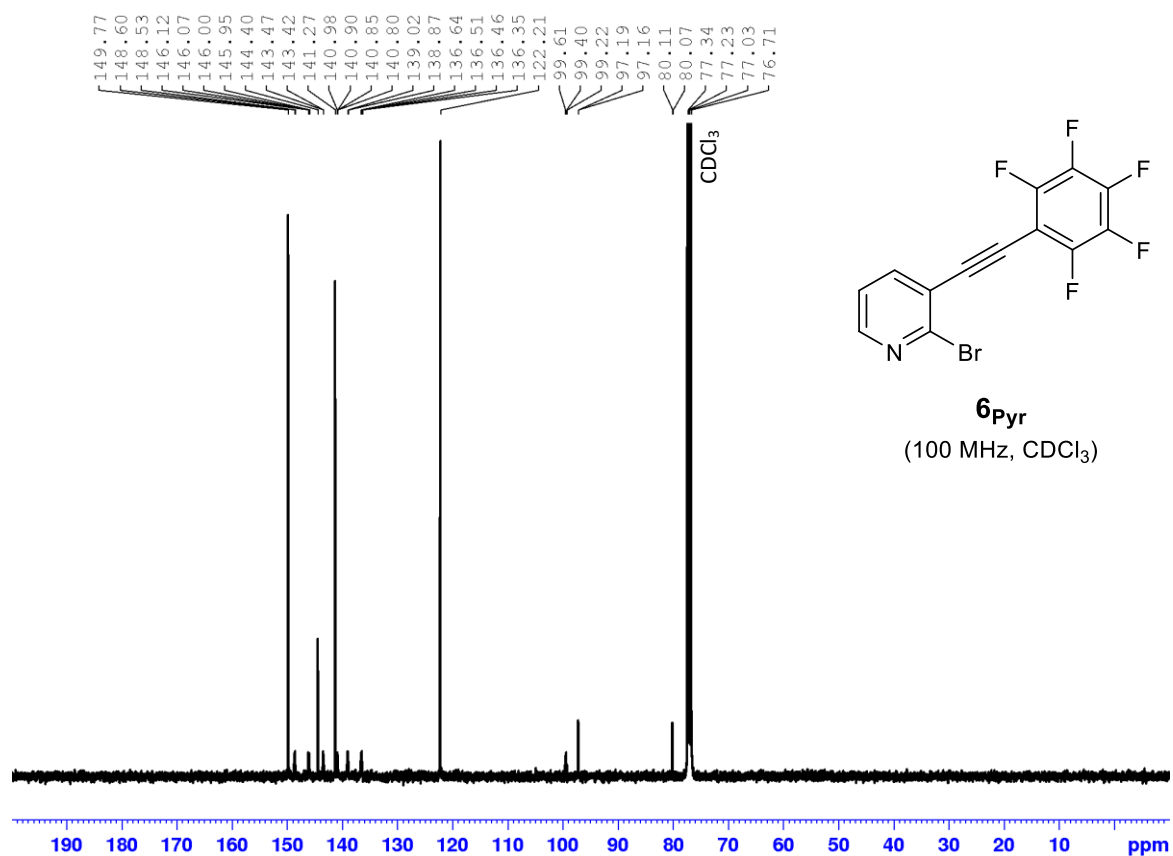
SUPPORTING INFORMATION

3.3 Characterization of 4_{Ph}Figure S7: 300 MHz ¹H NMR in CDCl₃ of molecule 4_{Ph}.Figure S8: 75 MHz ¹³C{¹H} NMR in CDCl₃ of molecule 4_{Ph}.

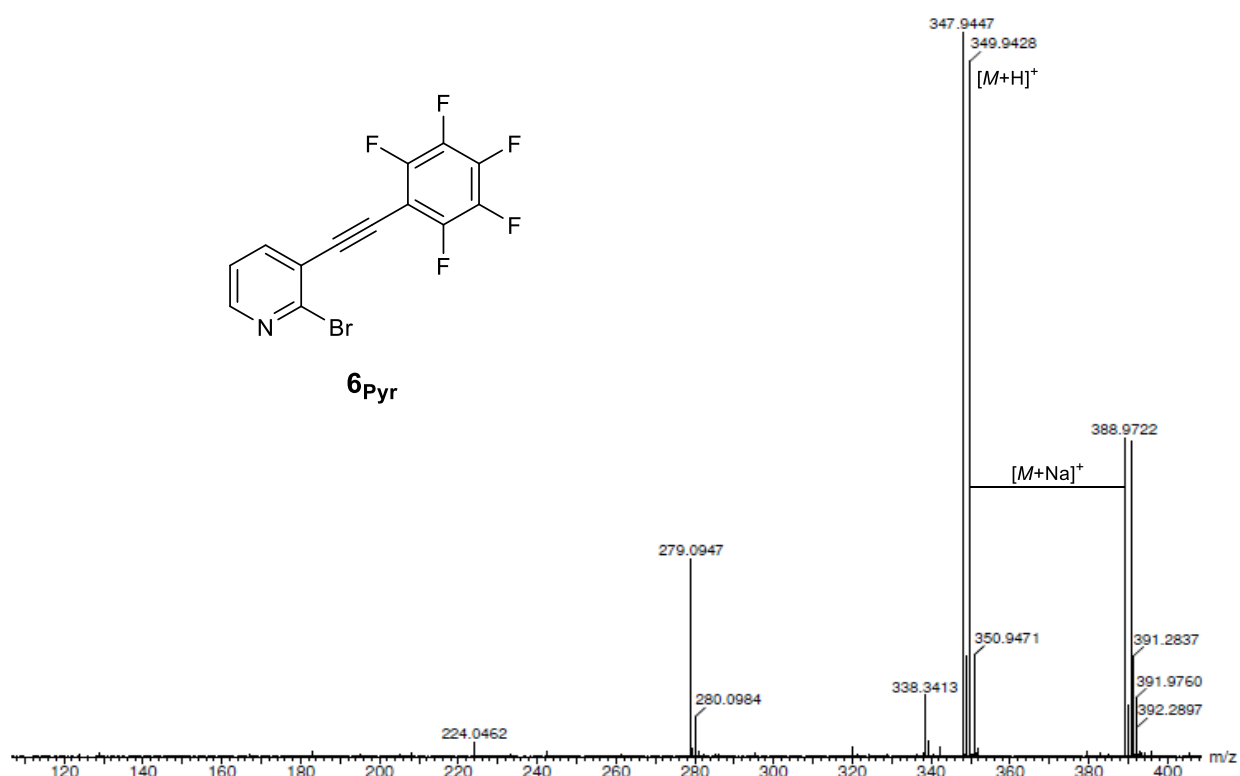
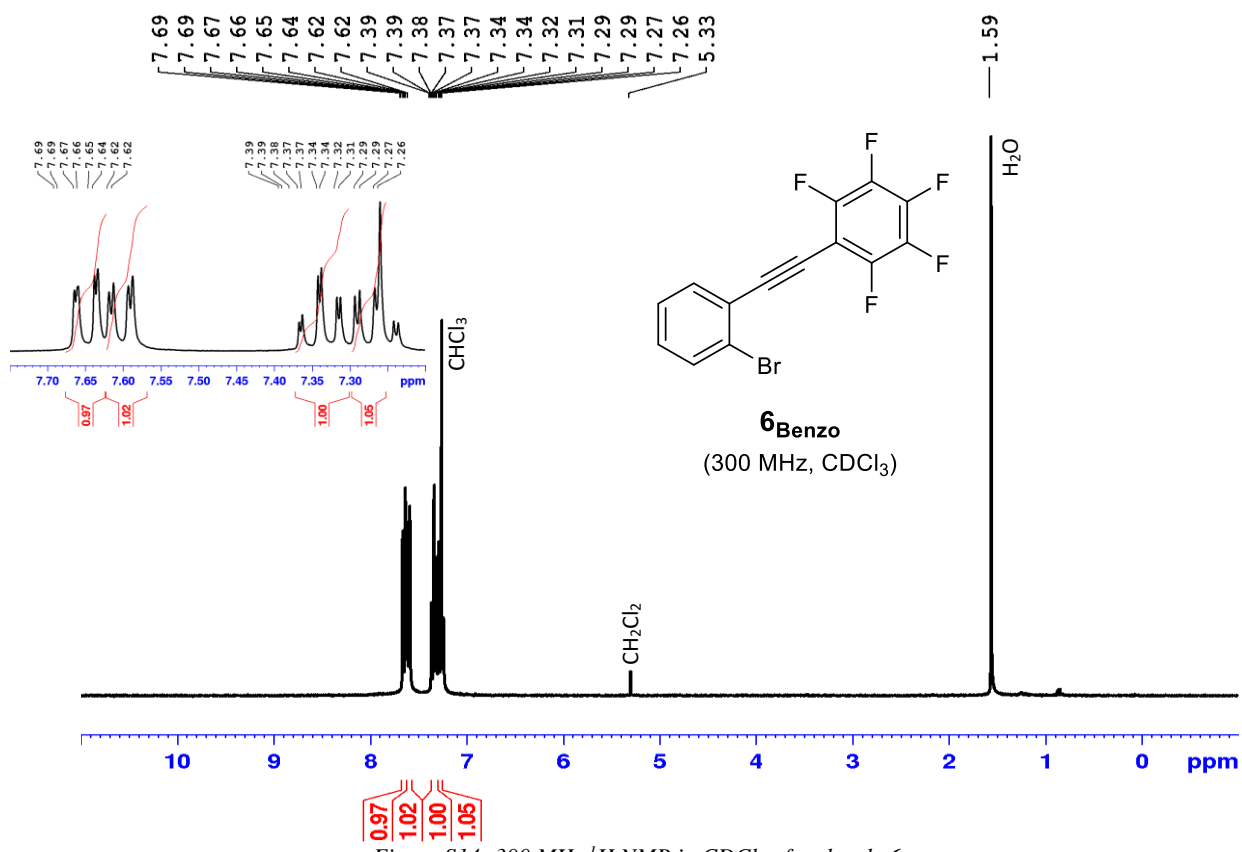
SUPPORTING INFORMATION

3.4 Characterization of **6Pyr**

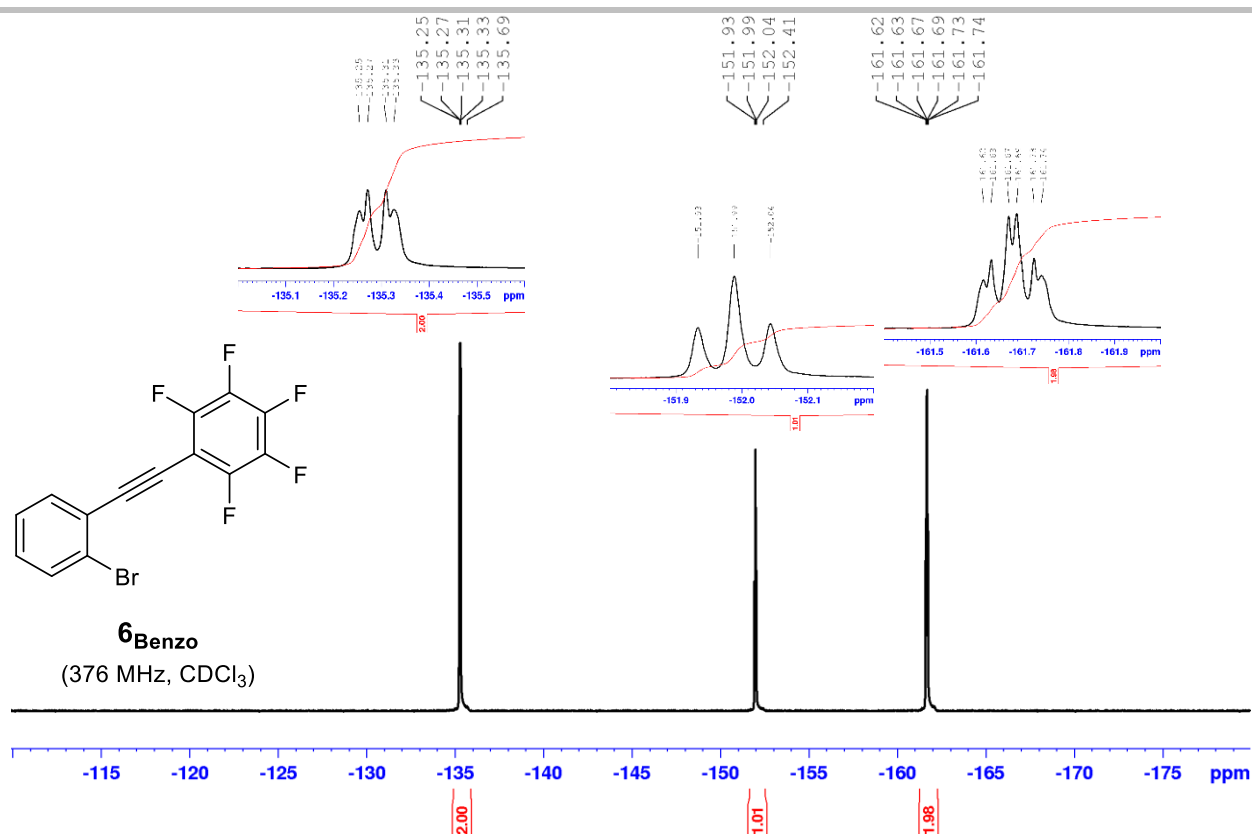
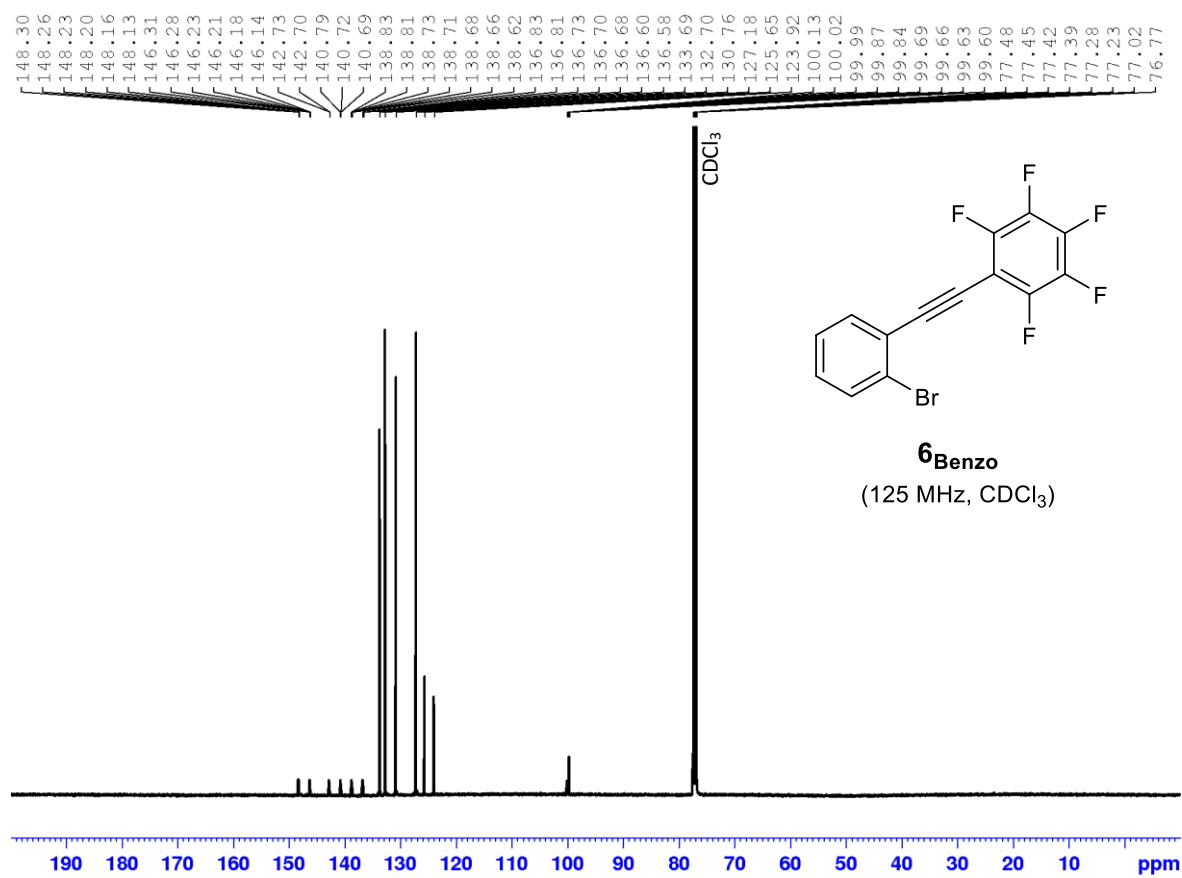
SUPPORTING INFORMATION

Figure S11: 376 MHz ^{19}F NMR in CDCl_3 of molecule **6Pyr**.Figure S12: 100 MHz $^{13}\text{C}\{^1\text{H}\}$ NMR in CDCl_3 of molecule **6Pyr**.

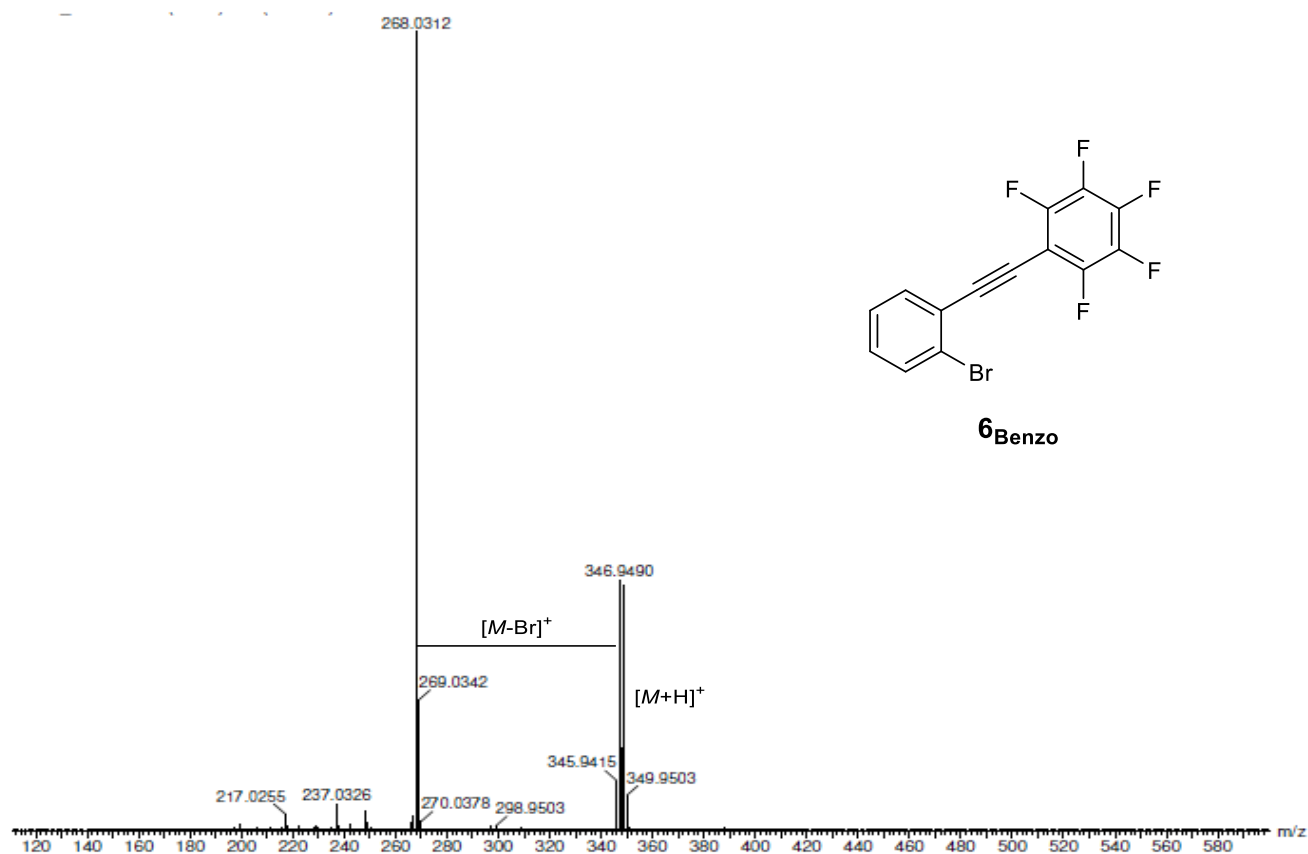
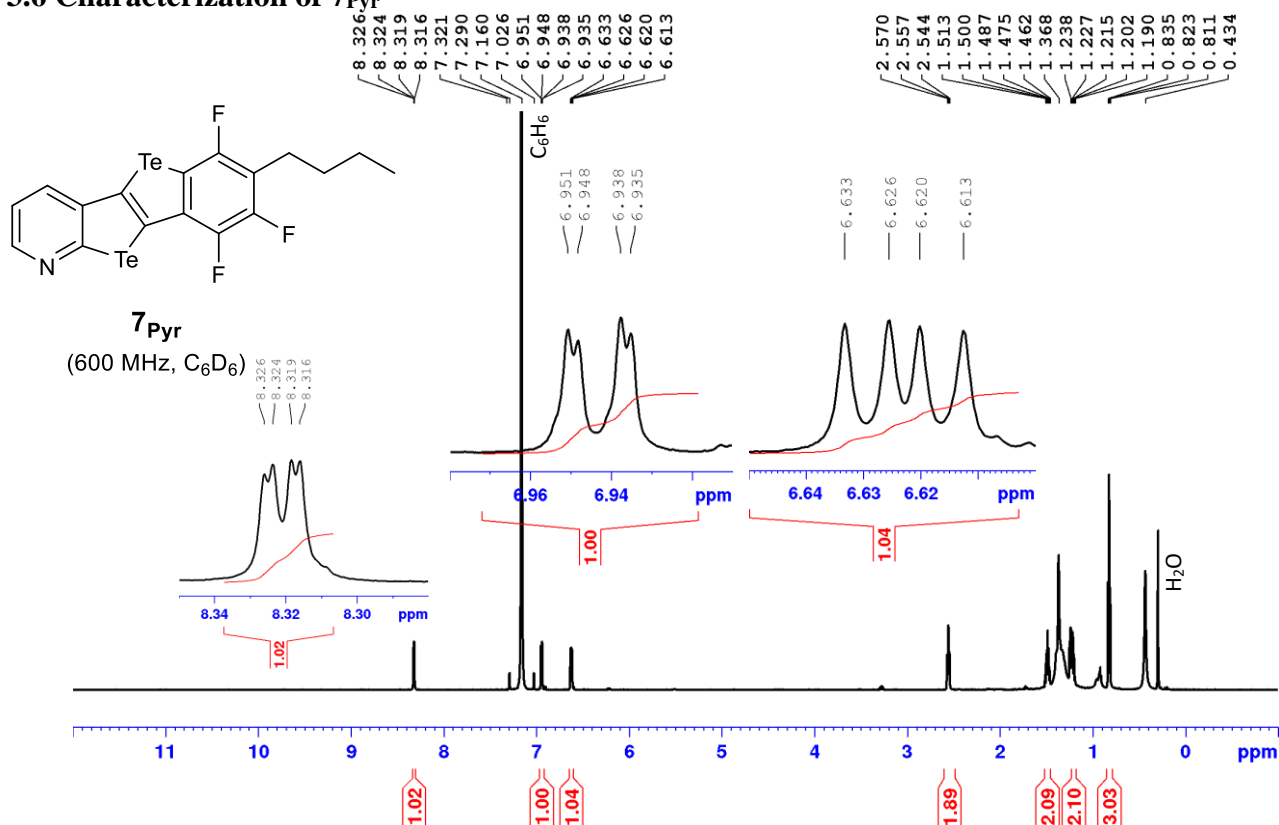
SUPPORTING INFORMATION

3.5 Characterization of **6_{Benzo}**

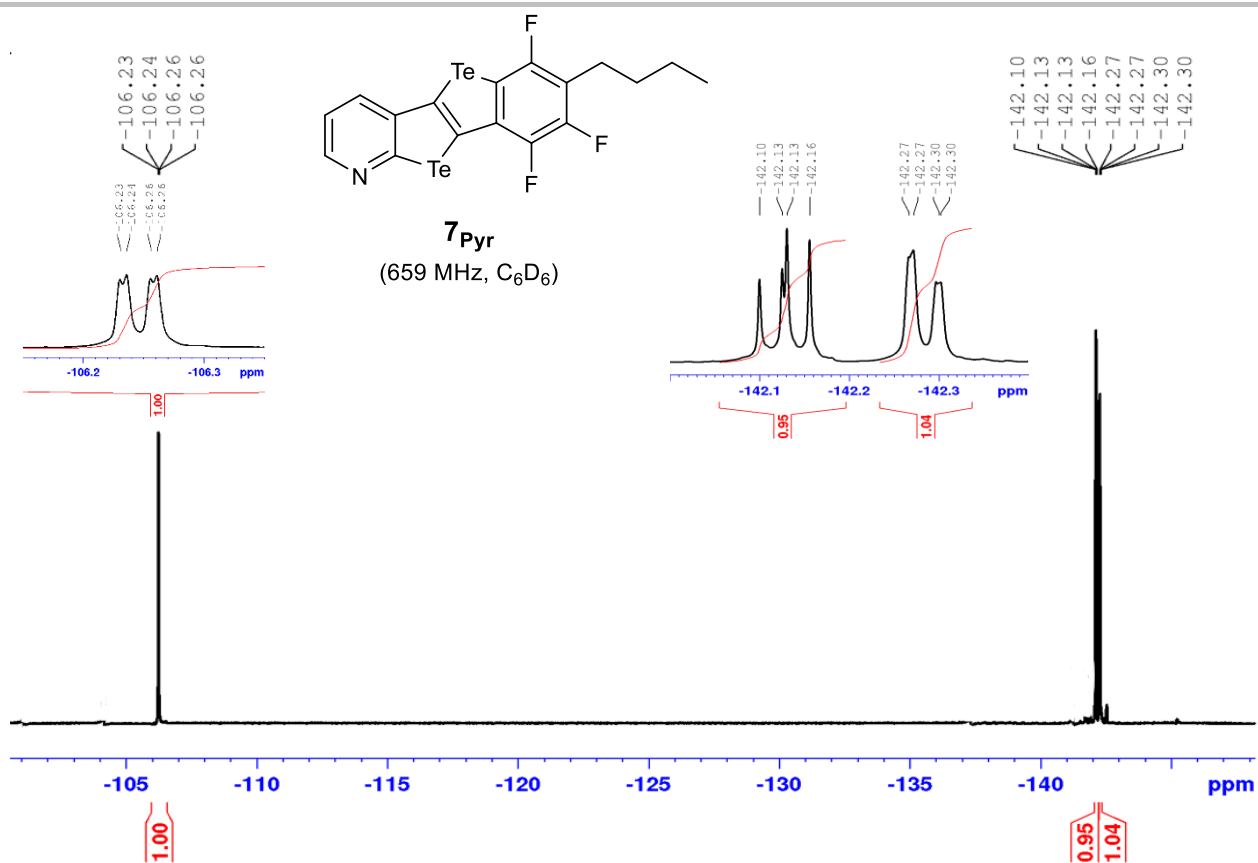
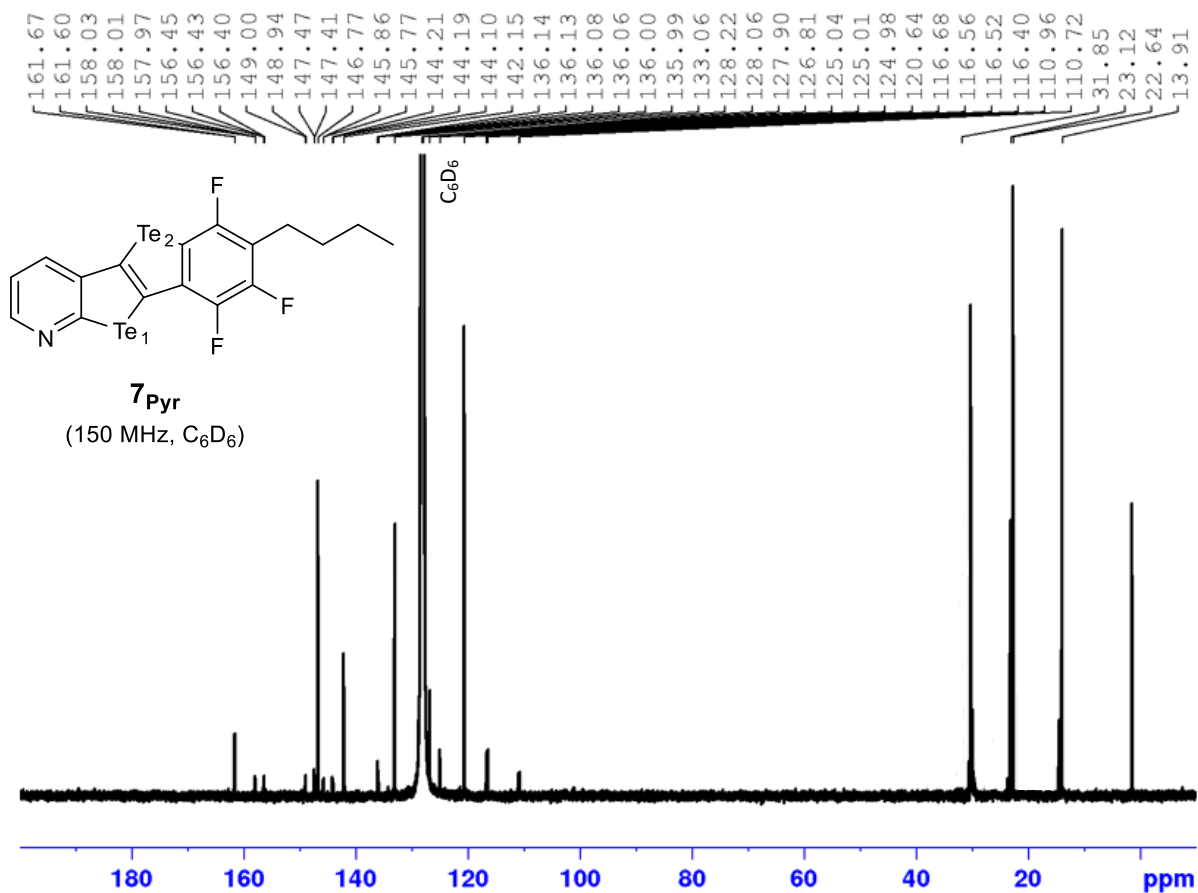
SUPPORTING INFORMATION

Figure S15: 376 MHz ^{19}F NMR in CDCl_3 of molecule **6Benzo**.Figure S16: 125 MHz $^{13}\text{C}\{^1\text{H}\}$ NMR in CDCl_3 of molecule **6Benzo**.

SUPPORTING INFORMATION

3.6 Characterization of **7Pyr**

SUPPORTING INFORMATION

Figure S19: 659 MHz ¹⁹F NMR in C₆D₆ of molecule **7Pyr**.Figure S20: 150 MHz ¹³C{¹H} NMR in C₆D₆ of molecule **7Pyr**.

SUPPORTING INFORMATION

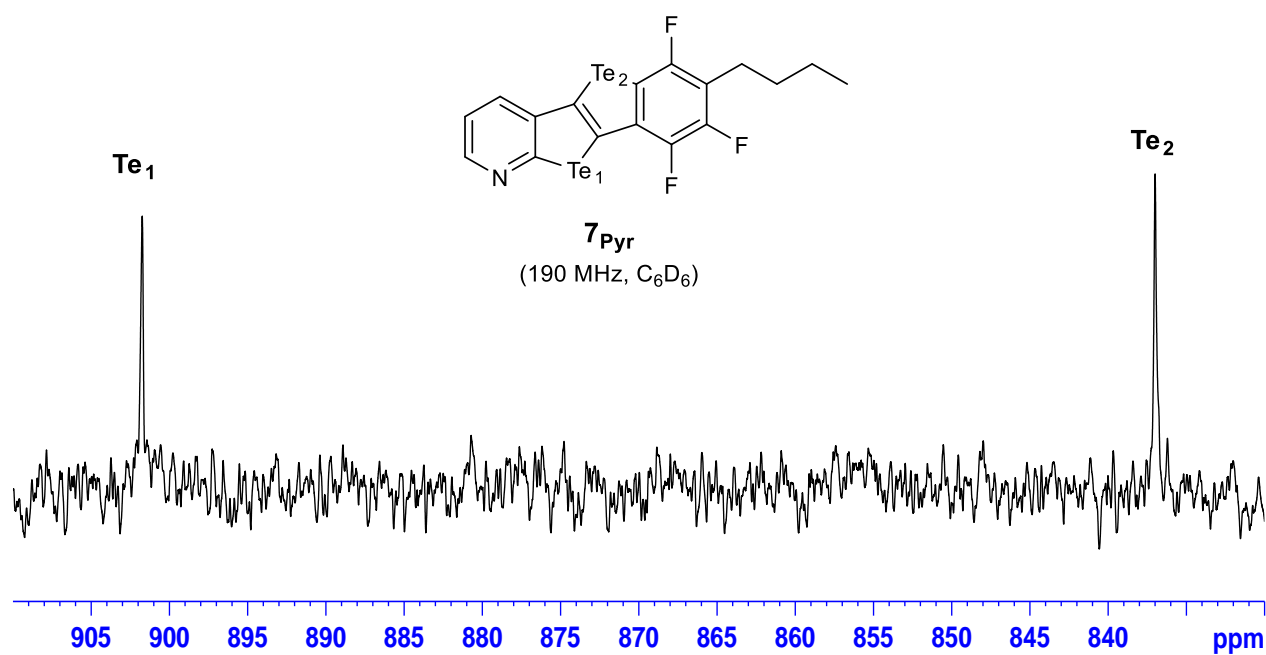


Figure S21: 190 MHz $^{125}\text{Te}\{^{19}\text{F}\}$ NMR in C₆D₆ of molecule **7_{Pyr}**.

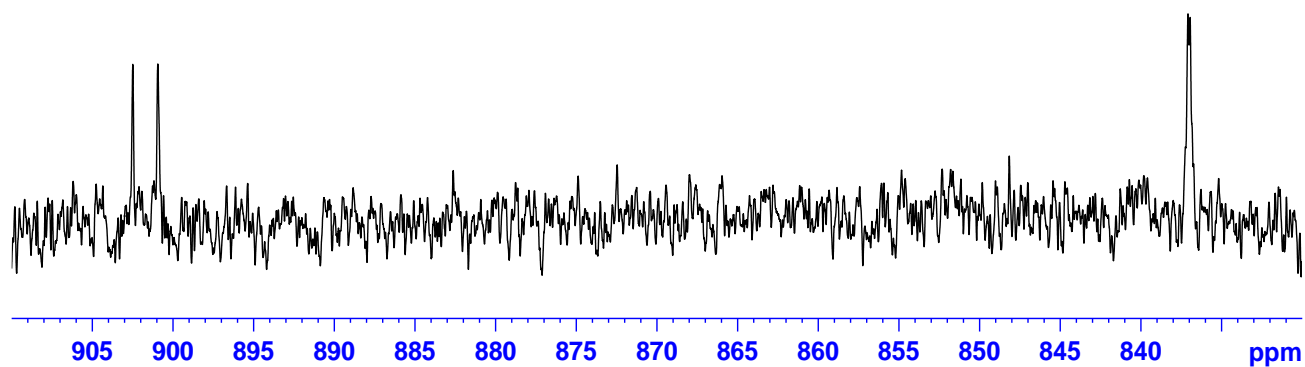
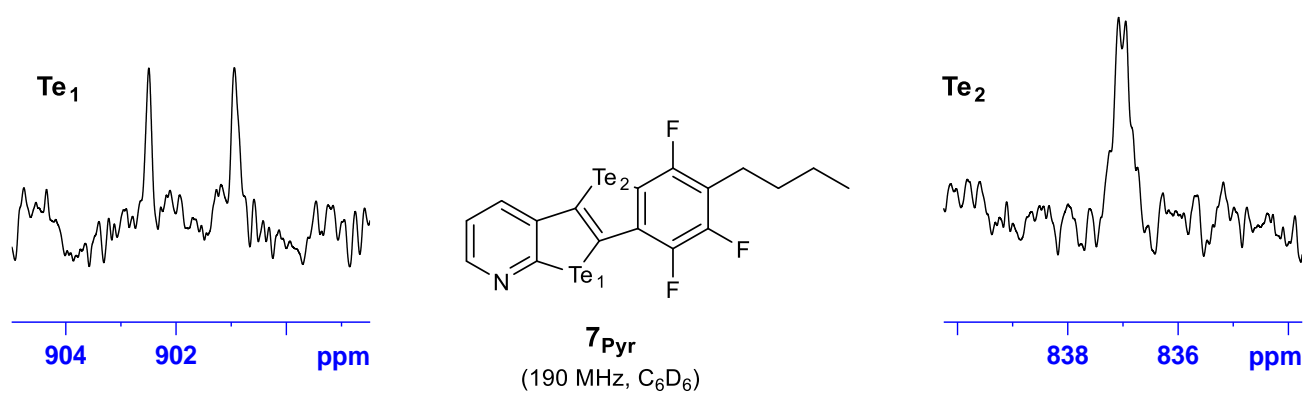


Figure S22: 190 MHz ^{125}Te NMR in C₆D₆ of molecule **7_{Pyr}**.

SUPPORTING INFORMATION

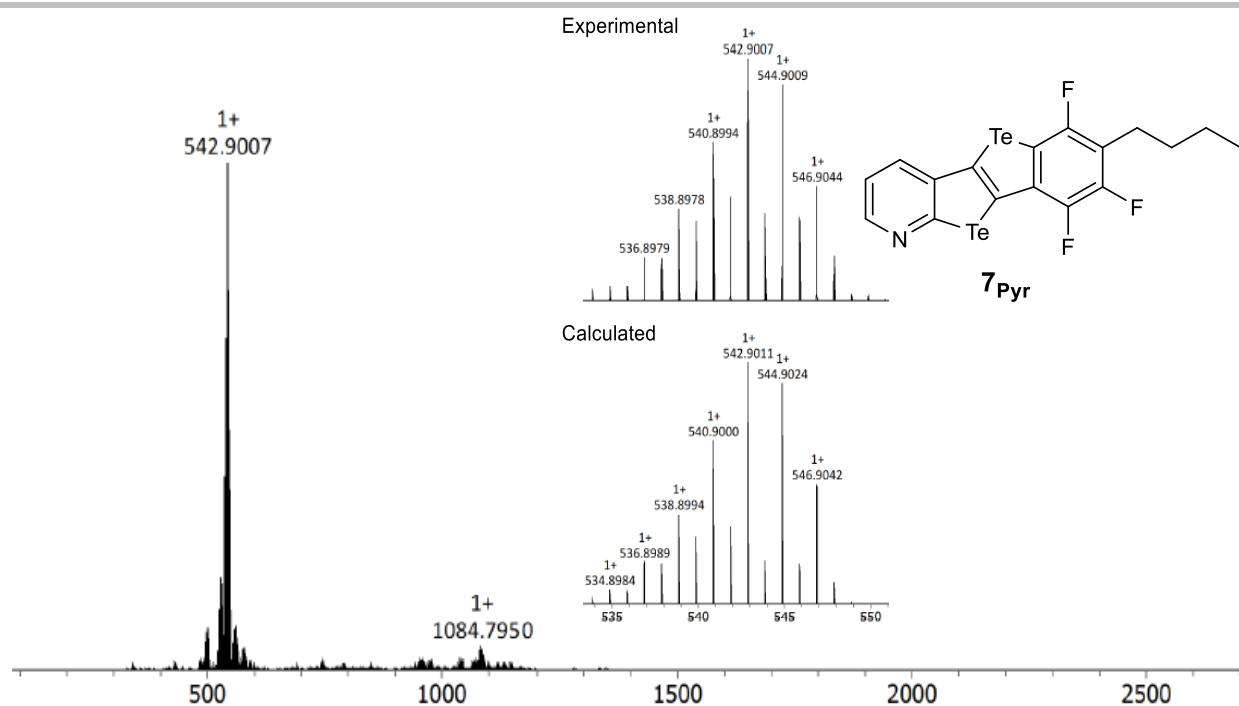


Figure S23: HRMS-LD mass spectrum of molecule **7Pyr** in the positive ion mode. The peak at 1084 corresponds to the dimeric species.

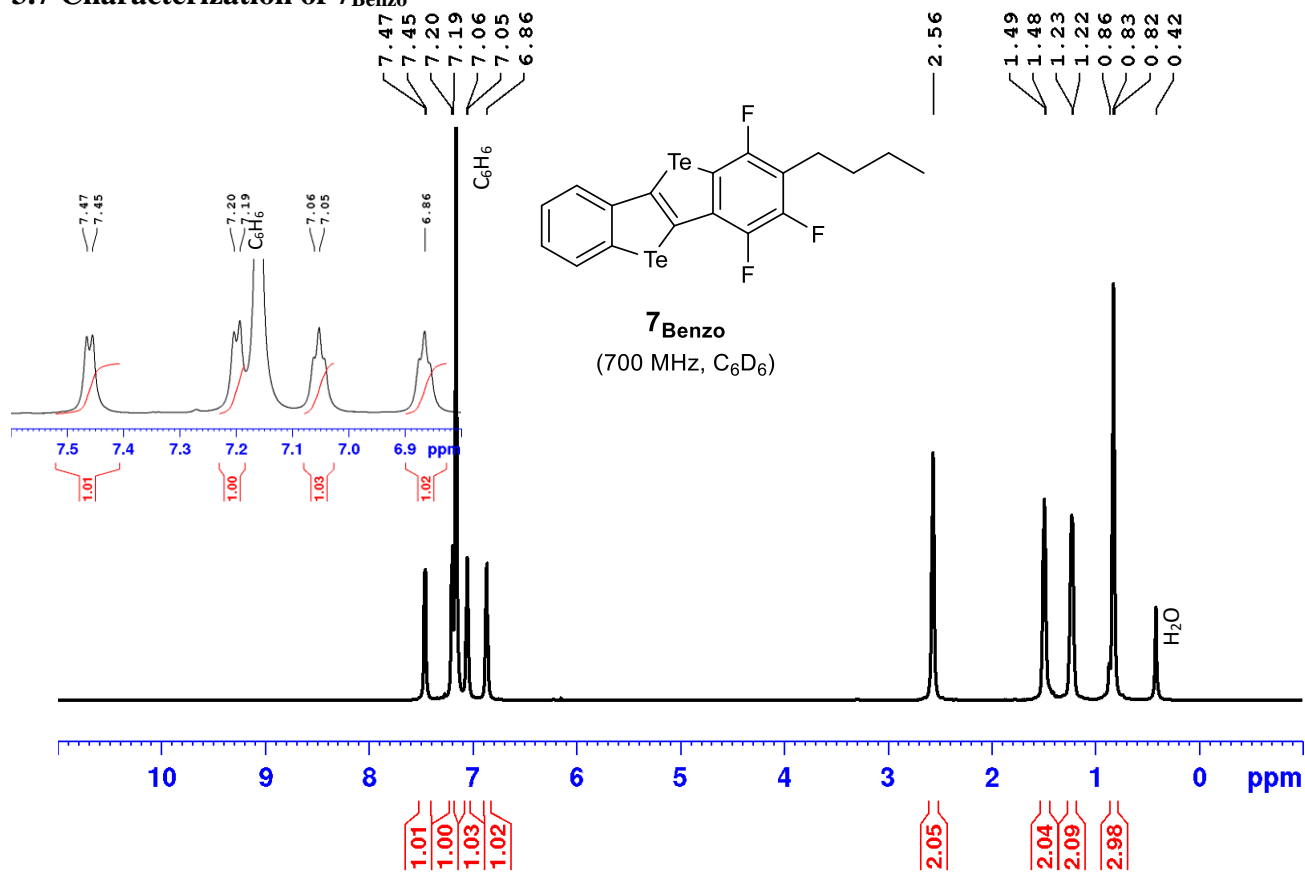
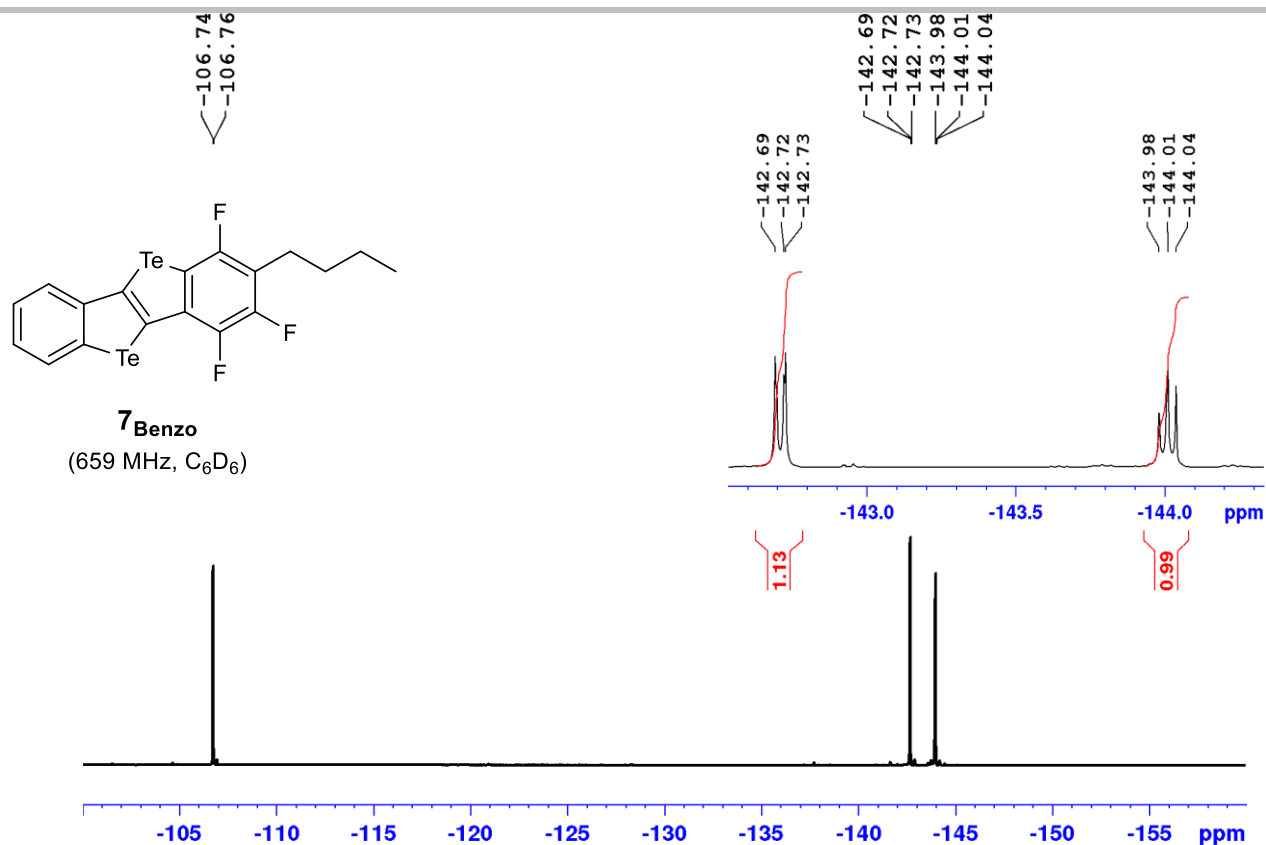
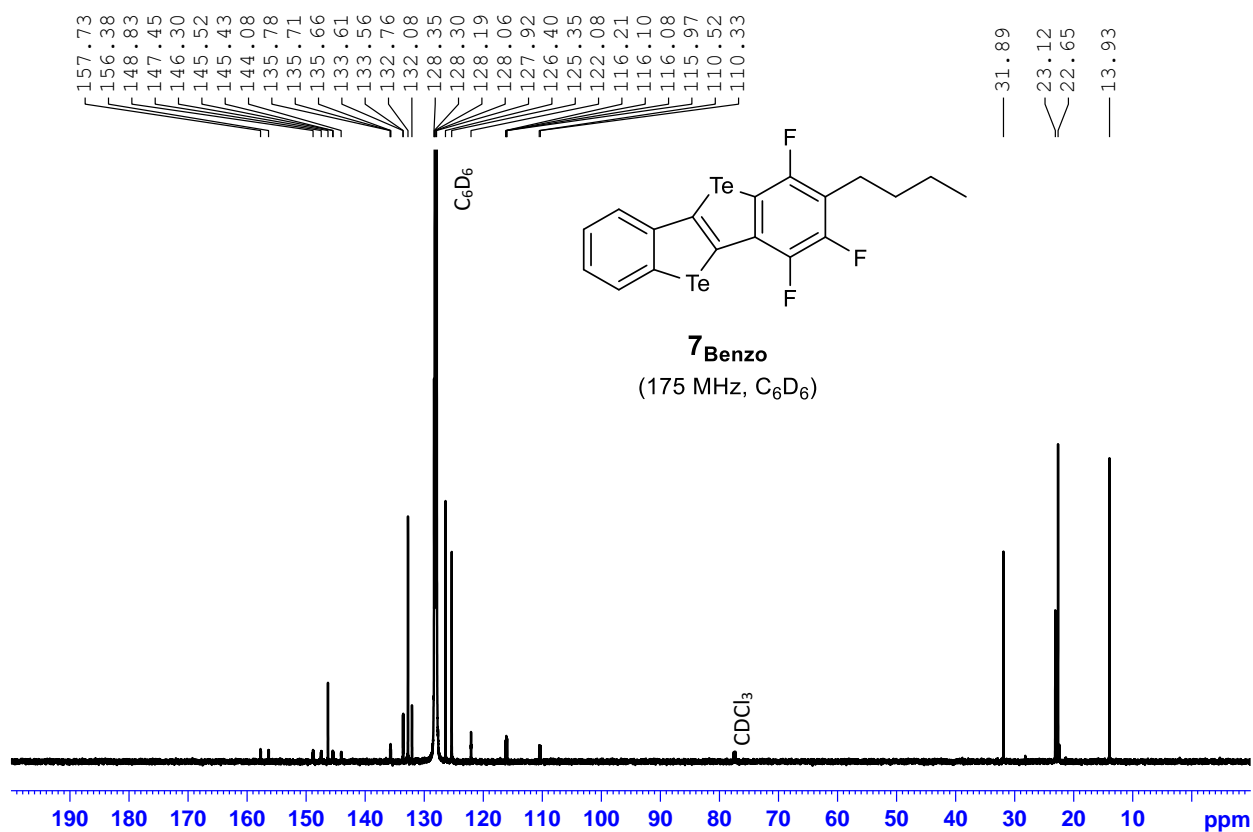
3.7 Characterization of **7Benzo**

Figure S24: 700 MHz ¹H NMR in C₆D₆ of molecule **7Benzo**.

SUPPORTING INFORMATION

Figure S25: 659 MHz ¹⁹F NMR in C₆D₆ of molecule **7_{Benzo}**.Figure S26: 175 MHz ¹³C{¹H} NMR in C₆D₆ of molecule **7_{Benzo}**.

SUPPORTING INFORMATION

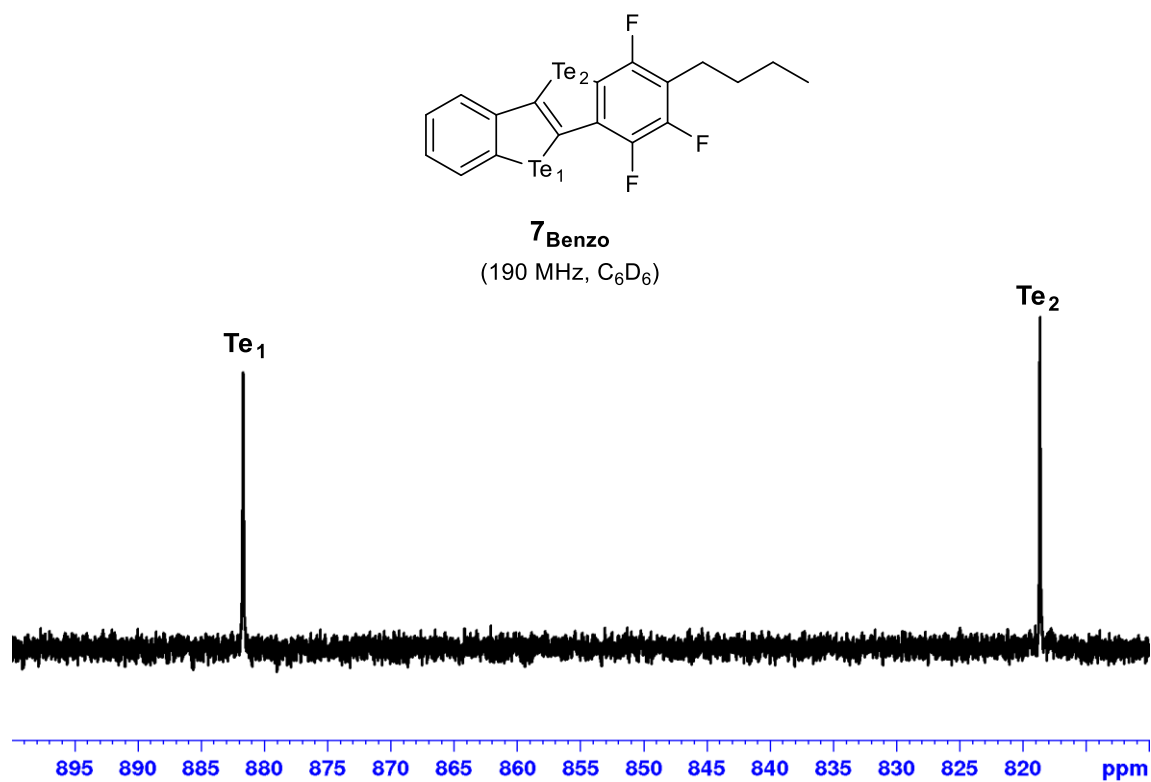


Figure S27: 190 MHz ¹²⁵Te{¹⁹F} NMR in C₆D₆ of molecule 7_{Benzo}.

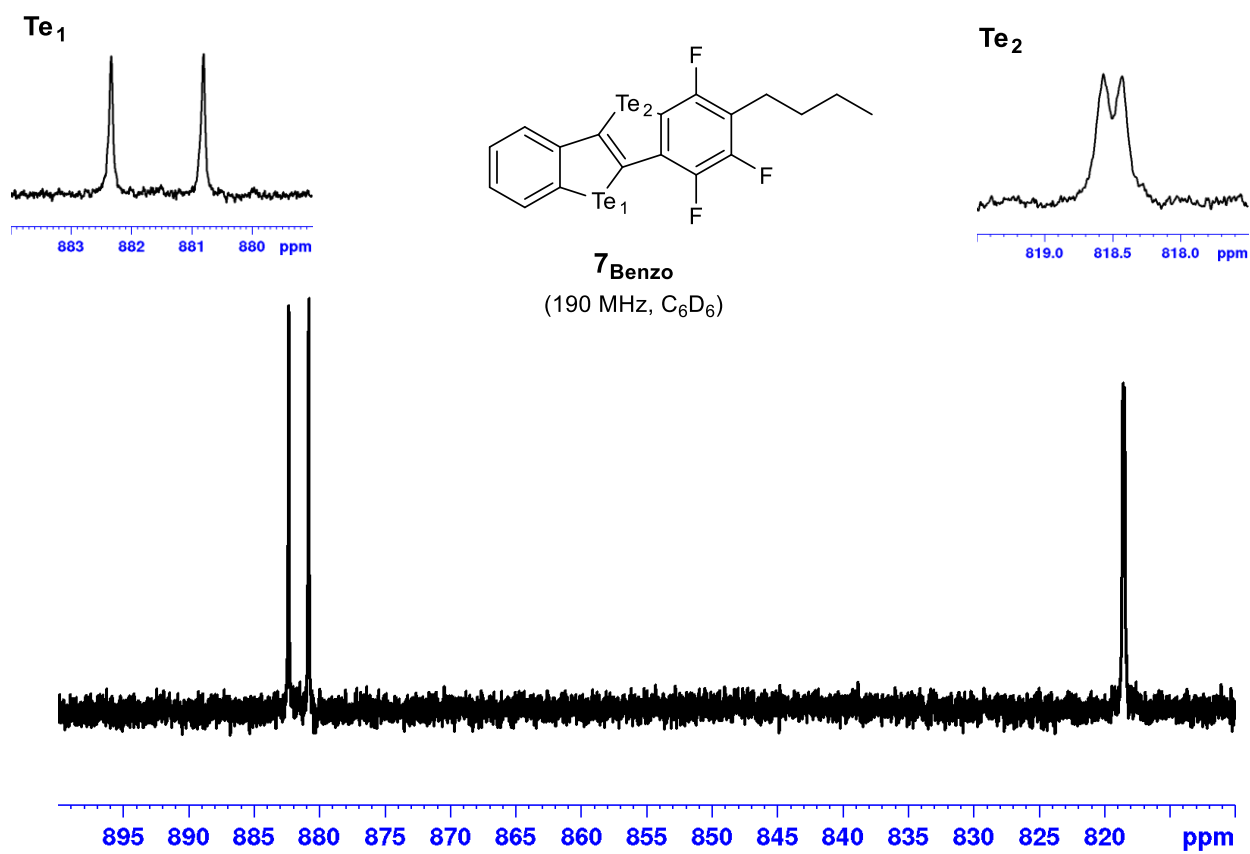


Figure S28: 190 MHz ¹²⁵Te NMR in C₆D₆ of molecule 7_{Benzo}.

SUPPORTING INFORMATION

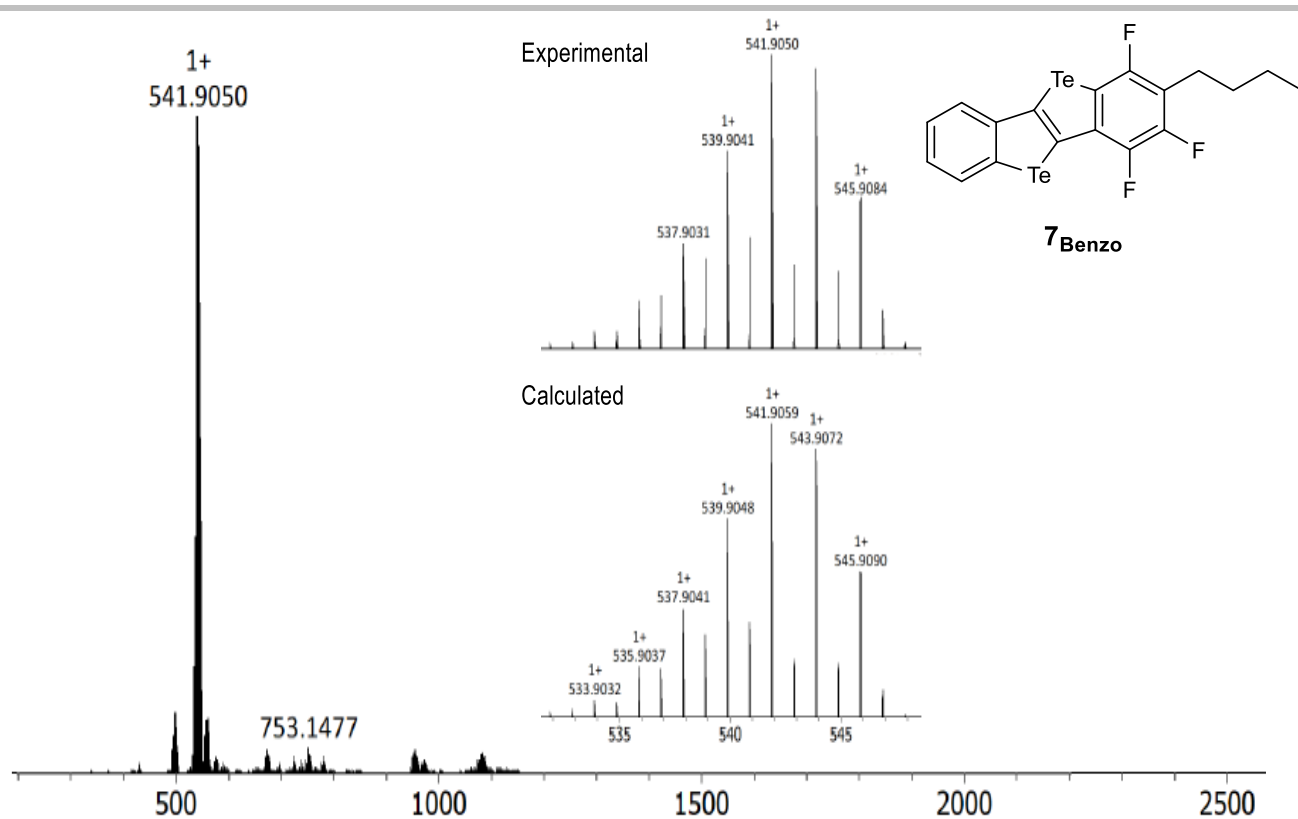
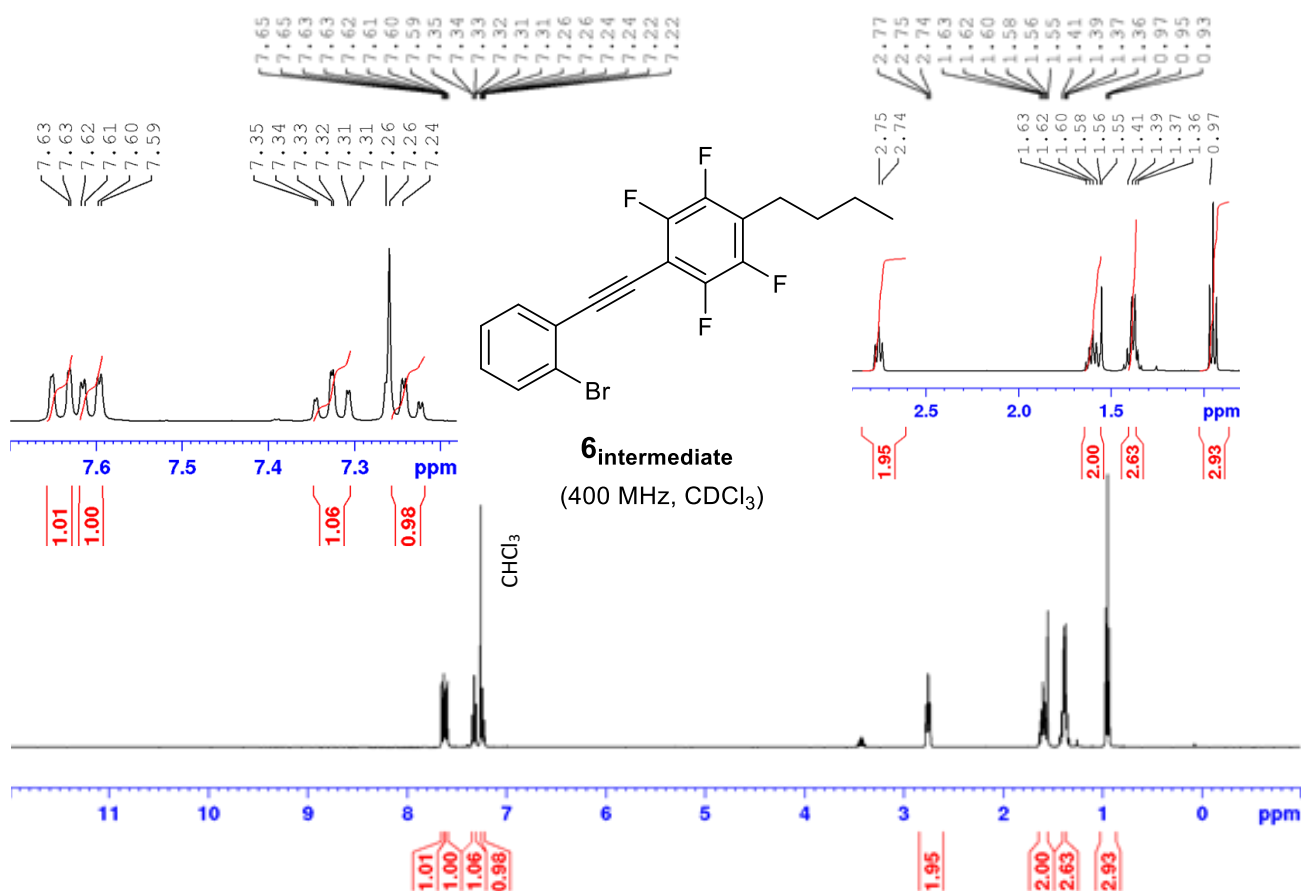
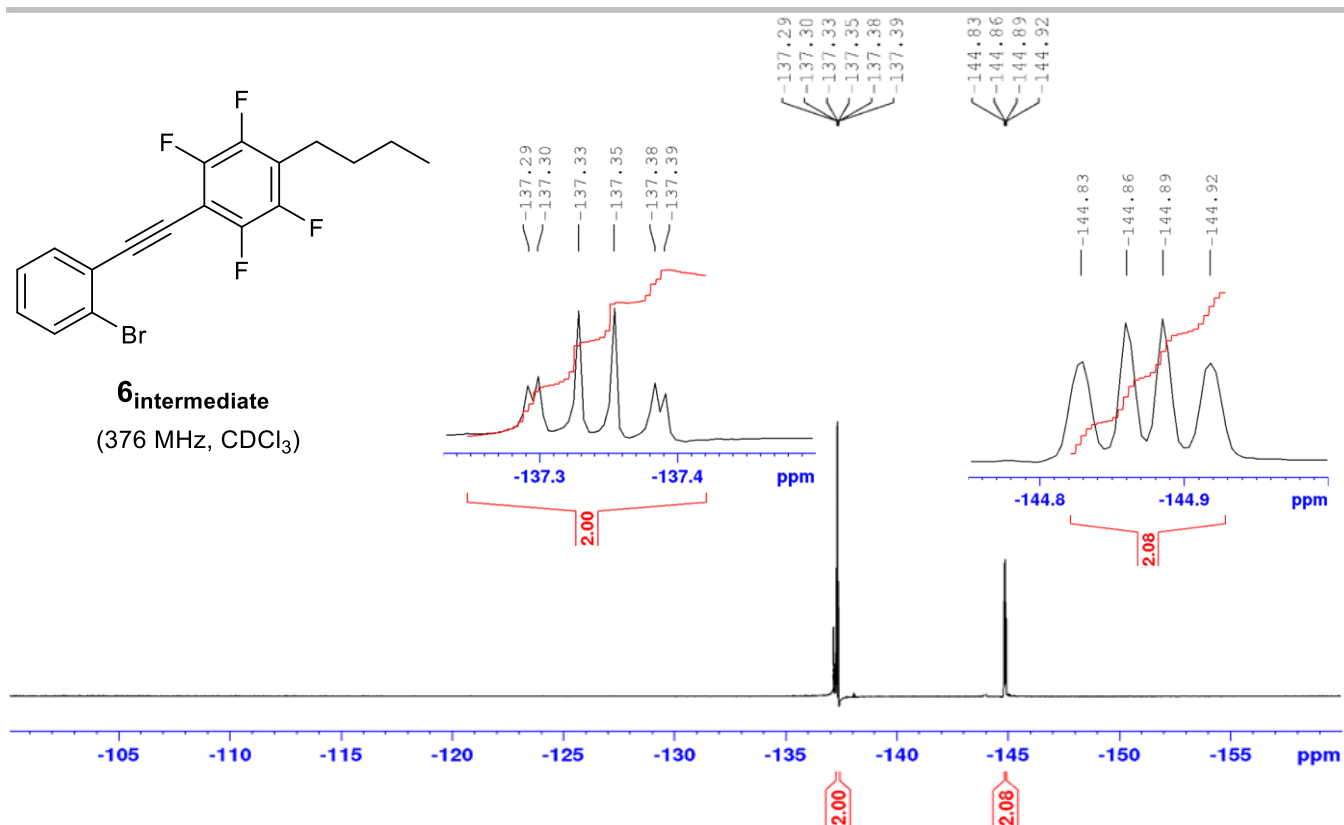
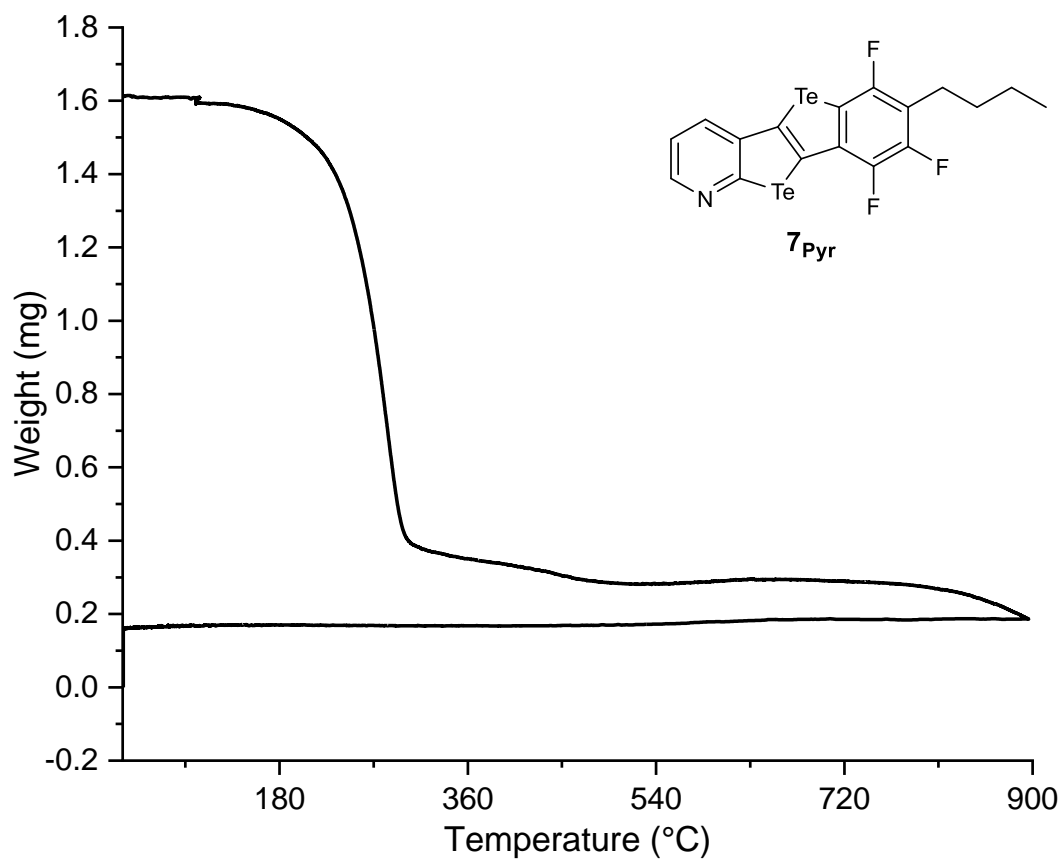


Figure S29: HRMS-LD mass spectrum of molecule 7Benzo in the positive ion mode.

Figure S30: 400 MHz ¹H NMR in CDCl₃ of molecule 6intermediate.

SUPPORTING INFORMATION

Figure S31: 376 MHz ¹⁹F NMR in CDCl₃ of molecule **6intermediate**.Figure S32: TGA analysis of **7Pyr** in the presence of N₂. Method: 1. Equilibrate at 30 °C; 2. Isothermal for 30'; 3. Ramp 20 °C/min to 100 °C; 4. Isothermal for 30'; 5. Ramp 10 °C/min to 900 °C; 6. Equilibrate at 30 °C.

SUPPORTING INFORMATION

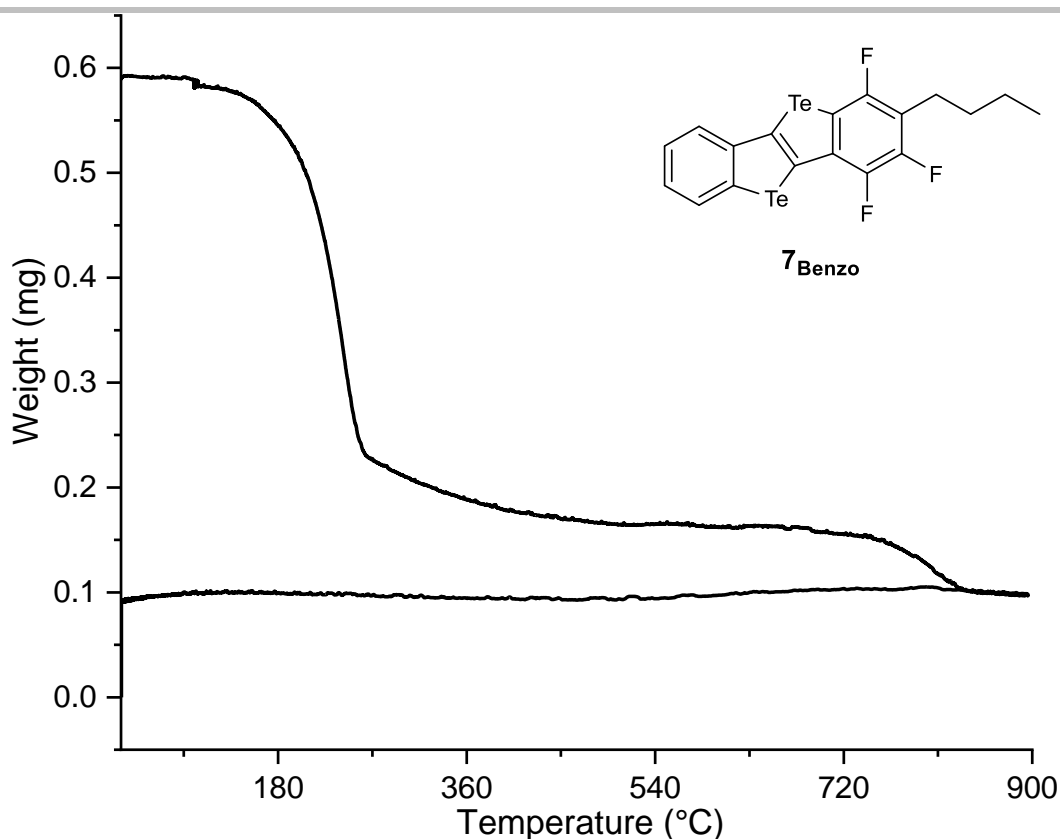


Figure S33: TGA analysis of **7Benzo** in the presence of N_2 . Method: 1. Equilibrate at 30 °C; 2. Isothermal for 30'; 3. Ramp 20 °C/min to 100 °C; 4. Isothermal for 30'; 5. Ramp 10 °C/min to 900 °C; 6. Equilibrate at 30 °C.

Table S1. Experimental ^{125}Te chemical shift tensors for both the Te sites of **7Pyr** and **7Benzo**.

	7Pyr		7Benzo	
	Te ₁	Te ₂	Te ₁	Te ₂
δ_{iso} [ppm]	898.5	845.5	852.4 ^[a]	835.8 ^[a]
LB ^[24]	1107.6	1364.6	1274.2	1197.9
δ (CSA) [ppm]	956.2	1272.8	1333.5	1180.2
η (CSA)	0.353	0.044	0.120	0.093
δ_{11} [ppm]	1854.7	2118.3	2185.8	2016.1
δ_{22} [ppm]	589.2	237.0	265.4	300.8
δ_{33} [ppm]	251.6	181.2	106.0	190.7
Ω [ppm]	1603.2	1937.1	2079.9	1825.4
κ	-0.58	-0.94	-0.85	-0.88

[a] Exchangeable.

^{125}Te ssNMR spectra acquired with different magic angle spinning speeds of samples containing **7Pyr** proved the position of δ_{iso} values, which turned to be 898.5 ppm and 845.5 ppm for Te₁ and Te₂ atoms, respectively. Moreover, a decreased value for the largest principal component δ_{11} could be observed for Te₁ (1854.7 ppm) when compared to that of Te₂ (from 2118.3 ppm). An increase in the shielded δ_{33} value

SUPPORTING INFORMATION

is also observed (251.6 ppm and 181.2 ppm for Te₁ and Te₂, respectively). These variations shrink the span values of the Te₁ resonance compared to that of Te₂ atom (1603.2 vs. 1937.1 ppm).

4. Optoelectronic characterization

In contrast to other Te-containing derivatives,^[25] the vibrational structure does not coalesce into an unique broadened peak, but it is surprisingly well-defined, suggesting a significant ligand-centered or intraligand character.

4.1 Photophysical properties

Table S2. Photophysical data for **7_{Pyr}** and **7_{Benzo}**

	Absorbance ^[a]		Phosphorescence ^[b]	
	λ_{max} (nm)	ϵ_{max} (M ⁻¹ cm ⁻¹)	λ_{max} (nm)	τ (μ s)
7_{Pyr}	330	12830	522	510
7_{Benzo}	336	13580	528	1460

[a] Recorded in CH₂Cl₂ at 298 K. [b] Recorded in CHCl₃/EtOH (1:1) glassy matrix at 77 K.

4.2 Electrochemical properties

Table S3. Half-wave potentials calculated versus the Fc/Fc⁺ couple for the experiments in the given solvent; TBAPF₆ 0.1 M used as electrolyte. Scan rate: 120 mV·s⁻¹. Only oxidation phenomena reported for analysis in thin films.^[a]

	7_{Pyr}		7_{Benzo}	
	$E_{1/2}^{ox}$ (V)	$E_{1/2}^{red}$ (V)	$E_{1/2}^{ox}$ (V)	$E_{1/2}^{red}$ (V)
CH₂Cl₂	+0.67	-2.47	+0.26	-2.81
TCE	+0.82	-1.66	+0.34	-1.53
Thin film	+0.79	-	+0.87	-

[a] All the values refer to irreversible phenomena.

SUPPORTING INFORMATION

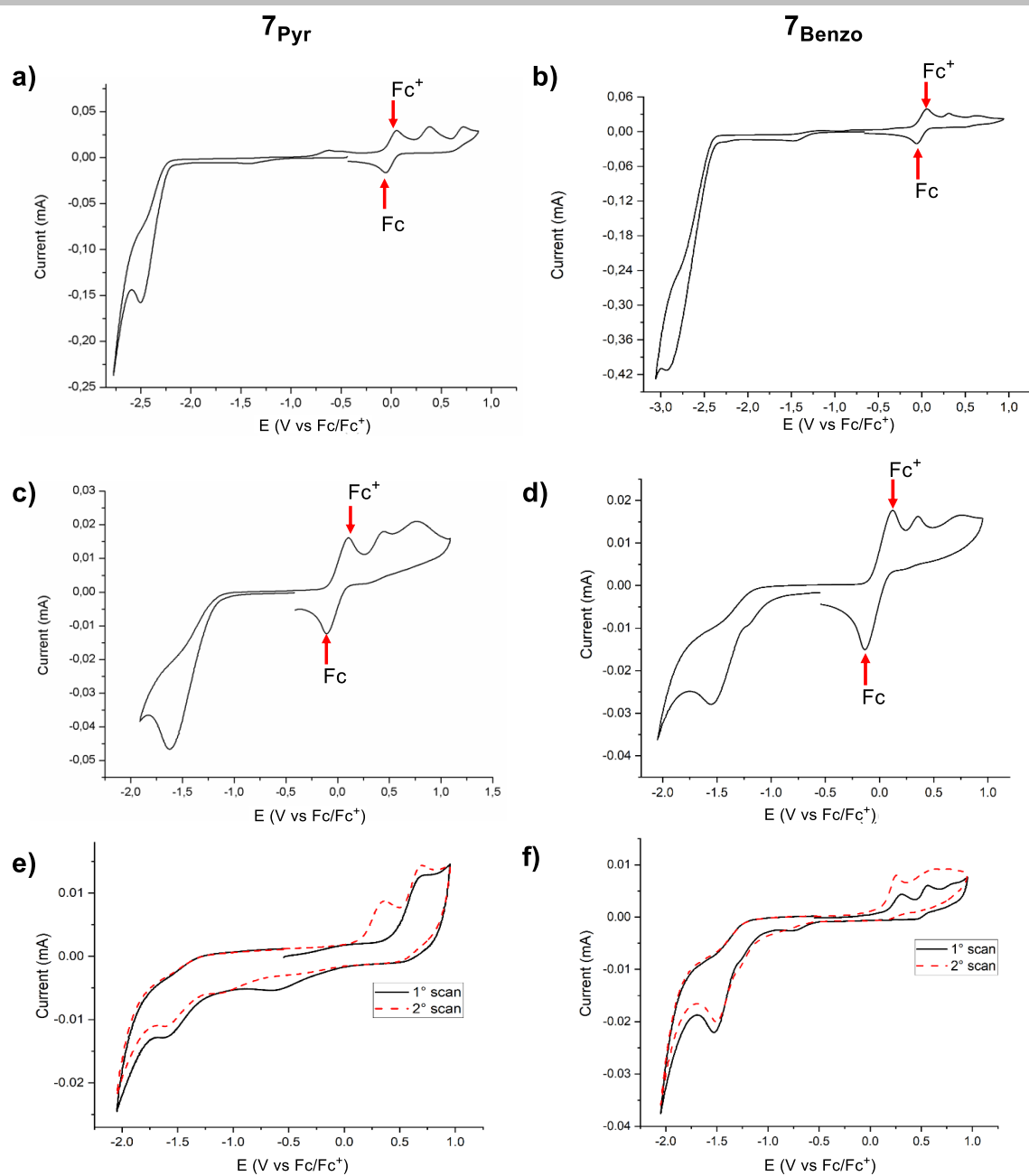


Figure S34: At the top, cyclic voltammograms in CH_2Cl_2 at r.t. with electrolyte TBAPF_6 0.1 M of a) 7_{Pyr} and b) 7_{Benzo} ; at the center, CV in TCE at r.t. with electrolyte TBAPF_6 0.1 M of c) 7_{Pyr} and d) 7_{Benzo} . Scan rate: $120 \text{ mV}\cdot\text{s}^{-1}$; at the bottom, multiple anodic traces in TCE at r.t. of e) 7_{Pyr} and f) 7_{Benzo} , using electrolyte TBAPF_6 0.1 M. Scan rates: $250 \text{ mV}\cdot\text{s}^{-1}$ for 7_{Pyr} , $120 \text{ mV}\cdot\text{s}^{-1}$ for 7_{Benzo} . Ferrocene was used as internal reference standard.

SUPPORTING INFORMATION

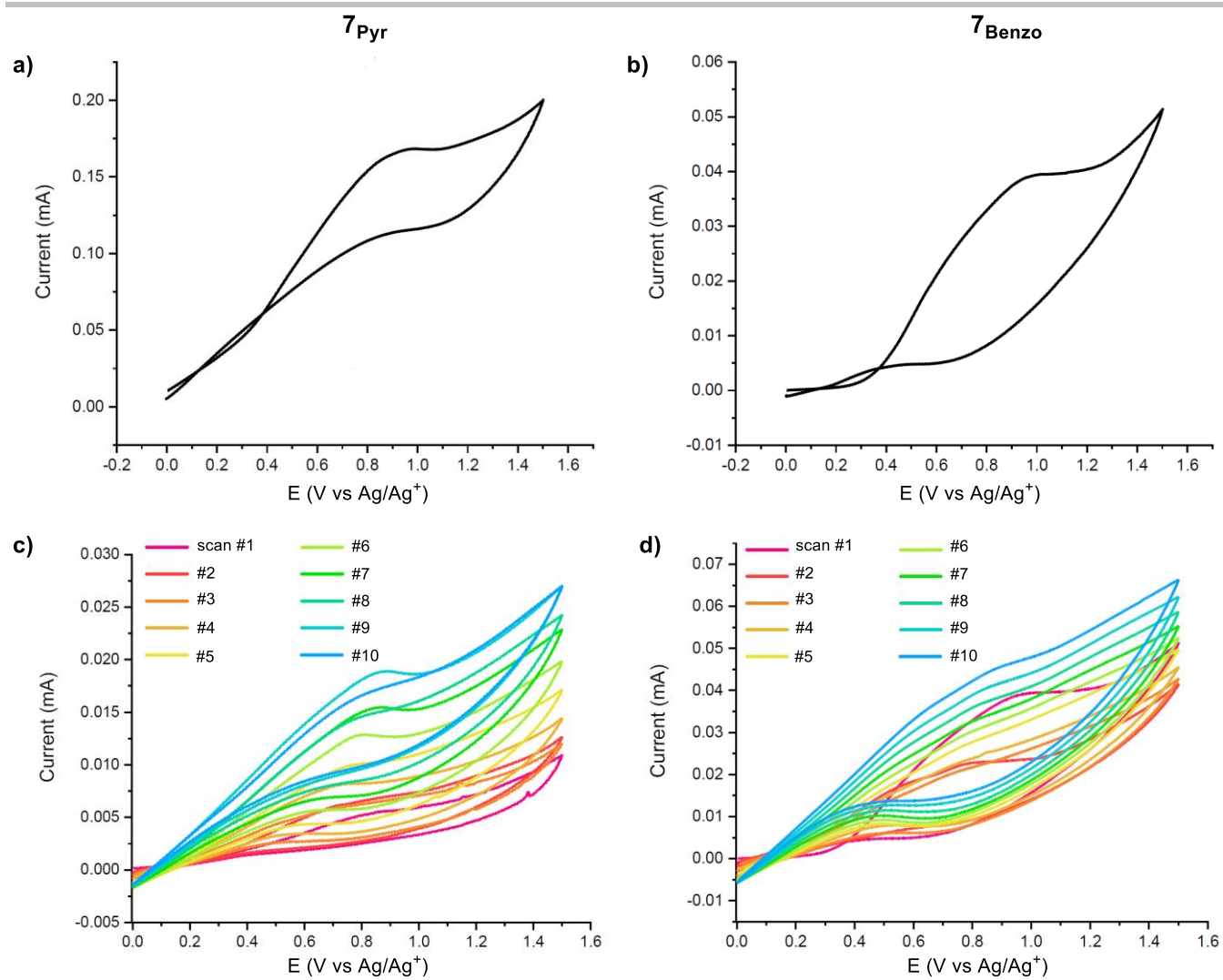


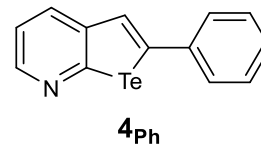
Figure S35: At the top, single anodic run of thin films of a) 7_{Pyr} and b) 7_{Benzo} ; at the bottom, multiple anodic traces of thin films of c) 7_{Pyr} and d) 7_{Benzo} . Scan rates: $100 \text{ mV}\cdot\text{s}^{-1}$. Solvent in which films were immersed: propyl carbonate.

SUPPORTING INFORMATION

5. Crystallographic data

Table S4. Crystal data and structure refinement for **4Ph** (2063971).

Empirical formula	C ₁₃ H ₉ NTe	
Formula weight	306.81	
Crystal system	Orthorhombic	
Space group	Pbca	
Unit cell dimensions	a = 11.9636(4) Å	α = 90°.
	b = 7.3711(3) Å	β = 90°.
	c = 24.2292(9) Å	γ = 90°.
Volume	2136.65(14) Å ³	
Z	8	
Density (calculated)	1.908 mg/m ³	
Absorption coefficient	2.746 mm ⁻¹	
F(000)	1168	
Crystal size	0.274 × 0.212 × 0.162 mm ³	
	Data collection	
Temperature	150(2) K	
Wavelength	0.71073 Å	
Theta range for data collection	3.353 to 29.748°.	
Index ranges	-16 ≤ h ≤ 12, -10 ≤ k ≤ 7, -27 ≤ l ≤ 32	
Reflections collected	10342	
Independent reflections	2697 [R(int) = 0.0249]	
Completeness to theta = 25.242°	99.9 %	
	Refinement	
Absorption correction	Gaussian	
Refinement method	Full-matrix least-squares on F ²	
Data / restraints / parameters	2697 / 0 / 136	
Goodness-of-fit on F ²	1.087	
Final R indices [I > 2σ(I)]	R1 = 0.0263, wR2 = 0.0572	
R indices (all data)	R1 = 0.0365, wR2 = 0.0636	
Extinction coefficient	n/a	
Largest diff. peak and hole	0.364 and -0.865 e ⁻ Å ⁻³	



SUPPORTING INFORMATION

Table S5. Crystal data and structure refinement for **7_{Pyr}** (2057472).

	Crystal data	
Empirical formula	C ₁₇ H ₁₂ F ₃ NTe ₂	
Formula weight	542.48	
Crystal system	Orthorhombic	
Space group	Pbca	
Unit cell dimensions	a = 9.4828(3) Å	α = 90°.
	b = 7.5010(3) Å	β = 90°.
	c = 44.1183(15) Å	γ = 90°.
Volume	3138.16(19) Å ³	
Z	8	
Density (calculated)	2.296 mg/m ³	
Absorption coefficient	29.623 mm ⁻¹	
F(000)	2016	
Crystal size	0.1 × 0.07 × 0.003 mm ³	
	Data collection	
Temperature	100(2) K	
Wavelength	1.54178 Å	
Theta range for data collection	4.006 to 121.648°.	
Index ranges	-10 ≤ h ≤ 10, -8 ≤ k ≤ 8, -48 ≤ l ≤ 48	
Reflections collected	36745	
	Refinement	
Absorption correction	multiscan	
Refinement method	Full-matrix least-squares on F ²	
Data / restraints / parameters	2304 / 27 / 209	
Goodness-of-fit on F ²	1.085	
Final R indices [I > 2σ(I)]	R1 = 0.0801, wR2 = 0.1910	
R indices (all data)	R1 = 0.1109, wR2 = 0.2126	
Extinction coefficient	n/a	
Largest diff. peak and hole	1.49 and -2.12 e·Å ⁻³	

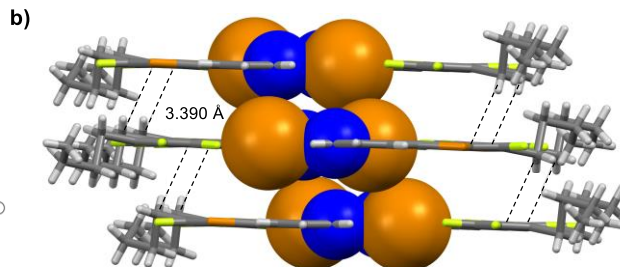
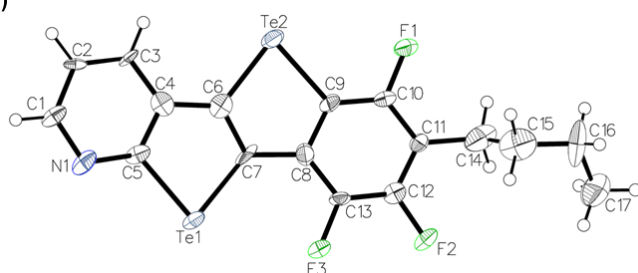
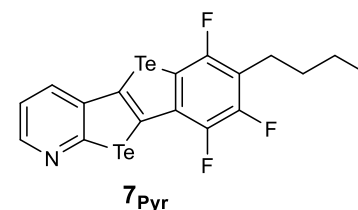
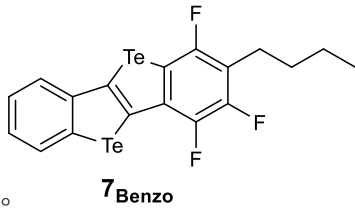


Figure S36: a) ORTEP representation of a single molecule of **7_{Pyr}**, drawn with 50% displacement ellipsoid; b) crystal structure of **7_{Pyr}** showing the flat conformation, with N and Te atoms represented with their vdW radii. π - π stacking is highlighted (distances are expressed in Å). Crystallization solvent: CHCl₃. Space group: Pbca.

SUPPORTING INFORMATION

Table S6. Crystal data and structure refinement for **7**_{Benzo} (2057473).

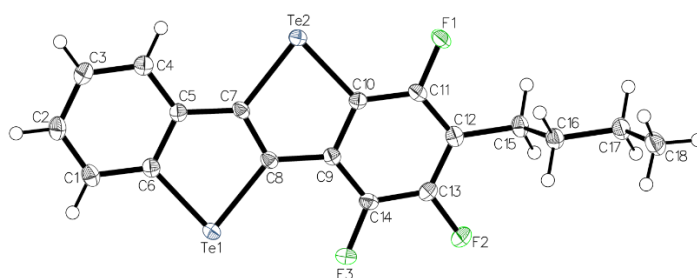
Empirical formula	C ₁₈ H ₁₃ F ₃ Te ₂	 <p style="text-align: center;">7_{Benzo}</p>
Formula weight	541.48	
Crystal system	Monoclinic	
Space group	P2 ₁ /c	
Unit cell dimensions	a = 22.9376(11) Å b = 4.5485(2) Å c = 15.8345(12) Å	
Volume	1625.54(16) Å ³	
Z	4	
Density (calculated)	2.213 mg/m ³	
Absorption coefficient	3.615 mm ⁻¹	
F(000)	1008	
Crystal size	0.337 × 0.128 × 0.014 mm ³	

Data collection

Temperature	114(2) K
Wavelength	0.71073 Å
Theta range for data collection	5.218 to 60.32°
Index ranges	-32 ≤ h ≤ 32, -6 ≤ k ≤ 6, -22 ≤ l ≤ 19
Reflections collected	44139

Refinement

Absorption correction	multiscan
Refinement method	Full-matrix least-squares on F ²
Data / restraints / parameters	4825 / 0 / 209
Goodness-of-fit on F ²	1.046
Final R indices [I > 2σ(I)]	R1 = 0.0191, wR2 = 0.0436
R indices (all data)	R1 = 0.0234, wR2 = 0.0448
Extinction coefficient	n/a
Largest diff. peak and hole	0.87 and -0.58 e ⁻ Å ⁻³

*Figure S37: ORTEP representation of a single molecule of 7*_{Benzo}*, drawn with 50% displacement ellipsoid.*

SUPPORTING INFORMATION

6. Computational studies

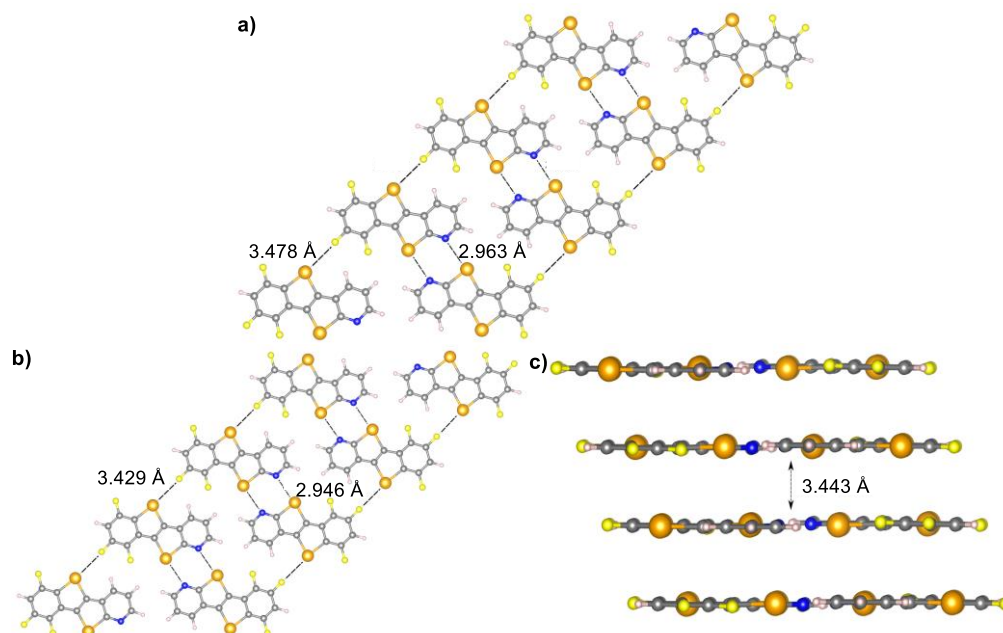


Figure S38: Atomic structures of a) monolayer, b) top-view and c) side-view of multilayers of $7P_{Yr}$ after structural optimization. C, Te, N, F and H atoms are represented by grey, orange, blue, yellow and white spheres, respectively.

In order to determine the effect of the absence of N and Te on the electronic structure, hypothetical atomic structures have been built substituting both Te and N atoms (model I), N atoms (model II) and Te atoms (model III) with C-H groups. For each model, the PDOS have been evaluated and compared to the C and Te p states of the $7P_{Yr}$ pristine monolayer, as depicted in Figure S39.

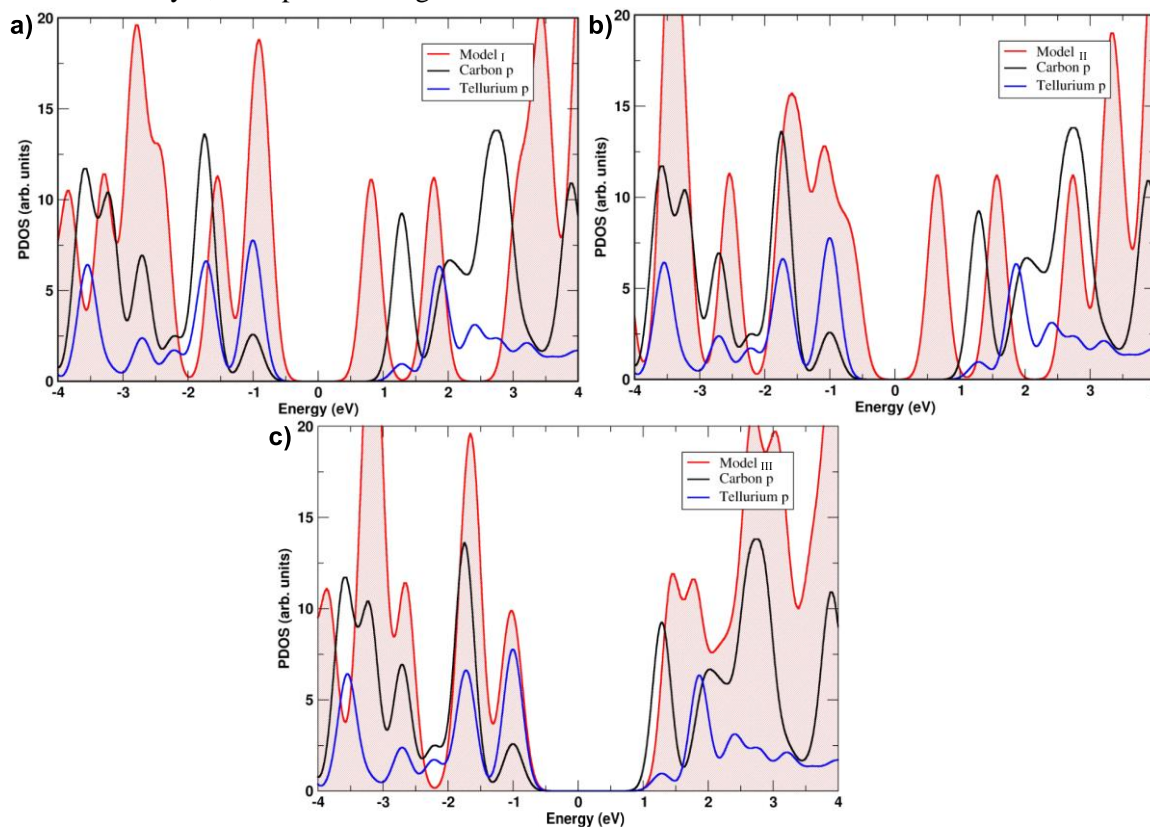


Figure S39: PDOS of hypothetical atomic structures (in red) compared to C and Te p states of pristine $7P_{Yr}$ (respectively in black and blue lines), determined by replacing a) both Te and N atoms, b) Te atoms and c) N atoms with C-H moieties.

SUPPORTING INFORMATION

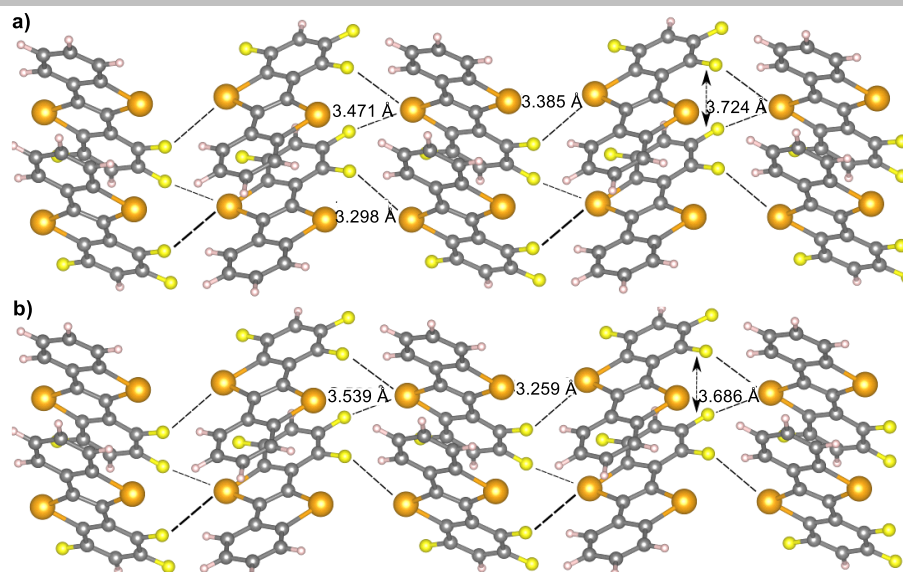


Figure S40: Atomic structure model for a) monolayer and b) multilayers of 7_{Benzo} after structural optimization. Color code: grey (Carbon), Orange (Tellurium), Yellow (Fluorine), White (Hydrogen).

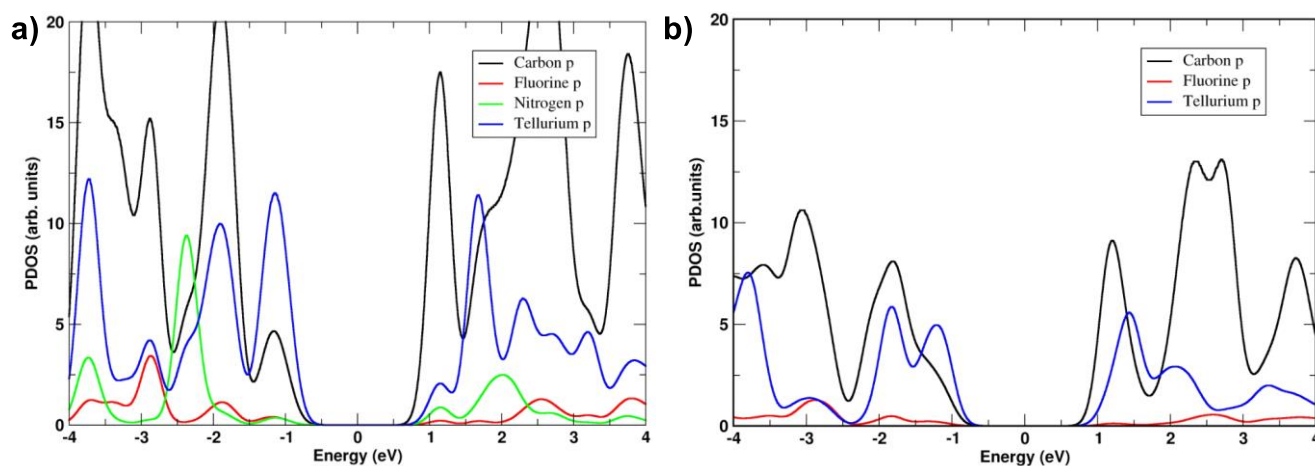


Figure S41: PDOS calculated for multi-layered structures of a) 7_{Pyr} and b) 7_{Benzo} .

7. Morphological features

Polarized Light Microscopy (PLM) imaging investigations show that surfaces, which are spin-coated with 7_{Pyr} are homogeneously covered with tiny crystalline domains, with the exception of the presence of few opaque bigger grains of about $10\ \mu\text{m}$ (circled in red in Figure S42a). This suggests the presence of aggregates of amorphous crystallites having casual crystallographic orientations in the film. Similar agglomerates, marked by multiple layers of randomly oriented crystallites, were mainly observed in drop-casted layers of 7_{Pyr} (Figure S42b). As expected, drop-casting deposition favors the growth of large crystalline aggregated grains, leading to thicker films (120 nm; 60 nm for spin coated films) with a higher surface roughness (RMS for the drop-casted and spin-coated films is of 20 nm and 3 nm, respectively). In contrast, no difference in the morphology was observed between thin 7_{Benzo} -films produced by either spin-coating (50 nm and RMS of 6 nm) or drop-casting (200 nm and RMS of 38 nm) techniques. Both layers exclusively contain several randomly oriented aggregates, which are amorphous since they look unaltered by changing the polarization angle (Figure S42c-d). Notably, significantly bigger domains constitute the drop-casted films, which reach sizes up to $10\ \mu\text{m}$.

SUPPORTING INFORMATION

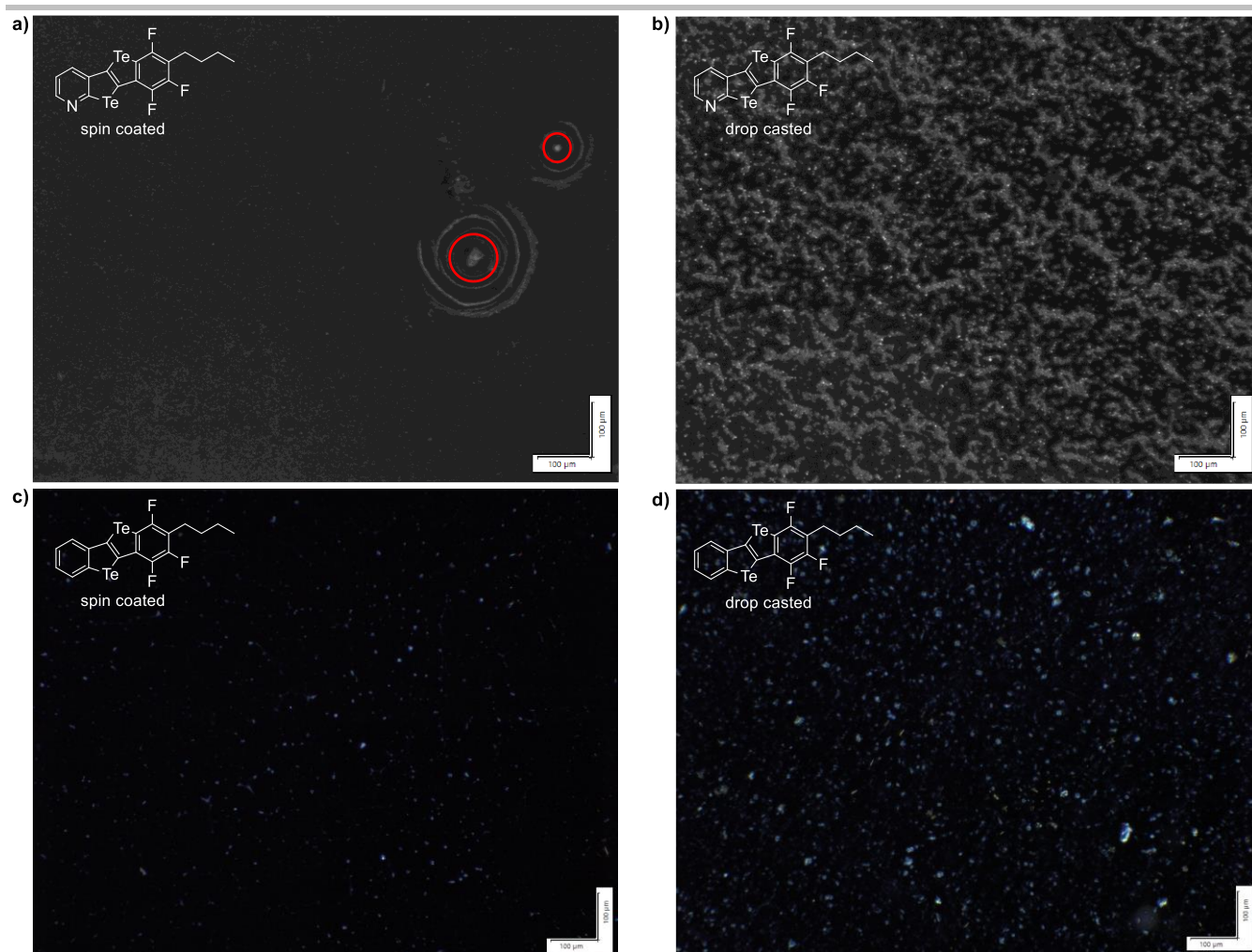


Figure S42: At the top, PLM images of naked glass substrates covered with a) spin coated and b) drop casted 7_{Pyr} , with the bigger aggregates pointed out in red circles; at the bottom, PLM images of naked glass substrates covered with c) spin coated and d) drop casted 7_{Benzo} . All the images are $100 \times 100 \mu\text{m}$.

Further studies with Scanning Electron Microscopy (SEM) imaging of spin-coated and drop-casted 7_{Pyr} - and 7_{Benzo} -films deposited on silicon wafers were performed. Once spin-coated, 7_{Pyr} arranges in well dispersed grains (Figure S43a) with a rhomboidal geometry (Figure S43b), having an average size of $\sim 2 \mu\text{m}$. The same rhomboidal morphologies were observed in the aggregates formed by drop casting (Figure S43c), marked by a bigger size (Figure S43d) which is comparable to that observed with the PLM studies on glass surfaces. Differently, the SEM analysis of 7_{Benzo} on silicon wafers revealed a different morphology than that emerged from the PLM images. Surfaces spin-coated with 7_{Benzo} are almost entirely covered with flat stripes (Figure S44a) with some regions featuring clusters of amorphous solid (Figure S44b). Drop-casting deposition of 7_{Benzo} led to amorphous material in the center of the substrate (Figure S44c), whereas having a higher concentration at the edges leads to the formation of elongated fibers (Figure S44d).

SUPPORTING INFORMATION

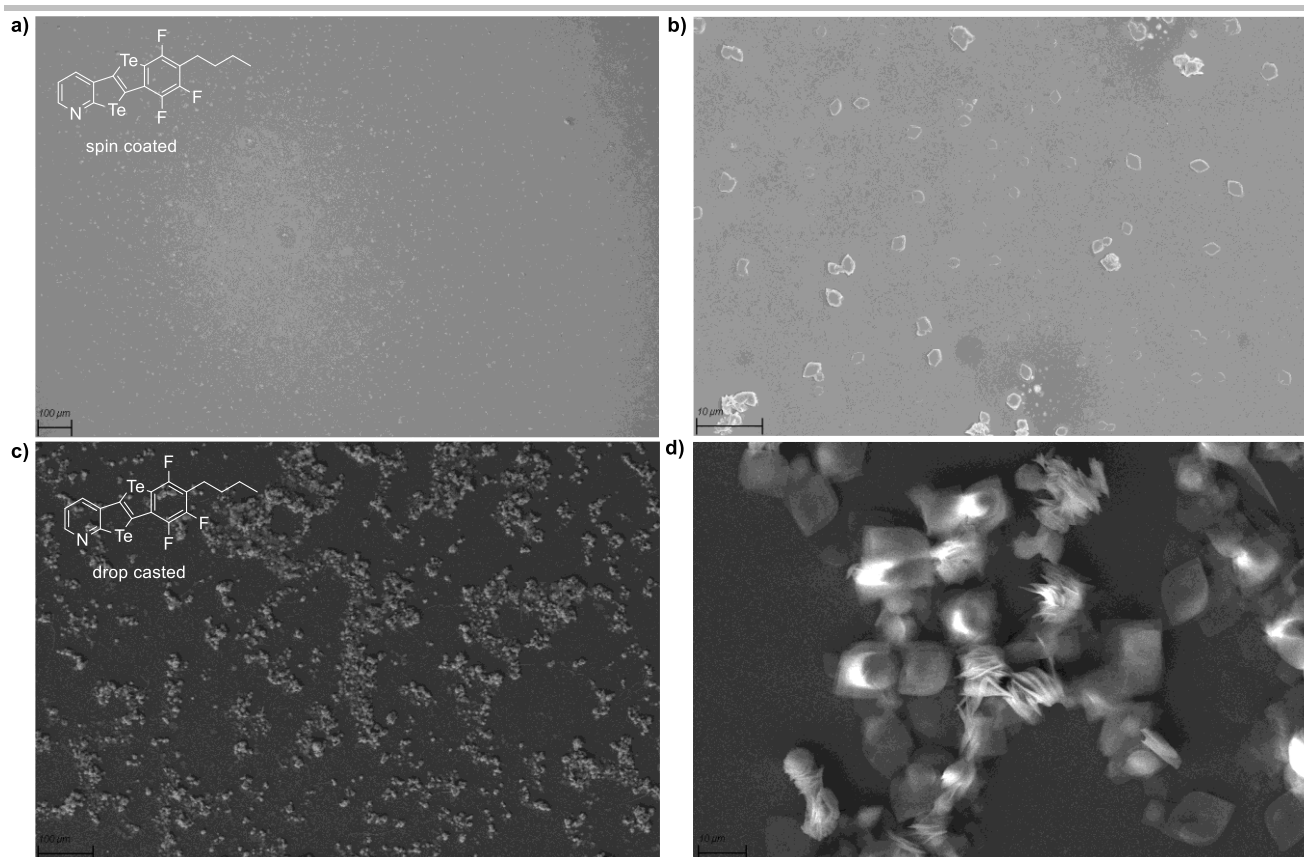


Figure S43: SEM images of silicon wafers covered with a, b) spin coated and c, d) drop casted **7Pyr**. Scale bars: 100 μm (a, c), 10 μm (b, d).

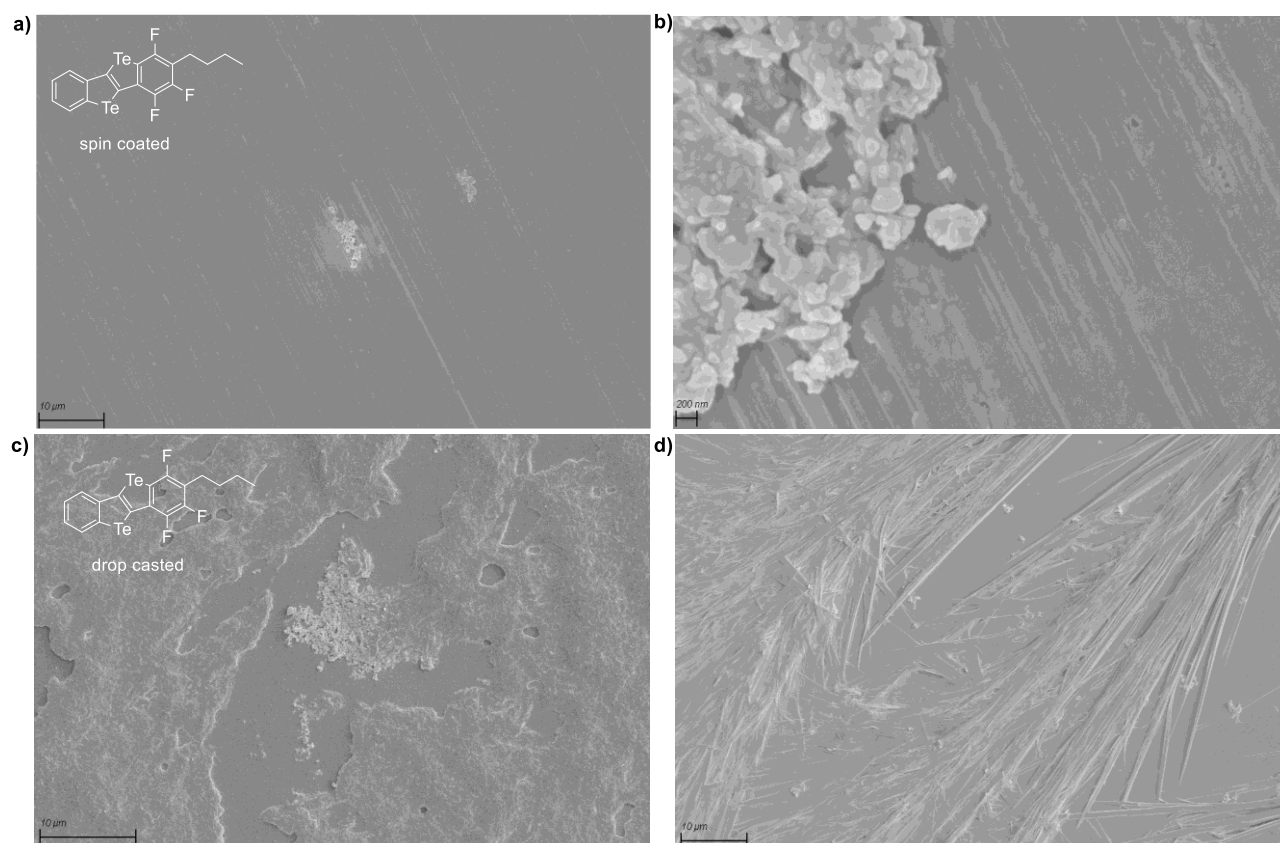


Figure S44: SEM images of silicon wafers covered with a, b) spin coated and c, d) drop casted **7Benzo**. Scale bars: 10 μm (a, c, d), 200 nm (b).

SUPPORTING INFORMATION

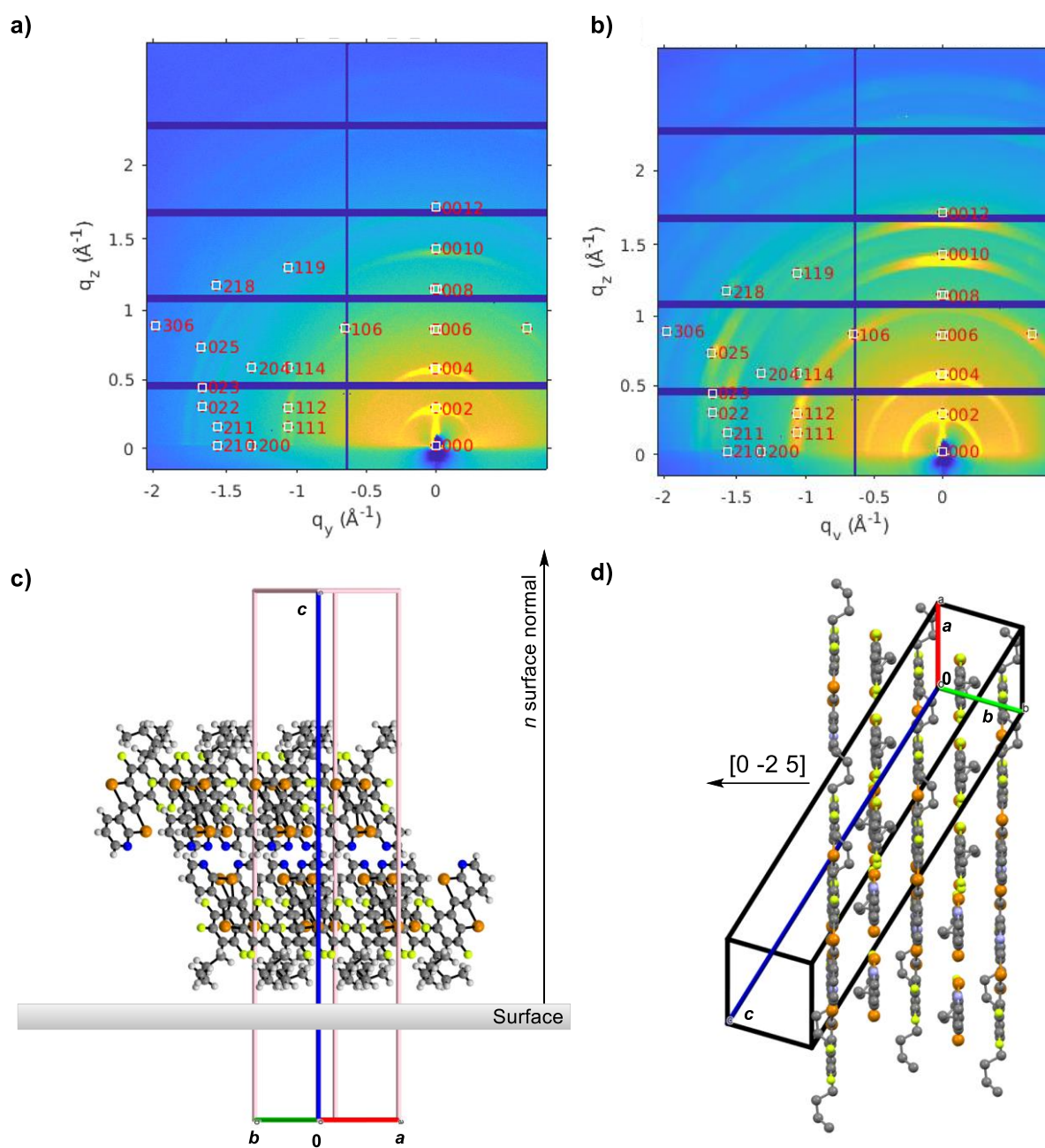


Figure S45: 2D-GIXRD pattern of thin films of $7P_{yr}$ a) spin-coated on Si-wafer and b) drop-casted on ITO/PEDOT:PSS covered glass. The indices of the GIXRD pattern determined from the crystal structure is overlaid with the c axis oriented in the out-of-plane direction and in-plane random orientation. Orientation of the molecules in thin films of $7P_{yr}$, namely c) representation of the crystal structure on the surface and d) visualization of the π - π stacking in the $[0 -2 5]$ direction.

SUPPORTING INFORMATION

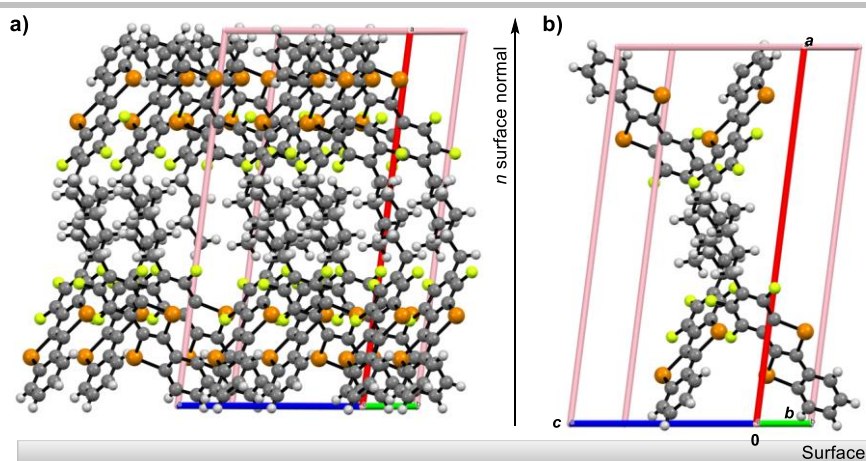


Figure S46: Orientation of the molecules in 7_{Benzo} thin films: a) crystal structure on the surface and b) visualization of the structural motive on the surface.

8. Thin-film transistors outcome

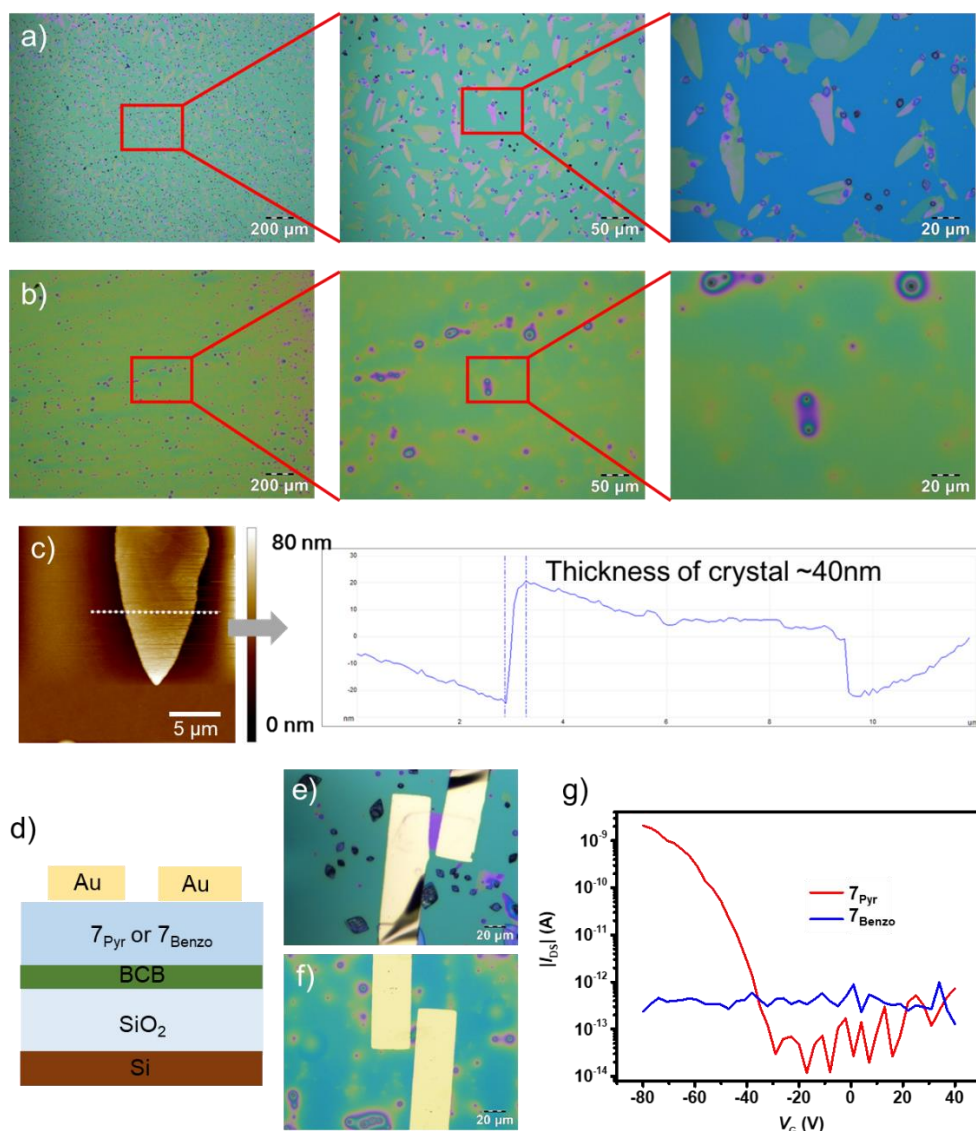


Figure S47: Optical image of a) crystals of 7_{Pyr} , b) aggregates of 7_{Benzo} . c) Atomic force microscope image of crystal of 7_{Pyr} , and its topographical profile revealing a crystal thickness of about 40 nm. Image size is 20 $\mu\text{m} \times 20 \mu\text{m}$. d) Device structure, optical microscopy image, top-view, of the e) 7_{Pyr} - and f) 7_{Benzo} - based transistor. g) Transfer curves of the transistors.

SUPPORTING INFORMATION

9. Implementation of dichalcogenides 7_{Pyr} and 7_{Benzo} in LEC devices

At first, devices with the architecture ITO/PEDOT:PSS/ 7_{Pyr} or 7_{Benzo} /Al were investigated as emitting layers. The devices were subjected to repetitive I-V scans, to study their electrical behavior, and were driven at pulsed 90 mA to determine their electrical stability (Figure S47). As expected, none of them exhibited electroluminescent response. However, 7_{Pyr} devices showed a very stable carrier injection and transport, reaching, for example, currents of 16 mA at 6 V. In addition, these devices displayed a stable average voltage at pulsed 90 mA. Reference 7_{Benzo} devices featured almost one order of magnitude lower currents in the I-V assays, while the average voltage quickly increases at pulsed 90 mA (Figure S49b). These findings suggest that the 7_{Pyr} -films are best suited for device applications.

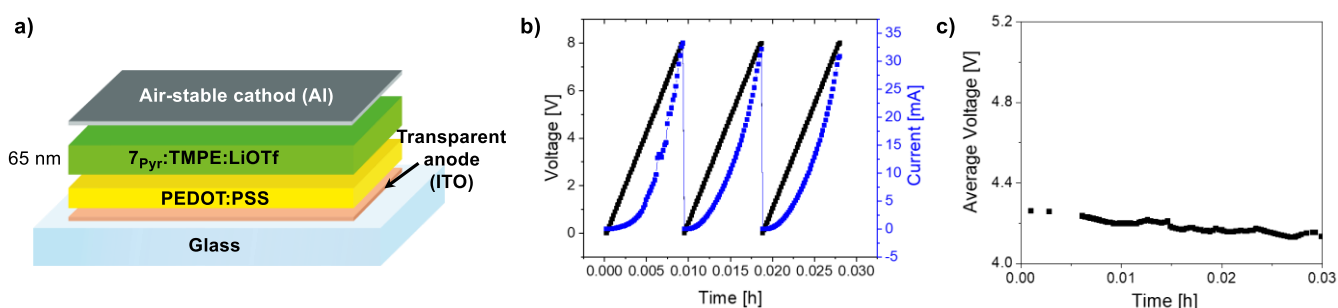


Figure S48: a) Scheme of the single-component LEC device having 7_{Pyr} as active layer; b) Luminescence-intensity-voltage (L-I-V) graph with voltage scans from 0 to 8 V; c) average voltage vs time recorded with a pulsed current of 90 mA.

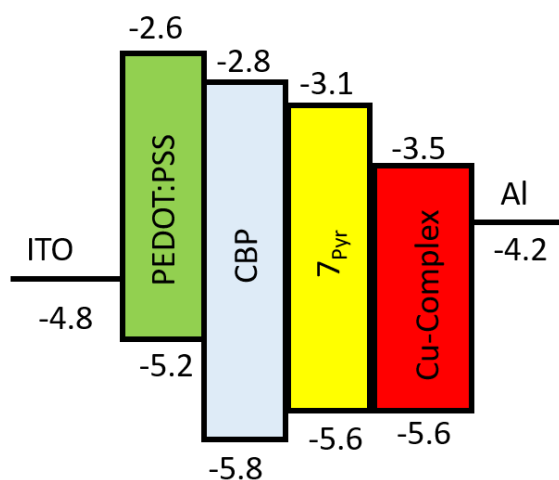


Figure S49: Schematic energy level diagrams of Cu-iTMCs-LECs with CBP or 7_{Pyr} as HTL. Please note that only one HTL is used in a device configuration. The levels are, when possible, calculated from the CV data (with $E_{\text{HOMO/LUMO}} = e(V_{\text{Fc}}/V_{\text{Fc}^+}) + 4.8 \text{ eV}$). Otherwise, we refer to the value obtained by theoretical calculations.

SUPPORTING INFORMATION

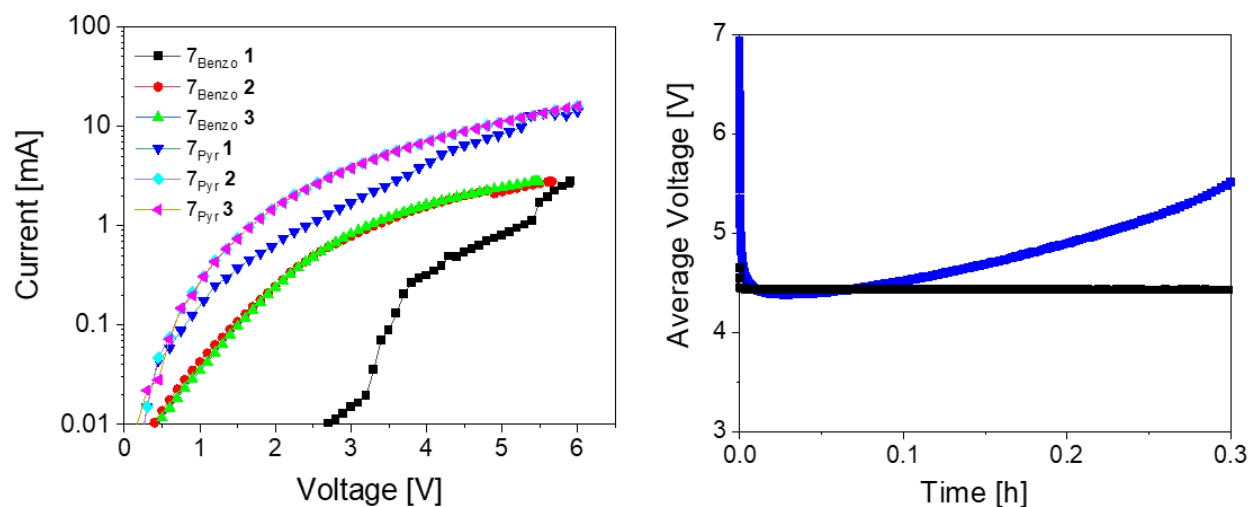


Figure S50: a) Scheme of the single-component LEC device having 7_{Pyr} as active layer (from previous figure); b) Measured currents upon 3 different 0-6 V voltage scans (see legend) for both 7_{Pyr} and 7_{Benzo} devices; c) Average voltage vs time for 7_{Benzo} (blue) and 7_{Pyr} (black) devices recorded with a pulsed current of 90 mA.

References

- [1] X.-F. Duan, X.-H. Li, F.-Y. Li, C.-H. Huang, *Synthesis* **2004**, 2004, 2614-2616.
- [2] G. Chelucci, S. Baldino, G. A. Pinna, B. Sechi, *Tetrahedron Lett.* **2008**, 49, 2839-2843.
- [3] A. Odedra, C.-J. Wu, T. B. Pratap, C.-W. Huang, Y.-F. Ran, R.-S. Liu, *J. Am. Chem. Soc.* **2005**, 127, 3406-3412.
- [4] R. K. Harris, E. D. Becker, S. M. Cabral De Menezes, P. Granger, R. E. Hoffman, K. W. Zilm, *eMagRes* **2007**.
- [5] A. T. CrysAlisPro, Version 1.171.37.33 (release 27-03-2014 CrysAlis171 .NET).
- [6] G. M. Sheldrick, *SHELX-2013: Program for the Solution of Crystal Structures*, University of Göttingen **2013**.
- [7] Bruker SAINT v8.38B Copyright © 2005-2019 Bruker AXS.
- [8] G. M. Sheldrick, *University of Göttingen, Germany* **1996**.
- [9] O. V. Dolomanov, L. J. Bourhis, R. J. Gildea, J. A. Howard, H. Puschmann, *J. Appl. Cryst.* **2009**, 42, 339-341.
- [10] C. B. Hübschle, G. M. Sheldrick, B. Dittrich, *J. Appl. Cryst.* **2011**, 44, 1281-1284.
- [11] G. M. Sheldrick, *SHELXS v 2016/4 University of Göttingen, Germany* **2015**.
- [12] A. L. Spek, *Acta Cryst.* **2009**, D65, 148-155.
- [13] H. Amenitsch, M. Rappolt, M. Kriechbaum, H. Mio, P. Laggner, S. Bernstorff, *J. Synchrotron Radiat.* **1998**, 5, 506-508.
- [14] Z. Jiang, *J. Appl. Cryst.* **2015**, 48, 917-926.
- [15] M. J. van Setten, M. Giantomassi, E. Bousquet, M. J. Verstraete, D. R. Hamann, X. Gonze, G.-M. Rignanese, *Comput. Phys. Commun.* **2018**, 226, 39-54.
- [16] P. Giannozzi, O. Andreussi, T. Brumme, O. Bunau, M. B. Nardelli, M. Calandra, R. Car, C. Cavazzoni, D. Ceresoli, M. Cococcioni, *J. Phys.: Condens. Matter* **2017**, 29, 465901.
- [17] J. P. Perdew, K. Burke, M. Ernzerhof, *Phys. Rev. Lett.* **1996**, 77, 3865.
- [18] S. Grimme, J. Antony, S. Ehrlich, H. Krieg, *J. Chem. Phys.* **2010**, 132, 154104.
- [19] W. Lin, L. Chen, P. Knochel, *Tetrahedron* **2007**, 63, 2787-2797.
- [20] H.-S. Lin, L. A. Paquette, *Synth. Commun.* **1994**, 24, 2503-2506.
- [21] F. Trécourt, G. Breton, V. Bonnet, F. Mongin, F. Marsais, G. Quéguiner, *Tetrahedron* **2000**, 56, 1349-1360.
- [22] A. Numata, Y. Kondo, T. Sakamoto, *Synthesis* **1999**, 1999, 306-311.

SUPPORTING INFORMATION

- [23] C. Körner, P. Starkov, T. D. Sheppard, *J. Am. Chem. Soc.* **2010**, *132*, 5968-5969.
- [24] M. T. Shehzad, A. Khan, M. Islam, S. A. Halim, M. Khat, M. U. Anwar, J. Hussain, A. Hameed, A. R. Pasha, F. A. Khan, *Bioorg. Chem.* **2020**, *94*, 103404.
- [25] A. Kremer, C. Aurisicchio, F. De Leo, B. Ventura, J. Wouters, N. Armaroli, A. Barbieri, D. Bonifazi, *Chem. Eur. J.* **2015**, *21*, 15377-15387.